

Electronic Thesis and Dissertation Repository

1-30-2023 2:00 PM

Synthesis of Ni(II) Complexes for Allylic C(sp³)-H Bond Activation for Aerobic Oxidation Catalysis

Shagana Kukendran, *The University of Western Ontario*

Supervisor: Blacquiere M. Johanna, *The University of Western Ontario*

A thesis submitted in partial fulfillment of the requirements for the Master of Science degree in Chemistry

© Shagana Kukendran 2023

Follow this and additional works at: <https://ir.lib.uwo.ca/etd>

 Part of the [Inorganic Chemistry Commons](#)

Recommended Citation

Kukendran, Shagana, "Synthesis of Ni(II) Complexes for Allylic C(sp³)-H Bond Activation for Aerobic Oxidation Catalysis" (2023). *Electronic Thesis and Dissertation Repository*. 9107.
<https://ir.lib.uwo.ca/etd/9107>

This Dissertation/Thesis is brought to you for free and open access by Scholarship@Western. It has been accepted for inclusion in Electronic Thesis and Dissertation Repository by an authorized administrator of Scholarship@Western. For more information, please contact wlsadmin@uwo.ca.

Abstract

Nickel is a widely abundant and inexpensive metal. Catalysts are substances that increase the rate of reactions by reducing the activation energy barrier, often by providing an alternative route and remaining unconsumed. The main goal of this study is to prepare Ni(II) complexes that can promote a catalytic aerobic oxidation reaction by breaking allylic C-H bonds. Based on previous studies, allylnickel *N*-heterocyclic carbene complexes react with molecular oxygen to give useful carbonyl compounds with a Ni(II)-OH by-product, which undergoes dimerization. In order to achieve catalysis, dimerization of the Ni(II)-OH should be prevented and C-H activation has to be achieved to complete the cycle. This project attempts to promote C-H activation via a Ni-OH moiety utilizing two different strategies that are described in Chapters 2 and 3, respectively. A known tridentate ligand structure proposed to inhibit dimer formation was targeted, which includes an imidazolium salt precursor that contains a hemilabile picolyl group. Studies on synthesizing a Ni(II)-OH monomer were conducted to test its ability toward C-H activation. No success was seen due to the instability of the intermediate leading to the formation of a bis-ligated Ni complex. A new allyl ligand *N*-8-quinolinyl-4-pentenamide with a bidentate directing group was chosen as an alternative approach. Preliminary studies indicated the formation of a dynamic paramagnetic complex with an unknown structure and a presumed bis-ligated by-product. Catalytic studies were done to test the ability of the unknown complex to activate allylic C-H bonds, but no success was achieved due to a competing reaction of the base with the ligand.

Keywords

Ni(II) complexes, aerobic oxidation catalysis, *N*-heterocyclic carbene, dimerization, C-H activation, tridentate ligand, imidazolium salt, hemilabile picolyl group, bis-ligated, bidentate, directing group, paramagnetic complex

Summary for Lay Audience

Catalysts are substances that make reactions faster without being used up. Aerobic oxidation is a chemical process that utilizes molecular oxygen from the air to form oxygen-containing organic molecules. Although oxygen is naturally available, the main challenge of using it in transition metal-catalyzed reactions to form useful compounds is its potential to form unwanted products after activation. The focus of this thesis is to carry out aerobic oxidation catalysis using nickel. Previous studies have shown successful results of Ni aerobically oxidizing molecules with no side reactions. The unstable Ni by-product formed in these reactions is the major challenge to making it catalytic. This project focuses on forming a stable Ni product through different strategies for aerobic oxidation catalysis. A successful catalytic reaction would be a cheaper alternative to other precious metals since Ni is a widely available metal.

Co-Authorship Statement

All experiments were performed by Shagana Kukendran, with the help of undergraduate students Kevin Deck and Lauren DiLoreto who contributed to the ligand scale-up. Crystal data collection and refinement were performed by P. D. Boyle. Chapters 1-5 were written by Shagana Kukendran and edited by J. M. Blacquiere.

Acknowledgment

First and foremost, I would like to thank my supervisor, Dr. Johanna Blacquiere. As an international student, I had no prior experience working in an inorganic lab, but she trusted me and let me work in her lab. Throughout my entire research journey, she was very supportive and provided me with guidance whenever I had questions. She also provided important insights on how to handle challenges and as a supervisor, she inspired me to be motivated and curious for that I am forever grateful.

I would also like to thank all the students of the Blacquiere group students, both current and past, that I have worked with over the last two years. I would especially like to thank the graduate students Kyle Jackman, Devon Chapple, and Jan-Willam for being around to answer any of my questions and Megan Hoffer and Amrit Singh for making my life in the lab (and outside) enjoyable with some amazing memories that I'll cherish forever. Thanks to Mat Willans for helping me run all my NMR experiments, to Paul Boyle for his crystallography work, and to Haidy Metwally and Chathu Pulukkody for the mass spec analysis.

I thank my family and friends (both in Canada and back in Sri Lanka) for their endless support over both my graduate and undergraduate career, especially my mom and sister. Finally, I would like to thank my amazing partner and best friend Nimantha who has been my forever support. I cannot imagine getting through my Master's without his guidance and constant motivation throughout the challenging times that I have faced. All of you have made my journey through grad school amazing and played an important part in achieving my dream.

Table of Contents

Abstract	ii
Summary for Lay Audience	iii
Co-Authorship Statement.....	iii
Acknowledgment	iv
Table of Contents	v
List of Tables	ix
List of Figures	x
List of Schemes.....	xiv
List of Abbreviations	xviii
Chapter 1	1
Introduction.....	1
1.1 Oxidation of C-H Bonds	1
1.2 Aerobic Oxidation Catalysis	3
1.2.1 Molecular Oxygen as an Oxidant	3
1.2.2 Transition Metal Catalyzed Allylic Aerobic Oxidation Catalysis	4
1.3 Ni(II) Allyl Complex Reactivity with Molecular Oxygen.....	6
1.4 Stability of Ni(II)-OH Monomers	8
1.5 C-H Bond Activation by Concerted Metalation-Deprotonation	9
1.5.1 General Features of the CMD Mechanism	9
1.5.2 Types of Internal Bases Involved in CMD	10
1.5.3 Role and Types of Directing Groups in CMD	12

1.5.4 Types of C-H bonds that Undergo CMD	14
1.5.5 Catalytic Ni(II) Reactions Involving CMD	15
1.6 Scope of Thesis	16
1.7. References	17
Chapter 2	21
Metalation of NHC Ligand and Attempts at the Formation of Ni(II)-OH Monomer	21
2.1 Synthesis of Bifunctional Tridentate NHC Ligand	21
2.1.1 Imidazole Synthesis	21
2.1.2 Picolyl Group Installation	22
2.1.3 Deprotection	23
2.2 Metalation of Ligand 3a with Ni to Form Complex 4a	25
2.3 Attempted Catalytic Aerobic Oxidations with 4a and <i>N</i> -8-quinolinyl-4-pentenamide	28
2.4 Conversion of 4a to Ni(II)-OH monomer 5a	31
2.4.1 Attempted Synthesis with KOH	31
2.4.2 Attempted Synthesis via a Ni-Amido Complex	32
2.4.3 Attempted Synthesis with NH ₄ OH	34
2.5 Synthesis and Characterization of Complex 6	35
2.6 Low Temperature UV-vis study to Determine 4a + NH ₄ OH Reaction Intermediates	40
2.7 Preliminary Synthesis of Ni(II) Allyl Complex 9a	42

2.8 Reactivity of 9a with Molecular Oxygen.....	43
2.9 Attempted Catalytic Aerobic Oxidations with 9a.....	46
2.9.1 Allyl Benzene as a Substrate.....	47
2.9.2 Allyl-4-(trifluoromethyl) Benzene as a Substrate.....	49
2.9.3 Allyldiphenyl Phosphine as the Substrate.....	50
2.10 Conclusions.....	51
2.11 References.....	52
Chapter 3.....	54
Synthesis of 8-Aminoquinoline Derived Allyl Ni(II) Complex for C(sp ³)-H Bond Activation Study.....	54
3.1 Reactivity of Ni(II) with <i>N</i> -8-Quinoliny-4-pentenamide.....	54
3.1.1 Reactivity of NiCl ₂ •6H ₂ O with QPAH.....	55
3.1.2 Reactivity of NiCl ₂ (PPh ₃) ₂ with QPAH.....	57
3.2 Catalysis to Test C-H Bond Activation with NaOH as the Base.....	66
3.3 Conclusions.....	68
3.4 References.....	70
Chapter 4.....	71
General Conclusions and Future Work.....	71
4.1 General Conclusions.....	71
4.2 Future Work.....	73
Chapter 5.....	76

Experimental	76
5.1 General Experimental Procedure	76
5.2 General Procedure for Imidazole Synthesis.....	77
5.3 General Procedure for Picolyl Group Installation.....	78
5.4 Synthesis of 1-(2-Pyridinylmethyl)-3-(2-hydroxyphenyl)-imidazolium Bromide (3a)	79
5.5 Synthesis of NHC Ni(II)-Br Complex (4a).....	80
5.6 Synthesis of Bis-ligated NHC Ni Complex (6).....	80
5.7.1 Representative Procedure for Attempted Catalytic Aerobic Oxidation of <i>N</i> -8- Quinoliny-4-pentenamide (QPAH) with 4a as Catalyst	81
5.7.2 Attempted Catalytic Aerobic Oxidation of QPAH at Low Concentration	82
5.7.3 Attempted Catalytic Aerobic Oxidation of QPAH with Different Bases	82
5.7.4 Attempted Catalytic Aerobic Oxidation of QPAH with IMes•HCl and Ni(OTf) ₂ as Catalyst	82
5.8 Low-Temperature UV-vis Spectroscopy Study to Trap Intermediates of the 4a + NH ₄ OH Reaction	83
5.9 Preliminary Synthesis of Ni(II) Allyl Complex (9a)	83
5.10 Preliminary Study on the Reactivity of 9a with O ₂	84
5.11.1 Representative Procedure for Attempted Catalytic Oxidation of Allylbenzene with 9a.....	84

5.11.2 Attempted Catalysis of Allylbenzene with 9a at High and Low Temperatures in MeCN- <i>d</i> ₃	85
5.11.3 Attempted Catalysis of Allylbenzene with 9a at Low Concentration in MeCN- <i>d</i> ₃	85
5.11.4 Attempted Catalytic Oxidation of 1-Allyl-4-(trifluoromethyl) Benzene with 9a	85
5.11.5 Attempted Catalytic Oxidation of Allyl Diphenylphosphine with 9a.....	86
5.12 References	87
Appendix	88
I NMR Spectra	88
II IR Spectra	97
III Crystallographic Detail	99
Curriculum Vitae	105

List of Tables

Table 2.1. Selected bond lengths (Å) and bond angles (°) for solid-state structures of 6 and 7 . ¹	38
Table 2.2. Conditions screened for attempted catalytic oxidation of allylbenzene. ^a	49
Table A1. Summary of Crystal Data for 6	102

List of Figures

- Figure 1.1.** Stabilization of Ni(II)-OH monomer by H bonding interactions from amide N-H reported by Borovik *et al.*¹⁸ 8
- Figure 1.2.** Different directing groups commonly used in catalysis involving CMD.....13
- Figure 1.3.** a) Proposed catalytic cycle involving the monomeric Ni(II)-OH intermediate. b) Proposed tridentate NHC ligand design inspired by known Ni(II)- halide complex to prevent dimerization of Ni(II)-OH monomer.....17
- Figure 2.1.** ¹H NMR stack plot of a) **3a** in DMSO-*d*₆ and b) **4a** in DMSO-*d*₆. Red dot (●) indicates the imidazolium peak on the ligand which disappears after metalation with Ni to form the **4a** complex. The purple dotted line indicates the slight upfield shift in the methylene signal of **4a** relative to **3a**. 26
- Figure 2.2.** MALDI MS of **4a** with pyrene as the matrix. The inset depicts the simulated and observed isotope pattern for the abundant signals. Signals that do not contain Ni (as judged by the isotope pattern) are labeled with an asterisk (*). 27
- Figure 2.3.** ¹H NMR stack plot of a) **4a** b) **3a** (2 eq) + NiCp₂ under reaction conditions and c) **3a** in DMSO-*d*₆. Red dot (●) indicates the imidazolium peak and blue dot (●) indicated the hydroxy peak of the ligand. Signals corresponding to **4a** are denoted by purple dots (●). 28
- Figure 2.4.** ¹H NMR stack plot of a) **4a** b) **4a** + KNHAr (2 eq) c) **4a** + KNHAr (2 eq) after washing with benzene to remove aniline d) KNHAr and e) 2, 6-diisopropyl aniline all taken in DMSO-*d*₆. Green dot (●) indicates the methylene peak of **4a**, which has disappeared after

the addition of KNHAr. The purple boxes highlight the similarity of amide signals formed in 4a + KNHAr reaction to diisopropyl aniline. (THF is denoted by ‘*’)	34
Figure 2.5. ORTEP drawing of 6 showing naming and numbering scheme for selected atoms of interest. Ellipsoids are at the 50% probability level and hydrogen atoms were omitted for clarity	37
Figure 2.6. complex 7 synthesized by Wang et al. analogous to 6 ¹	38
Figure 2.7. ESI-MS of 6 with DCM as the solvent. The inset depicts the observed isotope pattern for the most abundant signal.	39
Figure 2.8. Target Ni(II) allyl complex to favour formation of Ni(II)-OH monomer in situ for C-H activation.....	42
Figure 2.9. Solution of 9a in MeCN in 4 mL vial. Left picture taken before oxygen exposure, right picture taken 3h after exposure to oxygen.....	45
Figure 3.1. ¹ H NMR stack plot of a) QPAH + NiCl ₂ (PPh ₃) ₂ + NaOH (2 eq) (standard metalation reaction) b) NiCl ₂ (PPh ₃) ₂ c) NiCl ₂ (PPh ₃) ₂ + NaOH (2 eq) d) QPAH + NiCl ₂ (PPh ₃) ₂ all reactions heated at 110 °C in DMSO- <i>d</i> ₆ for 24 h, and e) QPAH + NiCl ₂ (PPh ₃) ₂ + NaOH (2 eq) heated at 60 °C in THF for 24 h. All spectra taken in DMSO- <i>d</i> ₆ . The ‘•’ indicate the major paramagnetic peaks observed in the standard reaction, ‘•’ indicate the peaks that have nearby peak shifts to spectrum e), and ‘•’ indicate the peaks that have nearby peak shifts to spectrum d). Peaks in the range of 0-10 ppm correspond to the QPAH ligand.....	60
Figure 3.2. Variable-temperature ¹ H NMR experiment of the reaction mixture QPAH + NiCl ₂ (PPh ₃) ₂ + NaOH (2 eq) kept at 110 °C for 24 h in DMSO- <i>d</i> ₆ . All spectra taken in DMSO- <i>d</i> ₆ , I600 MHz, except the spectrum at 25 °C which is taken by B600 MHz	

instrument. Signals corresponding to the neutral ligand QPAH are denoted in green (•). Signals corresponding to the major peaks of unknown product are denoted in red (•).....62

Figure 3.3. ^1H NMR stack plot of a) QPAH + $\text{NiCl}_2(\text{PPh}_3)_2$ + NaOH (2 eq) in the absence of sieves b) QPAH + $\text{NiCl}_2(\text{PPh}_3)_2$ + NaOH (2 eq) in the presence of 4 Å sieves. Both reactions heated at 110 °C in $\text{DMSO}-d_6$ for 24 h and taken in $\text{DMSO}-d_6$63

Figure 3.4. Wide range ^1H NMR stack plot of a) QPAH (1 eq) + $\text{NiCl}_2(\text{PPh}_3)_2$ (1 eq) + NaOH (2 eq) heated to 110 °C for 24 h in $\text{DMSO}-d_6$, b) QPAH (2.2 eq) deprotonated with KH (2.2 eq) followed by $\text{NiCl}_2(\text{PPh}_3)_2$ (1 eq) addition in THF at RT. Both spectra taken in $\text{DMSO}-d_6$. The ‘•’ indicate the peaks that have nearby peak shifts to spectrum b).....65

Figure 3.5. QPAH (1 eq) + $\text{NiCl}_2(\text{PPh}_3)_2$ (1 eq) + NaOH (2 eq) heated at different temperatures for 24 h in $\text{DMSO}-d_6$ in the presence of sieves.....66

Figure 3.6. ^1H NMR stack plot of a) QPAH b) Crude reaction mixture obtained from catalysis c) Isolated product obtained after QPAH removal through column chromatography. All spectra taken in CDCl_368

Figure 4.1. a) Synthesis of target NHC ligand attempted by previous group members. b) Proposed NHC ligand to prevent dimerization by having bulky groups in 2 and 4 positions of phenol.....73

Figure 4.2. Proposed ligand design to stabilize the Ni(II)-OH complex.....75

Figure A1. ^1H NMR spectrum (400 MHz, CDCl_3) of **2a**, DCM is denoted by ‘*’.....88

Figure A2. $^{13}\text{C}\{^1\text{H}\}$ NMR spectrum (101 MHz, CDCl_3) of **2a**, DCM denoted by ‘*’.....89

Figure A3. ^1H NMR spectrum (400 MHz, $\text{DMSO}-d_6$) of **3a**, water is denoted by ‘*’.....90

Figure A4. $^{13}\text{C}\{^1\text{H}\}$ NMR spectrum (101 MHz, DMSO- d_6) of 3a .	91
Figure A5. ^1H NMR spectrum (400 MHz, DMSO- d_6) of complex 4a . DCM peak is denoted by 'd', water peak is denoted by '*'. .	92
Figure A6. $^{13}\text{C}\{^1\text{H}\}$ NMR spectrum (101 MHz, DMSO- d_6) of complex 4a . Diethyl ether is denoted by 'e'.	93
Figure A7. ^1H NMR spectrum (400 MHz, DMSO- d_6) of complex 6 . THF is denoted by '*', grease denoted by 'g'. Mass purity = 53% (Contains mono cationic ligand 3a).	94
Figure A8. $^{13}\text{C}\{^1\text{H}\}$ NMR spectrum (101 MHz, DMSO- d_6) of 6 . THF is denoted by '*'. Mass purity = 53% (Contains mono cationic ligand 3a).	95
Figure A9. ^1H NMR stack plot (600 MHz, MeOH- d_4) of a) QPAH ligand b) QPAH treated with $\text{NiCl}_2 \cdot 6\text{H}_2\text{O}$ at 55 °C in MeOH- d_4 . Internal standard denoted as '*', traces of water and acetone denoted as 'c'.	96
Figure A10. ATR-FTIR spectrum of solid 2a .	97
Figure A11. ATR-FTIR spectrum of solid 3a .	97
Figure A12. ATR-FTIR spectrum of solid 4a .	98
Figure A13. ATR-FTIR spectrum of solid 6 .	98
Figure A14. Drawing of 6 showing naming and numbering scheme. Ellipsoids are at the 50% probability level and hydrogen atoms were omitted for clarity.	101
Figure A15. Kinetics trace of 1 mM 4a at -60 °C depicted in blue and after addition of NH_4OH (28-30% in water) over 1 h. The reaction time between each trace is 5 min.	104

List of Schemes

Scheme 1.1. Allylic C-H oxidation of 1-butene using the free radical bromination, hydroxylation, and Swern oxidation.	1
Scheme 1.2. Pd(II) catalyzed oxidation of allylic C-H bonds using H ₂ O as the oxygen source. ³	2
Scheme 1.3. Proposed mechanisms for Pd(II) catalyzed allylic oxidation reaction consisting of the C-H activation and oxidation step. ³	3
Scheme 1.4. Aerobic oxidation catalysis by Co(II) catalysts 3 and 4 on cyclohexene showing different chemoselectivities. ¹⁰	5
Scheme 1.5. Catalytic reaction of bimetallic Ni(II) perchlorate complex with cyclohexene under optimized conditions. ¹¹	5
Scheme 1.6. Reaction of NiCl(η^3 -allyl) NHC with O ₂ forming α,β -unsaturated carbonyl compounds. ¹³	6
Scheme 1.7. Proposed mechanism for aerobic oxidation of Ni(II) allyl NHC complex supported by kinetic data (UV-Vis spectroscopy).	7
Scheme 1.8. Reaction of Ni(II)-NHC complexes with O ₂ by the Blacquiere group. ¹⁶	7
Scheme 1.9. Ni(II)-OH monomer reported by Holm <i>et al.</i> which is stabilized by tridentate ligand and its reactivity with an acid.	8
Scheme 1.10. The Concerted metalation deprotonation pathway involving the deprotonation of the intramolecular base.....	10
Scheme 1.11. The difference between the (C-H) sigma and the agostic complex and an example for each complex. ^{25,26} (O = C atom, O = H atom).....	10
Scheme 1.12. Concerted-metalation deprotonation (CMD) with Pd(II)- carboxylate.	11

Scheme 1.13. C-H activation with Ir(III)-hydroxide complex. ³²	11
Scheme 1.14. Computational studies on C-H with Ni-OR by Cundari <i>et al.</i>	12
Scheme 1.15. Role of directing groups in catalysis. (DG = directing group, FG = functional group, M = transition metal)	12
Scheme 1.16. Alkylation of C(sp ²)-H bonds in aromatic amides with alkyl halides by Chatani (The 8-aminoquinoline directing group is highlighted in green).	13
Scheme 1.17. Primary and secondary C(sp ³)-H bond activation using Ni(II) complex by Beattie <i>et al.</i> (R ¹ = H, alkyl or aryl group) ⁴¹	14
Scheme 1.18. Ni(II) catalyzed direct arylation by activating C(sp ³)-H, proposed by Chatani in 2014.	15
Scheme 1.19. Amide directed Ni-NHC catalyzed C(sp ²)-H alkylation.	15
Scheme 2.1. Synthesis of 1-(2-methoxyphenyl)-imidazole (1a) and 1-(2-methoxy-3-methylphenyl)-imidazole (1b). Isolated yields are given in parentheses.....	22
Scheme 2.2. a) Neutralization of 2-(bromomethyl)pyridine hydrobromide to 2-(bromomethyl)pyridine and b) Synthesis of 1-(2-pyridinylmethyl)-3-(2-methoxyphenyl)-imidazolium bromide (2a) and 1-(2-pyridinylmethyl)-3-(2-methoxy-3-methylphenyl)-imidazolium bromide (2b). Isolated yields are given in parentheses.	23
Scheme 2.3. Deprotection of 1-(2-pyridinylmethyl)-3-(2-methoxyphenyl)-imidazolium bromide (2a) to synthesize 1-(2-pyridinylmethyl)-3-(2-hydroxyphenyl)-imidazolium bromide (3a).....	25
Scheme 2.4. Metalation of ligand 3a with Ni(II) to form 4a complex.....	25
Scheme 2.5. Possible formation of monodentate bis ligated Ni(II) complex.....	27

Scheme 2.6. Postulated mechanism for catalytic oxidation of <i>N</i> -8-quinolinyl-4-pentenamide utilizing 4a as catalysts (A = alkali metal)	29
Scheme 2.7. Attempted catalytic aerobic oxidation of <i>N</i> -8-quinolinyl-4-pentenamide with 4a , with conditions tested	30
Scheme 2.8. Attempted catalytic aerobic oxidation of <i>N</i> -8-quinolinyl-4-pentenamide with monodentate NHC Ni(II) catalyst and the expected products.	31
Scheme 2.9. Reaction of 4a with KOH, at variable solvent systems (DCM, THF, and DMSO) and temperatures (from room temperature gradually increased to 70 °C).....	32
Scheme 2.10. Reaction of 4a with NaNH ₂ followed by H ₂ O addition.	33
Scheme 2.11. Proposed reaction of 4a with KNHAr (Ar = 2,6- ⁱ Pr ₂ C ₆ H ₃) in THF	33
Scheme 2.12. Formation of 6 by reacting 4a with NH ₄ OH in THF.....	35
Scheme 2.13. Proposed pathway for the formation of bis ligated Ni(II) complex 6	40
Scheme 2.14. General reaction scheme for low temperature UV-Vis experiments.	41
Scheme 2.15. Formation of 9a by reacting 2-propenyl magnesium bromide with 4a in THF.....	43
Scheme 2.16. Reactivity of 9a with molecular oxygen.....	44
Scheme 2.17. Cinnamaldehyde Grignard formation by reacting (3-Bromo-1-propenyl)benzene with Mg followed by 4a addition to form 10a	46
Scheme 2.18. Proposed mechanism for catalytic aerobic oxidation of 9a through tridentate Ni(II)-OH monomer 5a intermediate.	47
Scheme 2.19. Attempted catalytic aerobic oxidation of allylbenzene with 9a , with conditions tested.....	48

Scheme 2.20. Reaction conditions of aerobic oxidation catalysis of 1-allyl-4-(trifluoromethyl) benzene with 9a with proposed products.....	50
Scheme 2.21. Attempted aerobic oxidation catalysis of allyl diphenyl phosphine with 9a	50
Scheme 3.1. Proposed CMD pathway through deprotonation by a hydroxo base for allylic C(sp ³)-H activation using 8-aminoquinoline (denoted in blue) derived allyl substrate....	54
Scheme 3.2. Synthesis of the 8-aminoquinoline derived allyl QPAH. (HATU = hexafluorophosphate azabenzotriazole tetramethyl uronium)	55
Scheme 3.3. Metalation attempts of Ni(II) with QPAH in DMSO- <i>d</i> ₆ and toluene- <i>d</i> ₈ with NaOH and the proposed product.....	56
Scheme 3.4. Proposed potential products from the metalation reaction in DMSO- <i>d</i> ₆ based on the ¹ H NMR spectrum.....	56
Scheme 3.5. Metalation attempt of <i>N</i> -8-quinolinyl-4-pentenamide using NiCl ₂ •6H ₂ O in MeOH in the absence of a base and proposed <i>in situ</i> formed products.....	57
Scheme 3.6. Metalation reaction of QPAH with NiCl ₂ (PPh ₃) ₂ in the presence of NaOH base and the proposed potential products.	58
Scheme 3.7. Proposed equilibrium for the metalation reaction forming free QPAH.....	62
Scheme 3.8. a) Bis-ligated Ni(II) complex formed in the metalation reactions by Johnson et al using NiCl ₂ (PPh ₃) ₂ with 8-aminoquinoline derived amide. ⁶ b) Synthesis of bis ligated Ni(II) complex 11	64
Scheme 4.1. Ni(II)-OH intermediate trapping experiment at low temperature through phosphine groups.....	73

List of Abbreviations

Å (angstrom)

Ar (aryl)

Cp (cyclopentadienyl)

°C (degrees Celsius)

CMD (Concerted Metalation Deprotonation)

δ (chemical shift)

DCM (dichloromethane)

DDQ (2,3-Dichloro-5,6-dicyano-1,4-benzoquinone)

DMF (dimethylformamide)

DMSO (dimethyl sulfoxide)

DFT Density functional theory

h (hour)

HMBC (heteronuclear multiple bond correlation) xviii

HSQC (heteronuclear single quantum correlation)

Hz (hertz)

η (Hapticity)

IR (infrared)

IMes (1,3-bis(2,4,6-trimethylphenyl)imidazol-2-ylidene)

J (coupling constant (in Hz))

MALDI-MS (Matrix Assisted Laser Desorption Ionization Mass Spectrometry)

Me (methyl)

MeCN (acetonitrile)

min (minutes)

mmol (millimole)

M (molarity)

mM (millimolar)

m/z (mass to charge ratio)

NHC (*N*-heterocyclic carbene)

NMR (nuclear magnetic resonance)

Ph (phenyl)

ppm (parts per million)

pKa (acid dissociation constant)

RT (room temperature)

tBu (tert-butyl)

THF (tetrahydrofuran)

TMS (tetramethylsilane)

UV-Vis (ultraviolet-visible)

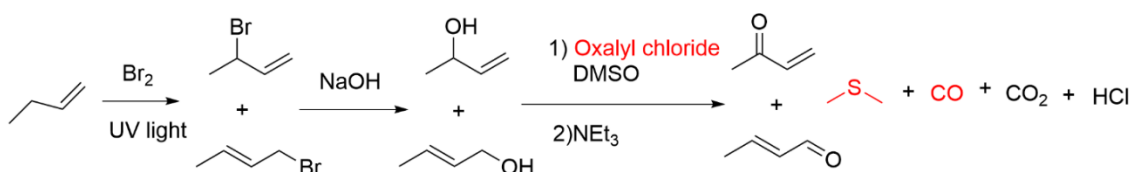
Chapter 1

Introduction

1.1 Oxidation of C-H Bonds

Oxidation of C-H bonds to C-O bonds is highly beneficial and these reactions are commonly found in many essential organic syntheses.¹ The formation of carbonyl bonds (C=O) from hydrocarbon oxidation is of specific interest, due to the prevalence of carbonyl functionalities in many useful organic compounds such as ketones, aldehydes, carboxylic acids, and esters. Activated C-H functionalities such as allylic groups are often targeted to achieve easier oxidation.²

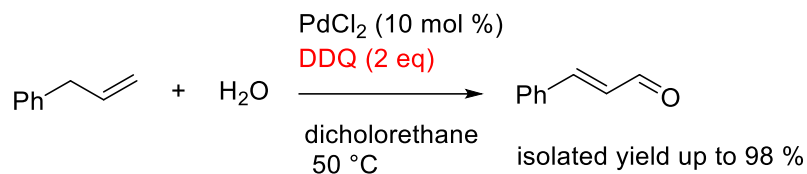
There are a few ways in which allylic C-H bonds can be oxidized to carbonyl groups using traditional organic methods. One such example involves halogenation by a free radical pathway, hydroxylation by S_N2 substitution, followed by a Swern oxidation (Scheme 1.1). Several drawbacks are associated with these reactions. The multiple synthetic steps involved increases the cost and may decrease the final yield compared to a single-step reaction. The production of toxic byproducts that are harmful to the environment and people, the use of harsh oxidants, and often poor selectivity are other disadvantages of the above traditional organic reactions.



Scheme 1.1. Allylic C-H oxidation of 1-butene using the free radical bromination, hydroxylation, and Swern oxidation.

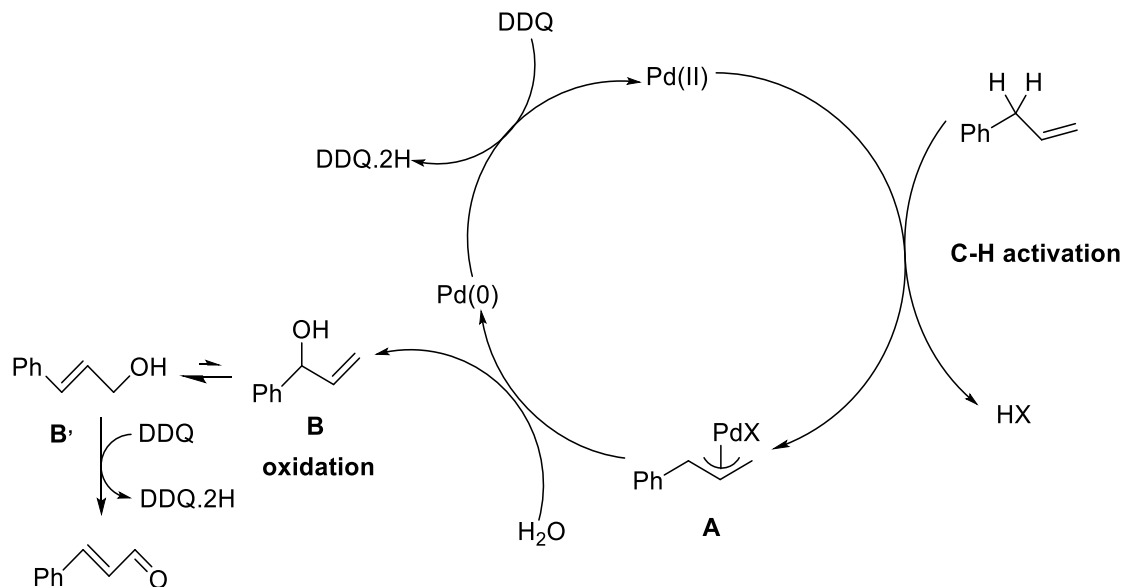
Some of these disadvantages can be solved by the use of transition metal catalysis, which can reduce the number of steps involved, improve selectivity, and permit the use of less aggressive/different oxidants. An example is palladium catalysts that were used to convert allyl benzene and water to cinnamaldehyde using 2,3-dichloro-5,6-dicyano-1,4-

benzoquinone (DDQ) as the oxidant (Scheme 1.2).³ Although the reaction takes place in a single step and has good yields and selectivity under mild conditions, the oxidant DDQ can be carcinogenic in its reduced form.



Scheme 1.2. Pd(II) catalyzed oxidation of allylic C-H bonds using H₂O as the oxygen source.³

The proposed mechanism for the above reaction consists of two major steps (Scheme 1.3). The first step involves the Pd(II) reacting with the allyl benzene to produce the π -allyl palladium species **A** by activating the allylic C-H bond. The second step is the oxidation step in which intermediate **A** is subjected to nucleophilic attack by H₂O forming Pd(0) and the enols **B** and **B'** as the oxidative products. The enols are oxidized by DDQ to give the cinnamaldehyde product. The Pd(0) is reoxidized to Pd(II) by DDQ so it can enter the catalytic cycle again.



Scheme 1.3. Proposed mechanisms for Pd(II) catalyzed allylic oxidation reaction consisting of the C-H activation and oxidation step.³

1.2 Aerobic Oxidation Catalysis

1.2.1 Molecular Oxygen as an Oxidant

Molecular oxygen (O_2) is a green oxidant that can be used rather than conventional oxidants such as DDQ since it is readily available, inexpensive, and less harmful to human health and the environment.^{4,5} O_2 mediated catalytic oxidation reactions can be classified into two types: oxidase and oxygenase reactions. In oxidase catalysis, the oxygen atom is not incorporated into the oxidized product even though it is involved in the oxidation reaction. Whereas in oxygenase catalysis O_2 acts as the oxidant as well as the oxygen source for the final product.⁶ Oxygenase reactions are very atom economical since they produce water as the only byproduct.

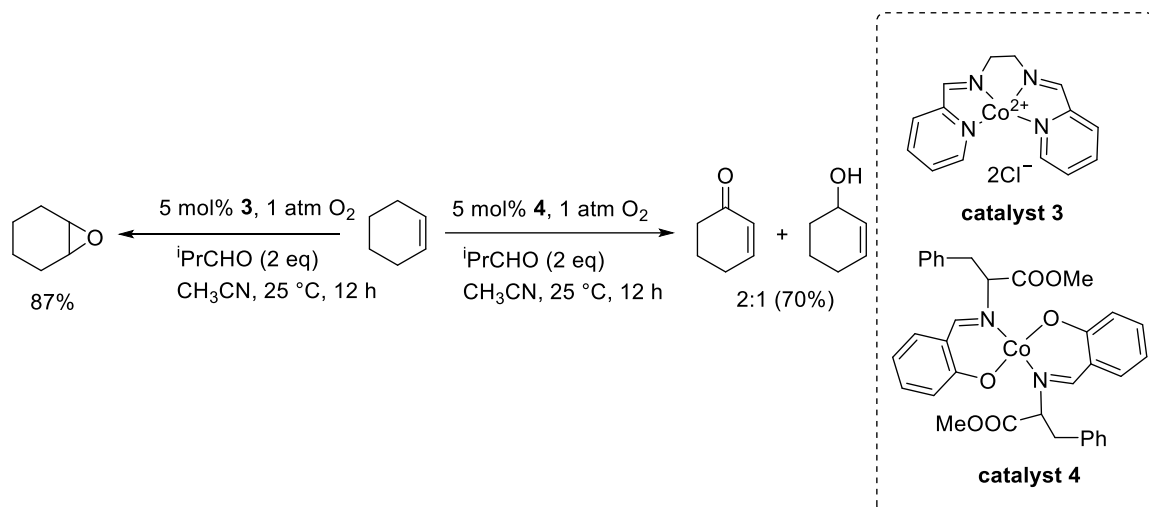
However, utilizing molecular oxygen as an oxidant has certain safety concerns due to O_2 being a potential fire hazard. O_2 is a promoter of combustion, hence large-scale use of it in industries can be a challenge. New reaction designs such as continuous flow chemistry, which uses dilute air as an oxidant can be used to overcome the safety hazard.⁷ Molecular

oxygen also has selectivity issues producing undesirable side products by forming reduced oxygen species after activation by the metal catalyst.⁸ New catalyst designs which improve selectivity, can provide a solution for these limitations. Hence, continued research on catalysts for aerobic oxidation is desired.

1.2.2 Transition Metal Catalyzed Allylic Aerobic Oxidation Catalysis

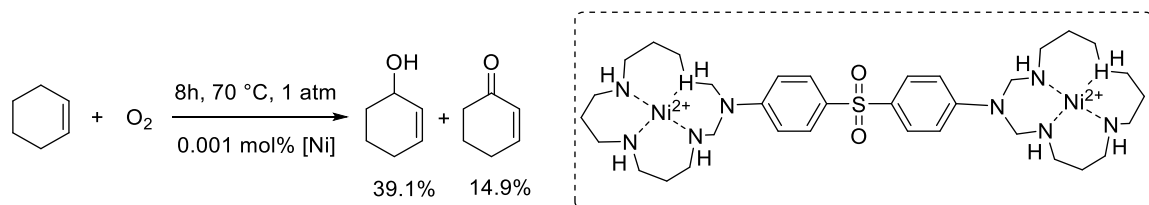
Transition metal catalyzed aerobic oxidation reactions are limited due to challenges such as: difficulty in activating O₂ at mild conditions, the requirement of co-catalysts to achieve complete oxidation, and poor chemoselectivity control.⁹ The usage of activated C-H bonds such as allylic C-H bonds in aerobic oxidation catalysis is one way to overcome some of these challenges. A few examples of catalytic allylic oxidation involving molecular oxygen are noteworthy.

Iqbal and co-workers reported two cobalt(II) complexes derived from Schiff bases that oxidize cyclic alkenes in the presence of molecular oxygen and 2-methylpropanal under mild conditions (Scheme 1.4).¹⁰ The two Co(II) catalysts show interesting chemoselectivities. One catalyst (catalyst 3) gives epoxide as the major product and the other catalyst (catalyst 4) dominantly forms allylic alcohols and enones. The difference in the chemoselectivity was observed due to the ligand effects around cobalt, which were responsible for forming various reactive species such as O₂⁻ and O₂²⁻ resulting in different products.



Scheme 1.4. Aerobic oxidation catalysis by Co(II) catalysts 3 and 4 on cyclohexene showing different chemoselectivities.¹⁰

A study involving Ni(II) catalyzed aerobic oxidation reaction was also reported in 2007.¹¹ Bis(macrocyclic) binuclear nickel(II) complexes are found to act as catalysts and selectively oxidize cyclohexene to give 2-cyclohexene-1-one and 2-cyclohexene-2-ol as the major products (Scheme 1.5). The catalytic reaction was more selective towards the enol (72.5%) and was optimized to achieve a maximum conversion of 53.9% at a catalyst loading of 0.001 mol% at 70 °C in the absence of a solvent. The study provides evidence for Ni(II) catalysts activating allylic C-H bonds and oxidizing them aerobically.

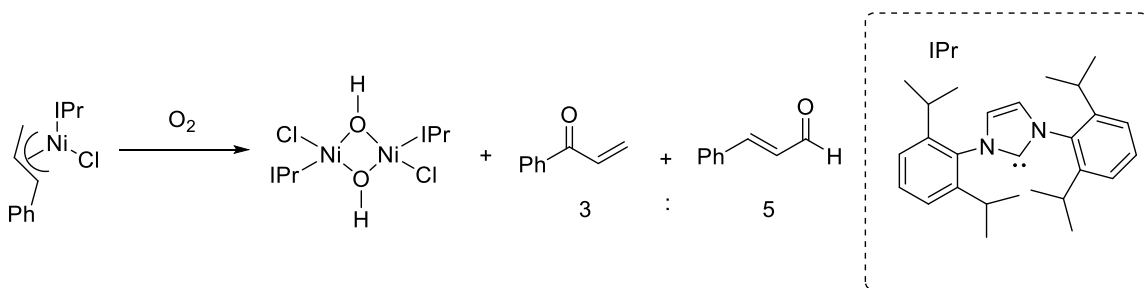


Scheme 1.5. Catalytic reaction of bimetallic Ni(II) perchlorate complex with cyclohexene under optimized conditions.¹¹

1.3 Ni(II) Allyl Complex Reactivity with Molecular Oxygen

The reactivity of Ni(II) with molecular oxygen is rare due to the difficulty in oxidizing Ni(II) to Ni(III).¹² The oxidation potential of oxidizing Ni from +2 to +3 oxidation state is more electropositive than the reduction potential of O₂ making the reaction thermodynamically unfavorable. Utilization of electron donating ligands such as *N*-heterocyclic carbene (NHC) can reduce the redox potential of Ni(II) to Ni(III) and make the oxidation reaction favorable.

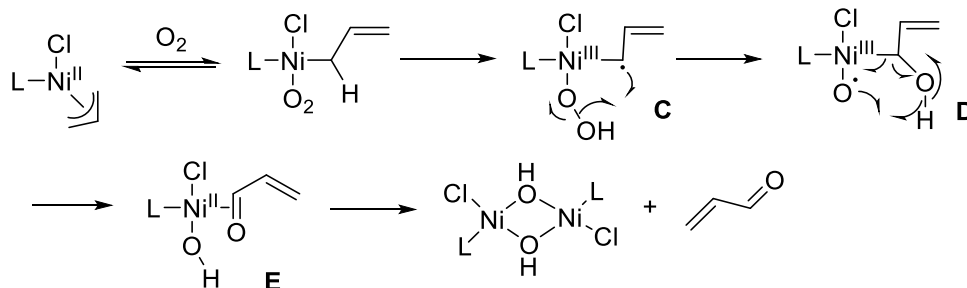
Sigman *et al.* published a finding, in which the C-H bond of the coordinated anionic allyl ligand in the NiCl(η³-allyl) (NHC: IPr; 1,3-bis(2,6-diisopropylphenyl)imidazole-2-ylidene) complex undergoes oxidation (Scheme 1.6). Aerobic oxidation was performed on the Ni(II) allyl complex, which resulted in the formation of two organic products: cinnamaldehyde and phenyl vinyl ketone. The reaction also produced a nickel-based byproduct Ni(II)-OH monomer, which dimerizes to form a bis-μ-hydroxonickel(II) compound.¹³ The Ni(II)-OH dimer is more stable than its monomer, but it undergoes decomposition in solution after several days.¹⁴ Another significance of this study is that there was an improvement in selectivity compared to other known aerobic allylic oxidation reactions.¹⁵



Scheme 1.6. Reaction of NiCl(η³-allyl) NHC with O₂ forming α,β-unsaturated carbonyl compounds.¹³

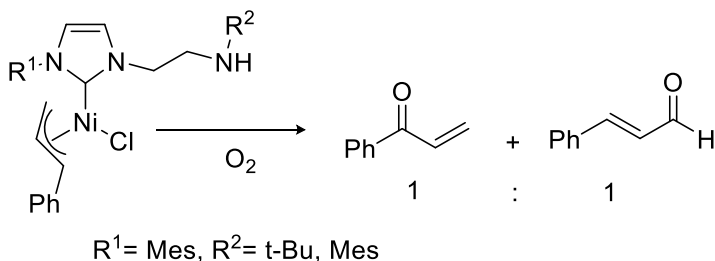
The proposed mechanism for the formation of the oxidized products for the above reaction involves the reversible binding of O₂ to Ni(II) to give the superoxide (Scheme 1.7). The superoxide then forms the Ni(III)-peroxide intermediate **C** through H atom

transfer from the allylic carbon. The oxygen radical of **D** abstracts a hydrogen atom from the neighboring hydroxy group and undergoes intramolecular hydroxylation to yield **E**, which ultimately leads to the formation of carbonyl products and a Ni(II)-OH byproduct.¹³



Scheme 1.7. Proposed mechanism for aerobic oxidation of Ni(II) allyl NHC complex supported by kinetic data (UV-Vis spectroscopy).

The Blacquiere group also worked with NHC Ni(II)-cinnamyl and allyl complexes, with bifunctional ligands having a secondary amine functionality as a substituent, and probed the significance of second-coordination sphere ligand properties on aerobic oxidation reactivity.¹⁶ The complexes when reacted with O₂ produced cinnamaldehyde and phenyl vinyl ketone in a rough ratio of 1:1 and a Ni(II) by-product (Scheme 1.8). Although the secondary amine group had no significant influence on the yield or selectivity of the obtained oxidation products, it did lower the stability of the Ni(II)-OH, based on preliminary data. This suggests the bifunctional nature of the ligand, through H bonding and hemilability might have influenced the stability and fate of the nickel oxidation products.



Scheme 1.8. Reaction of Ni(II)-NHC complexes with O₂ by the Blacquiere group.¹⁶

1.4 Stability of Ni(II)-OH Monomers

Stability of monomeric Ni(II)-OH from dimerization can be achieved in the two ways. First by using a group to form an H-bond between the OH group and a functional group in the secondary coordination sphere.¹⁷ Borovik *et al.* were able to stabilize a Ni(II)-OH monomer using two H-bonding interactions from amide N-H groups (Figure 1.1).¹⁸

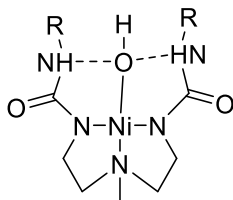
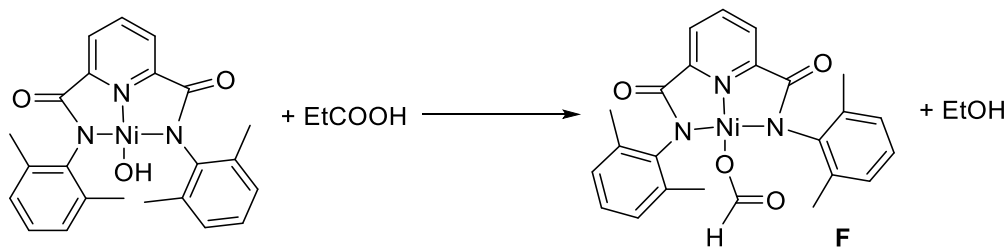


Figure 1.1. Stabilization of Ni(II)-OH monomer by H bonding interactions from amide N-H reported by Borovik *et al.*¹⁸

The second method involves the use of a ligand with a higher coordination number so that the coordination sites at the metal center are decreased to prevent dimerization through μ -OH bridging. Holm *et al.* were able to isolate Ni(II)-OH monomeric species using a tridentate ligand (Scheme 1.9).¹⁹ The reactivity of the monomeric Ni(II)-OH with different species involving ligand exchange, insertion, and metathesis reactions was studied. When the monomeric Ni(II) complex was exposed to EtCOOH it underwent a ligand exchange reaction producing the carbonate complex **F** and a base.



Scheme 1.9. Ni(II)-OH monomer reported by Holm *et al.* which is stabilized by tridentate ligand and its reactivity with an acid.

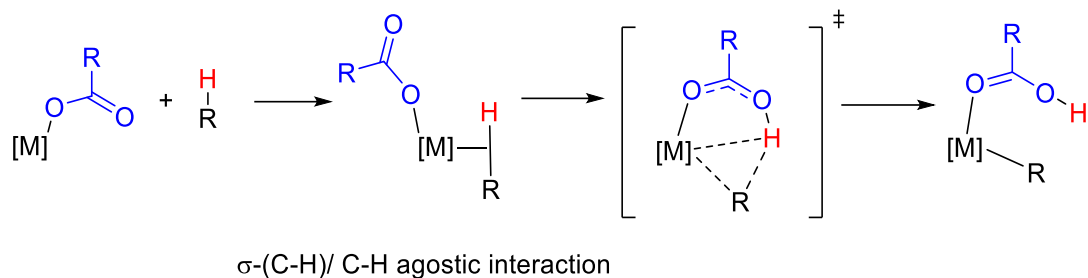
1.5 C-H Bond Activation by Concerted Metalation-Deprotonation

1.5.1 General Features of the CMD Mechanism

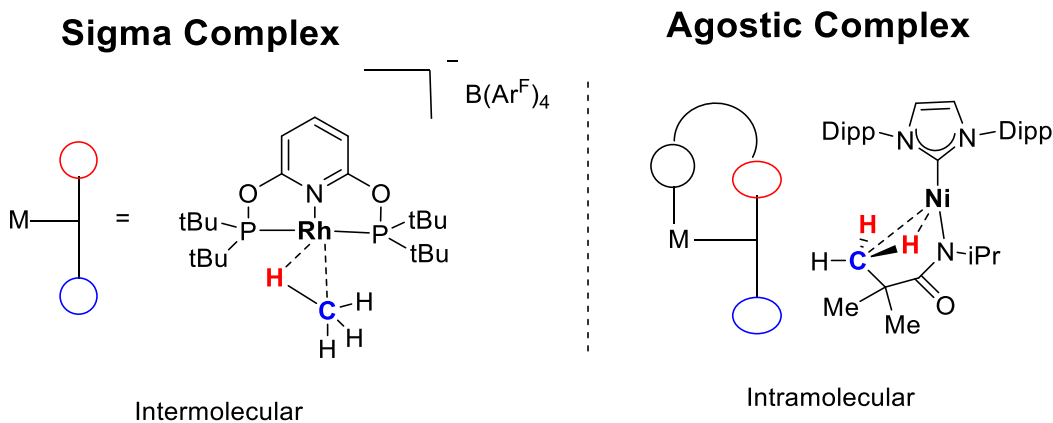
To oxidize a methylene unit to a carbonyl, two C-H bonds must be broken. In the last few decades, many known metals and ligands were used as catalysts for C-H activation reactions. The group 10 metals, notably Pd, play a major role.^{20,21}

Several mechanisms that are involved in the cleavage of C-H bonds have been studied or proposed over the years and they can be classified into three main categories such as oxidative addition, electrophilic substitution, and σ -bond metathesis.²² Each of these categories can be further described based on many factors such as the nature of the transition metal, change in metal oxidation state, etc.²³ The concerted metalation-deprotonation (CMD) pathway, also referred to as internal electrophilic substitution (IES) falls under the electrophilic mechanism.²⁴

Various well established late transition metal catalysts such as Pd, Ru, Ir, Rh, and Ni activate the C-H bond, via a redox neutral concerted metalation deprotonation pathway. The pathway involves the electrophilic metal forming a sigma bond or an agostic interaction with a hydrocarbon, which weakens the C-H bond by polarizing the bond and increasing the acidity of the proton (Scheme 1.10). This allows a weak base to cleave the bond by deprotonation leading to a new metal-carbon bond and a conjugated acid of the base.²² The C-H sigma complex and the agostic interaction are formed in the same way but they differ in the connectivity of the molecules that are undergoing the interaction (Scheme 1.11). The sigma complex is formed from an intermolecular reaction whereas an agostic interaction occurs through an intramolecular reaction. Hence, it is much easier to form an agostic interaction over a sigma complex.



Scheme 1.10. The Concerted metalation-deprotonation pathway involving the deprotonation of the intramolecular base.

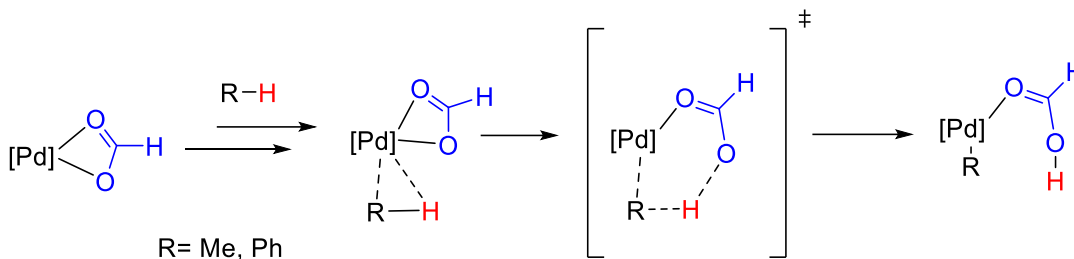


Scheme 1.11. The difference between the (C-H) sigma and the agostic complex and an example for each complex.^{25,26} (O = H atom, \circ = C atom)

1.5.2 Types of Internal Bases Involved in CMD

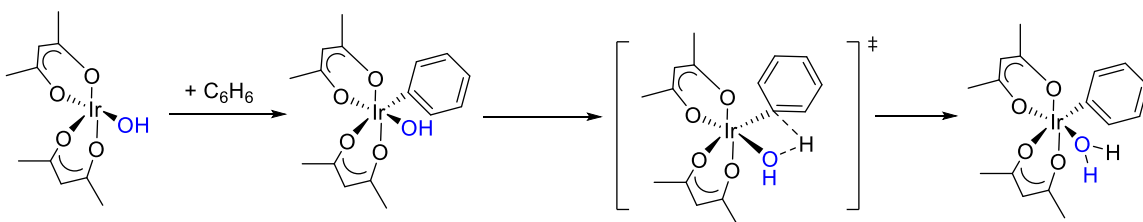
Among the several base-assisted CMD pathways, the bidentate carboxylate base is the most used base for deprotonation.²⁷ Intermolecular C-H activation of both benzene and methane were theoretically analyzed using Density Functional Theory (DFT) for Pd(II) carboxylate systems (Scheme 1.12).²⁸ The study theoretically provided evidence that the carboxylate base was involved in the proton abstraction by analyzing electron distribution changes in transition states. During the C-H activation process, the metal's atomic

population increased while that of H decreased significantly. Many well established Pd(II)-carboxylate catalysts are involved in CMD reactions.²⁹



Scheme 1.12. Concerted-metalation-deprotonation (CMD) with Pd(II)-carboxylate.

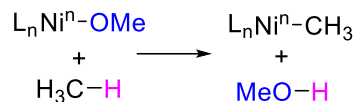
Internal monodentate bases like -OH and -OR have also been used based on recent studies.^{30, 31} Periana, Goddard, and co-workers did experimental and computational studies on stoichiometric and catalytic C(sp²)-H bond activation reactivity with an air stable iridium-hydroxide complex (Scheme 1.13).³² The hydroxo group was involved in the metalation and activation of benzene. This study indicated the possibility of a hydroxo group acting as an internal base for the CMD pathway.



Scheme 1.13. C-H activation with Ir(III)-hydroxide complex.³²

In 2018, a computational study was done on C(sp³)-H activation through CMD pathway using neutral and cationic Ni(II)-methoxide pincer complexes to activate methane and produce methanol (Scheme 1.14).³³ The study investigated ways to reduce the high activation energy barrier for the C(sp³)-H bond activation by analyzing various factors affecting the kinetics and thermodynamics of the reaction. Promising outcomes were obtained with the usage of bidentate supporting ligands and cationic complexes with counter ions, which helps to reduce the activation barrier by stabilizing the transition state.

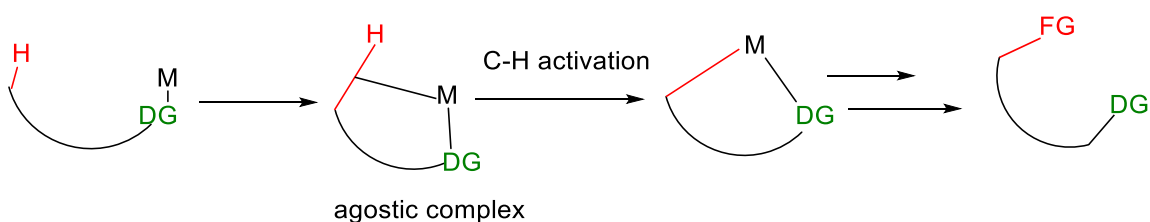
Although the solvent polarity had no major effect on the activation kinetics, the use of weakly coordinating solvents was recommended. A possible radical reaction was also identified due to the weaker 3d metal M-C bond compared to 4d and 5d metals, which may prevent catalytic activity. The study indicates the possibility of structurally similar Ni(II)-OH reactivity toward C-H activation even though studies involving the use of Ni(II) catalysts with internal hydroxo bases have not been conducted as of yet.



Scheme 1.14. Computational studies on C-H with Ni-OR by Cundari *et al.*

1.5.3 Role and Types of Directing Groups in CMD

A directing group is a part of a substrate molecule that facilitates the CMD reaction by temporarily coordinating with the transition metal through specific sites (i.e. the donor atoms) (Scheme 1.15). The chelation of metal to substrate promotes the C-H bond activation by making the reaction intramolecular forming the agostic complex. It also brings the C-H bond of interest in proximity to the transition metal catalyst which helps in controlling selectivity. Hence directing groups are useful tools in CMD reactions.^{34,35}



Scheme 1.15. Role of directing groups in catalysis. (DG = directing group, FG = functional group, M = transition metal)

An ideal directing group should easily coordinate to the catalyst, efficiently control the reactivity/selectivity, and easily dissociate from the catalyst.³⁶ They can be classified based on their structural features such as denticity, coordinating atoms, and moieties.

Directing groups that bind to the metal through a single coordination site or two coordination sites are known as monodentate and bidentate directing groups, respectively. Examples of commonly used monodentate and bidentate directing groups that are structurally different are shown in Figure 1.2.^{34,36,37}

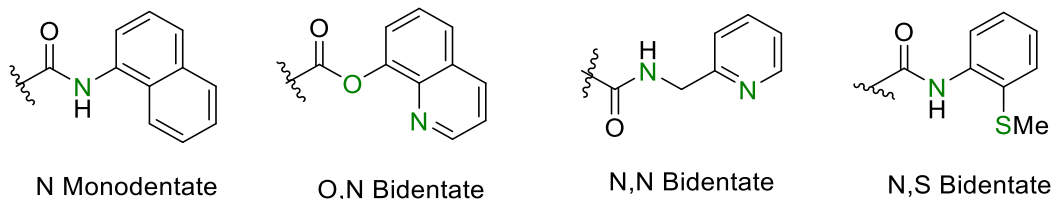
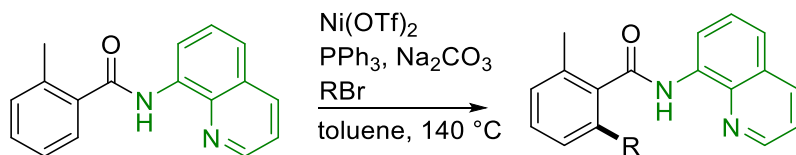


Figure 1.2. Different directing groups commonly used in catalysis involving CMD.

Many Ni(II) catalyzed reactions involving the CMD pathway have utilized directing groups. Direct alkylation by activating ortho C(sp²)-H bonds in an aryl ring and subsequent C-C bond formation with alkyl halides were studied using Ni(II) catalysts (Scheme 1.16). The study analyzed the effect of different monodentate and bidentate directing groups coordinating through different atoms on the catalytic activity. The 8-aminoquinoline moiety gave the best outcome, possibly due to the stronger binding of the substrate compared to other chelating groups.³⁸ The utilization of the bidentate chelation strategy by directing groups leads to tighter substrate binding, enhancing the C-H bond activation reaction.³⁹ N,N bidentate 8-aminoquinoline directing group is a commonly used group in many Ni(II) mediated catalytic studies.⁴⁰

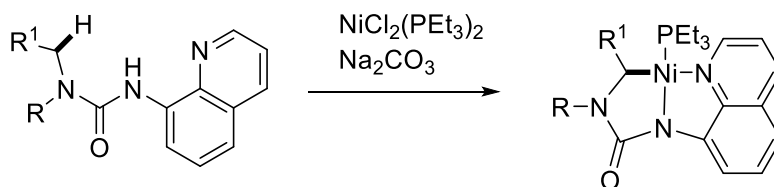


Scheme 1.16. Alkylation of C(sp²)-H bonds in aromatic amides with alkyl halides by Chatani (The 8-aminoquinoline directing group is highlighted in green).

1.5.4 Types of C-H bonds that Undergo CMD

C-H bonds can be classified into different types based on different factors. Based on the hybridization of the carbon atom connected to the hydrogen atom it can be classified as C(sp³)-H, C(sp²)-H, and C(sp)-H bonds. Both C(sp²)-H and C(sp³)-H bonds undergo activation through the CMD pathway. Catalytic reactions with C(sp²)-H activation are commonly found. But C(sp³)-H catalyzed reactions are quite rare due to the low polarity of these bonds and selectivity issues. These issues can be overcome by the utilization of directing groups and appropriate ligand designs.

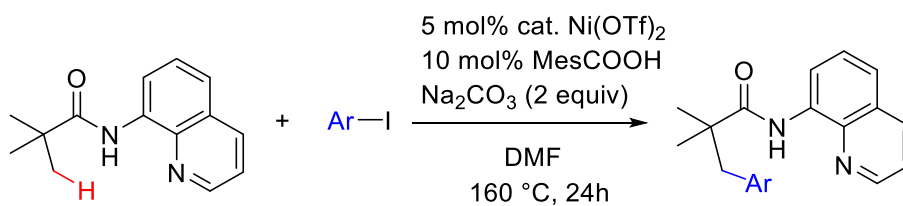
C(sp³)-H bonds can be further categorized as primary, secondary, and tertiary bonds based on the number of carbons bonded to the C atom. Beattie *et al* were able to mechanistically study the Ni(II) mediated C(sp³)-H activation by using 8-aminoquinoline substituted ureas as model systems, and they were able to isolate the products from both primary and secondary C(sp³)-H activation (Scheme 1.17).⁴¹ The studies showed that tertiary C(sp³)-H bonds cannot be activated due to steric limitations, whereas the secondary C(sp³)-H can be activated but at a slower rate relative to the primary C(sp³)-H bonds. The benzyl substrates (i.e. R¹ = aryl) with electron rich aryl rings had activation rates comparable to the primary C(sp³)-H bonds activation, which was proposed due to stronger agostic C-H interactions that were favoured by increased C-H electron density.



Scheme 1.17. Primary and secondary C(sp³)-H bond activation using Ni(II) complex by Beattie *et al.* (R¹ = H, alkyl or aryl group)⁴¹

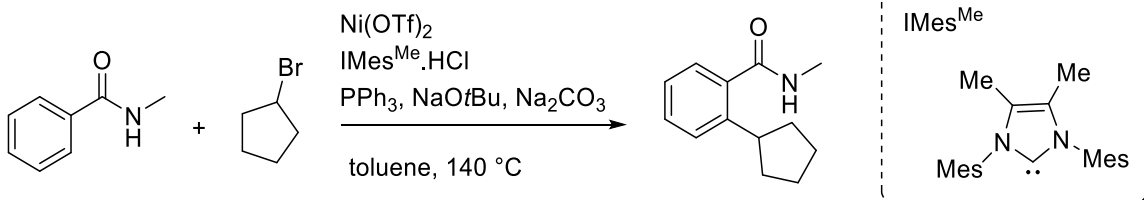
1.5.5 Catalytic Ni(II) Reactions Involving CMD

Recently there has been a significant interest in nickel complexes as a catalyst due to its wide availability and inexpensive nature in comparison to other metals such as Pd, Ir and Rh.⁴² It can activate both C(sp³)-H and C(sp²)-H bonds via a CMD mechanism and carry out catalysis reactions.⁴³ Chatani *et al.* were able to perform a direct arylation reaction using Ni(II) catalyst by activating methyl and methylene C(sp³)-H bonds, in the presence of a bidentate directing group and Na₂CO₃ as the base for deprotonation (Scheme 1.18). These reactions showed good compatibility with different functional groups on the aryl halide.³⁷



Scheme 1.18. Ni(II) catalyzed direct arylation by activating C(sp³)-H, proposed by Chatani in 2014.

The Chatani group also developed a Ni-NHC catalyst system with PPh₃ for intermolecular alkylation of secondary halides and arenes by activating C(sp²)-H bonds in the presence of N,N bidentate directing group (Scheme 1.19). The addition of the NHC ligand IMes^{Me} was essential for the formation of the product, although its exact role in the reaction mechanism is still under study.⁴⁴



Scheme 1.19. Amide directed Ni-NHC catalyzed C(sp²)-H alkylation.

1.6 Scope of Thesis

Using the above-mentioned studies on Ni(II) mediated aerobic oxidation reactions, an ideal catalytic reaction can be proposed to provide a cheaper and more environmentally friendly way to obtain carbonyl products. By investigating the reactivity of Ni(II)-OH towards CMD mediated C(sp³)-H activation this could be achieved. Hence, the primary focus of this project is to establish a synthetic route to a stable monomeric Ni(II)-OH complex whose reactivity towards allylic C(sp³)-H bond activation can be investigated. The C-H activation reaction could hypothetically complete the proposed catalytic cycle depicted in Figure 1.3a. The first goal of the project is to synthesize the proposed tridentate NHC ligand design (Figure 1.3b) inspired from a known Ni-Br complex by Wang *et al.*⁴⁵ The ligand is hypothesized to stabilize the reactive Ni(II)-OH monomer from dimerization, which is undesirable. The ligand design consists of: an NHC donor group to increase the electron density of Ni required for O₂ activation; an aryloxy group to enforce a bidentate coordination mode, at minimum; and a hemi-labile picolyl group which will reversibly open/close a coordination site, during and following the C-H bond activation. This stabilized Ni(II)-OH monomer may be basic enough to promote CMD with an allylic C-H bond, producing a Ni(allyl) species and the byproduct water. The second goal is promoting a CMD mediated C(sp³)-H activation through a hydroxo base by utilizing a directing group on the allylic substrate. Formation of a Ni-OH moiety from an allyl ligand consisting of an 8-aminoquinoline directing group will be targeted and its reactivity will be explored.

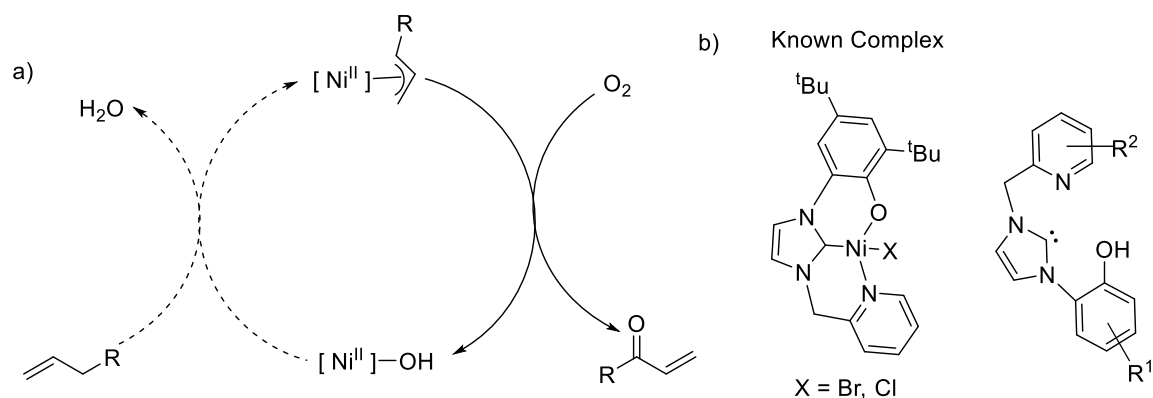


Figure 1.3. a) Proposed catalytic cycle involving the monomeric Ni(II)-OH intermediate. b) Proposed tridentate NHC ligand design inspired by known Ni(II)-halide complex to prevent dimerization of Ni(II)-OH monomer.

1.7. References

- (1) Shi, Z.; Zhang, C.; Tang, C.; Jiao, N. *Chem. Soc. Rev.* **2012**, *41* (8), 3381–3430.
- (2) Nakamura, A.; Nakada, M. *Synth.* **2013**, *45* (11), 1421–1451
- (3) Chen, H.; Jiang, H.; Cai, C.; Dong, J.; Fu, W. *Org. Lett.* **2011**, *13* (5), 992–994.
- (4) Shi, Z.; Zhang, C.; Tang, C.; Jiao, N. *Chem. Soc. Rev.* **2012**, *41* (8), 3381–3430.
- (5) Punniyamurthy, T.; Velusamy, S.; Iqbal, J. *Chem. Rev.* **2005**, *105* (6), 2329–2363.
- (6) Scheuermann, M. L.; Goldberg, K. I. *Chem. Eur. J.* **2014**, *20* (45), 14556–14568.
- (7) Ye, X.; Johnson, M. D.; Diao, T.; Yates, M. H.; Stahl, S. S. *Green Chem.* **2010**, *12* (7), 1180–1186.
- (8) Osterberg, P. M.; Niemeier, J. K.; Welch, C. J.; Hawkins, J. M.; Martinelli, J. R.; Johnson, T. E.; Root, T. W.; Stahl, S. S. *Org. Process Res. Dev.* **2015**, *19* (11), 1537–1543.
- (9) Shi, Z.; Zhang, C.; Tang, C.; Jiao, N. *Chem. Soc. Rev.* **2012**, *41* (8), 3381–3430.
- (10) Reddy, M. M.; Punniyamurthy, T.; Iqbal, J. *Tetrahedron Lett.* **1995**, *36* (1), 159-162.

- (11) Salavati-Niasari, M. *J. Mol. Catal. A Chem.* **2007**, *272* (1–2), 207–212.
- (12) Kieber-Emmons, M. T.; Riordan, C. G. *Acc. Chem. Res.* **2007**, *40*, 618–625.
- (13) Dible, B. R.; Sigman, M. S. *J. Am. Chem. Soc.* **2003**, *125* (4), 872–873.
- (14) Dible, B. R.; Sigman, M. S.; Arif, A. M. *Inorg. Chem.* **2005**, *44* (11), 3774–3776.
- (15) Drago, R. S. *Coord. Chem. Rev.* **1992**, *117* (C), 185–213.
- (16) Hazlehurst, R. J.; Hendriks, S. W. E.; Boyle, P. D.; Blacquiere, J. M. *ChemistrySelect* **2017**, *2* (23), 6732–6737.
- (17) Park, Y. J.; Cook, S. A.; Sickerman, N. S.; Sano, Y.; Ziller, J. W.; Borovik, A. S. *Chem. Sci.* **2013**, *4* (2), 717–726.
- (18) Powell-Jia, D.; Ziller, J. W.; Dipasquale, A. G.; Rheingold, A. L.; Borovik, A. S. *A Dalton Trans.* **2009**, *16*, 2986–2992.
- (19) Huang, D.; Holm, R. H. *J. Am. Chem. Soc.* **2010**, *132* (13), 4693–4701.
- (20) Sivaramakrishna, A.; Suman, P.; Goud, E. V.; Janardan, S.; Sravani, C.; Sandeep, T.; Vijayakrishna, K.; Clayton, H. S. *J. Coord. Chem.* **2013**, *66* (12), 2091–2109.
- (21) Khake, S. M.; Chatani, N. *Chem.* **2020**, *6* (5), 1056–1081.
- (22) Altus, K. M.; Love, J. A. *Commun. Chem.* **2021**, 1–4.
- (23) Rogge, T.; Kaplaneris, N.; Chatani, N.; Kim, J.; Chang, S.; Punji, B.; Schafer, L. L.; Musaev, D. G.; Wencel-Delord, J.; Roberts, C. A.; Sarpong, R.; Wilson, Z. E.; Brimble, M. A.; Johansson, M. J.; Ackermann, L. *Nat. Rev. Methods Primers* **2021**, *1* (1), 43.
- (24) Lapointe, D.; Fagnou, K. *Chem. Lett.* **2010**, *39*, 1118–1126.
- (25) Beattie, D. D.; Bowes, E. G.; Drover, M. W.; Love, J. A.; Schafer, L. L. *Angew Chem.* **2016**, *128* (42), 13484–13489.
- (26) Bernskoetter, W. H., Schauer, C. K., Goldberg, K. I. & Brookhart, M. *Science* **2009**, *326*, 553–556.

- (27) Ackermann, L. *Chem. Rev.* **2011**, *111*, 1315–1345.
- (28) Biswas, B.; Sugimoto, M.; Sakaki, S. *Organometallics* **2000**, *19* (19), 3895–3908.
- (29) Campeau, L. C.; Parisien, M.; Jean, A.; Fagnou, K. *J. Am. Chem. Soc.* **2006**, *128* (2), 581–590.
- (30) Ruan, Z.; Ghorai, D.; Zanoni, G.; Ackermann, L. *Chem. Commun.* **2017**, *53* (65), 9113–9116.
- (31) Harry, N. A.; Saranya, S.; Ujwaldev, S. M.; Anilkumar, G. *Catal. Sci. Technol.* **2019**, *9* (8), 1726–1743.
- (32) Ess, D. H.; Nielsen, R. J.; Goddard, W. A.; Periana, R. A. *J. Am. Chem. Soc.* **2009**, *131* (33), 11686–11688.
- (33) Najafian, A.; Cundari, T. R. *Organometallics* **2018**, *37* (18), 3111–3121.
- (34) Zarkadoulas, A.; Zgouleta, I.; Tzouras, N. v.; Vougioukalakis, G. C. *Catalysts* **2021**, *11*(5), 554
- (35) Hartwig, J. F.; Larsen, M. A. *ACS Cent. Sci.* **2016**, *2* (5), 281–292.
- (36) Rousseau, G.; Breit, B. *Angew. Chem. Int. Ed.* **2011**, *50* (11), 2450–2494.
- (37) Aihara, Y.; Chatani, N. *J. Am. Chem. Soc.* **2014**, *136*, 898–901.
- (38) Aihara, Y.; Chatani, N. *J. Am. Chem. Soc.* **2013**, *135* (14), 5308–5311.
- (39) Tang, H.; Zhou, B.; Huang, X. R.; Wang, C.; Yao, J.; Chen, H. *ACS Catal.* **2014**, *4* (2), 649–656.
- (40) Omer, H. M.; Liu, P. *J. Am. Chem. Soc.* **2017**, *139* (29), 9909–9920.
- (41) Beattie, D. D.; Grunwald, A. C.; Perse, T.; Schafer, L. L.; Love, J. A. *J. Am. Chem. Soc.* **2018**, *140* (39), 12602–12610.
- (42) Ananikov, V. P. *ACS Catal.* **2015**, *5* (3), 1964–1971.

- (43) Gandeepan, P.; Müller, T.; Zell, D.; Cera, G.; Warratz, S.; Ackermann, L *Chem. Rev.* **2019**, *119* (4), 2192–2452.
- (44) Zhao, Q.; Meng, G.; Nolan, S. P.; Szostak, M. *Chem. Rev.* **2020**, *120* (4), 1981–2048.
- (45) Yang, D.; Dong, J.; Wang, B. *Dalton Trans.* **2018**, *47* (1), 180–189.

Chapter 2

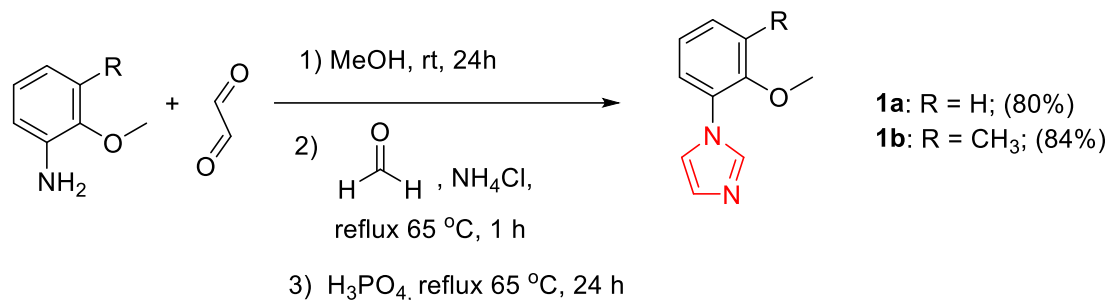
Metalation of NHC Ligand and Attempts at the Formation of Ni(II)-OH Monomer

2.1 Synthesis of Bifunctional Tridentate NHC Ligand

The synthesis of the NHC ligands used in this study involved three major steps: formation of imidazole, installation of the picolyl group, and deprotection. The preparation follows known procedures for closely related compounds which have *t*-butyl groups in the 2- and 4- positions of the aryl ring.¹ The next few sections will explain how each molecule was synthesized, highlighting important aspects of the reactions, including yields and purity.

2.1.1 Imidazole Synthesis

1-(2-Methoxyphenyl)-imidazole (**1a**) and 1-(2-methoxy-3-methylphenyl)-imidazole (**1b**) were synthesized following a three-step procedure from previously published work with modifications made to the equivalents of formaldehyde and NH₄Cl used and the purification step, which included the chromatography.² The product identities were confirmed using ¹H NMR spectroscopy where all peaks matched the reported values. Notably, the diagnostic imidazolium peak was observed at 7.81 and 7.85 ppm for **1a** and **1b**, respectively. No further purification was required, as the NMR spectra did not show any prominent impurity peaks. Both the compounds were formed as dark brown oils with a yield of 80% for compound **1a** and 84% for compound **1b** (Scheme 2.1).

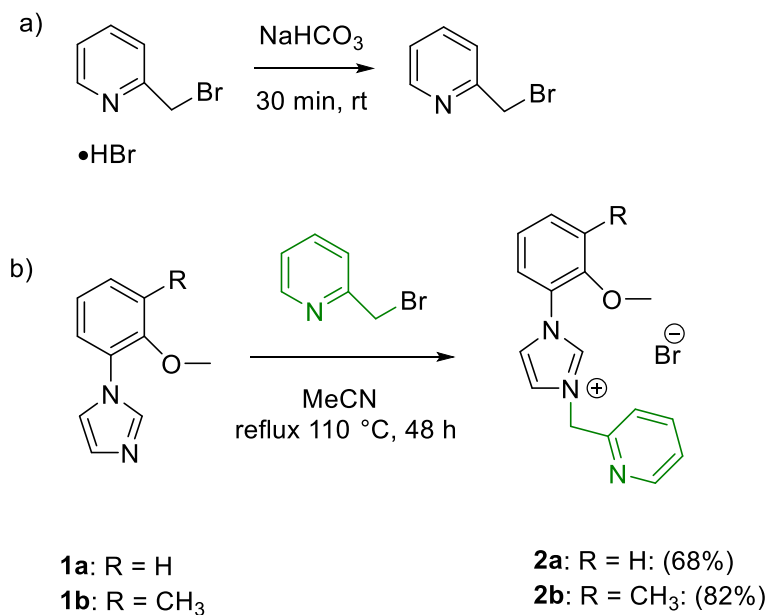


Scheme 2.1. Synthesis of 1-(2-methoxyphenyl)-imidazole (**1a**) and 1-(2-methoxy-3-methylphenyl)-imidazole (**1b**). Isolated yields are given in parentheses.

2.1.2 Picolyl Group Installation

The next step involved the installation of a picolyl group to compounds **1a** and **1b** using 2-(bromomethyl)pyridine. The picolyl precursor was obtained by neutralizing 2-(bromomethyl)pyridine hydrobromide with saturated NaHCO_3 , based on a published procedure (Scheme 2.2a).³ A bright pink product was obtained, which was immediately used for the next reaction.

The neutralized 2-(bromomethyl)pyridine was refluxed in acetonitrile with **1a** or **1b** for 48 hours (Scheme 2.2b). This procedure was obtained from the literature of a closely related compound having a hydroxy group instead of a methoxy group and *t*-butyl substituents in the *ortho* and *para* positions relative to OMe of the aryl group.¹ The purification step was changed by excluding column chromatography and instead removing the impurities by filtration.¹ The resulting sticky orange-brown solid, obtained after concentrating under vacuum, was confirmed to be the expected product 1-(2-pyridinylmethyl)-3-(2-methoxyphenyl)-imidazolium bromide (**2a**). The ^1H NMR spectrum in $\text{DMSO}-d_6$ showed all the expected peaks and the characteristic methylene peak at 5.67 ppm. 1-(2-Pyridinylmethyl)-3-(2-methoxy-3-methylphenyl)-imidazolium bromide (**2b**) was obtained as a brown oily solid with its diagnostic methylene peak at 6.39 ppm in the ^1H NMR spectrum (Figure A1).



Scheme 2.2. a) Neutralization of 2-(bromomethyl)pyridine hydrobromide to 2-(bromomethyl)pyridine and b) Synthesis of 1-(2-pyridinylmethyl)-3-(2-methoxyphenyl)imidazolium bromide (**2a**) and 1-(2-pyridinylmethyl)-3-(2-methoxy-3-methylphenyl)imidazolium bromide (**2b**). Isolated yields are given in parentheses.

2.1.3 Deprotection

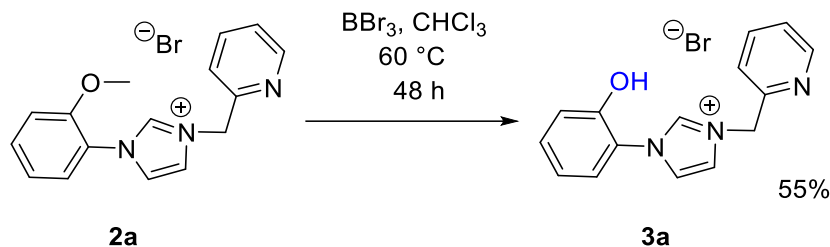
The final step of ligand synthesis was the deprotection of the methoxy group on the imidazolium bromide **2a**. 1-(2-Pyridinylmethyl)-3-(2-methoxy-3-methylphenyl)imidazolium bromide (**2b**) was kept aside for the time being, as it was rationalized it would be better to work with one ligand, optimize its metalation first and then explore the other, as they have very similar chemical properties.

This step was the most challenging step, as the deprotecting reagent must not be too harsh that it results in the decomposition of **2a**. When the deprotection was attempted with 8.9 M HBr following a reported literature procedure,⁴ it resulted in the decomposition of the molecule according to the NMR spectroscopy results.

BBr₃ was selected as the most appropriate deprotecting agent as it is a good demethylating agent for ether cleavage.⁵ The deprotection of the ligand using BBr₃ was carried out,

following a previously published procedure for a different molecule with modifications in the number of BBr_3 equivalents used and the workup steps.⁶ The insolubility of the ligand after the addition of BBr_3 in DCM was one of the major problems faced during the reaction as it resulted in very low yields. This was likely due to the formation of an adduct, formed by the coordination of BBr_3 with the N atom of the picolyl group in **2a** that may have prevented further reaction of BBr_3 with the ether.⁷ To overcome this issue, a solvent with a higher boiling point than DCM was chosen to provide the energy required to cleave the B-N adduct. Based on various attempts and considering the solubility of **2a**, the reaction was successfully done in chloroform at 60 °C for 48 hours (Scheme 2.3). The ^1H NMR spectrum of the crude material in $\text{DMSO-}d_6$ showed the disappearance of the methoxy peak at 3.96 ppm indicating successful deprotection. There was also a broad peak observed with variable chemical shift values, which may have been due to the acid byproduct. To remove this acid and yield the clean ligand, several neutralization attempts were made with various bases (triethylamine, sodium bicarbonate, and sodium hydroxide), and finally, NH_3 a weak base was chosen. After removing the ammonium salts via filtration by dissolving the ligand in DCM, the ligand was isolated in a 55% yield.

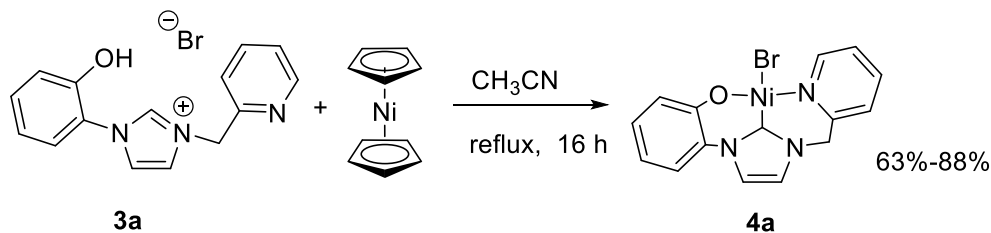
The ligand **3a** was characterized by ^1H and $^{13}\text{C}\{^1\text{H}\}$ NMR spectroscopy, IR, and high-resolution mass spectrometry (HRMS). The ^1H NMR spectrum of compound **3a** exhibited a characteristic singlet at 9.73 ppm for the imidazolium proton (Figure A2), which is consistent with values between 9–10 ppm observed, for similar imidazolium salts.⁸ The ligand **3a** is soluble in CH_2Cl_2 , CHCl_3 , CH_3CN , and MeOH, but insoluble in hexane, THF, and diethyl ether.



Scheme 2.3. Deprotection of 1-(2-pyridinylmethyl)-3-(2-methoxyphenyl)-imidazolium bromide (**2a**) to synthesize 1-(2-pyridinylmethyl)-3-(2-hydroxyphenyl)-imidazolium bromide (**3a**).

2.2 Metalation of Ligand **3a** with Ni to Form Complex **4a**

The tridentate nickel complex **4a** was obtained by the reaction of the corresponding NHC ligand **3a** with 1.1 equiv of nickelocene ($\text{Ni}(\text{Cp})_2$) in CH_3CN at reflux for 16 hours. Brown solids in 63-88% isolated yields were obtained after washing with diethyl ether and DCM (Scheme 2.4). This procedure was followed based on a formerly published work with changes made to the duration of the reaction and the workup, which required a DCM/ether wash instead of column chromatography.¹



Scheme 2.4. Metalation of ligand **3a** with Ni(II) to form **4a** complex.

The nickel complex **4a** is air and moisture stable. It is completely soluble in MeOH, DMF, and DMSO, partially soluble in CH_2Cl_2 and CH_3CN , but, insoluble in THF, CHCl_3 , hexane, and diethyl ether. The evidence for the formation of the complex was indicated by the ^1H and $^{13}\text{C}\{^1\text{H}\}$ NMR spectroscopy. In the ^1H NMR spectrum, the signal of the imidazole proton at the C-2 position at 9.73 ppm and the hydroxy peak at 10.93 ppm of ligand **3a** disappeared completely. In addition, the methylene peak shifted from 5.67 ppm to 5.64 ppm. All the aromatic signals shifted as well when compared to **3a** (Figure 2.1). The IR

spectrum of **4a** had a broad peak at 3377 cm^{-1} indicating a hydroxy stretch, this may have been due to the possibility of water being present in the sample during the DCM/ether wash or coordination of moisture with **4a** when exposed to the atmosphere.

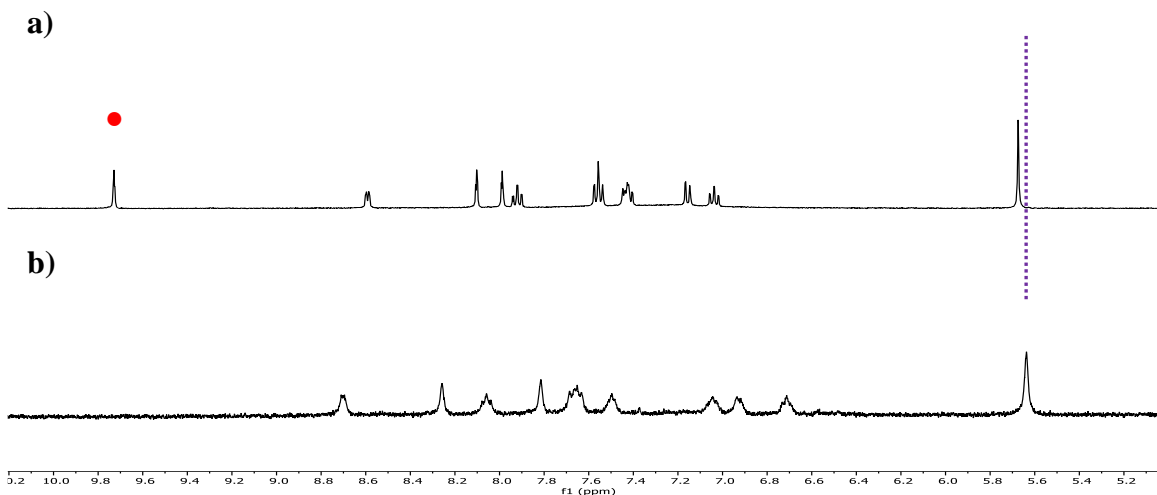


Figure 2.1. ^1H NMR spectra stack plot of a) **3a** in $\text{DMSO-}d_6$ and b) **4a** in $\text{DMSO-}d_6$. Red dot (●) indicates the imidazolium peak on the ligand which disappears after metalation with Ni to form the **4a** complex. The purple dotted line indicates the slight upfield shift in the methylene signal of **4a** relative to **3a**.

The Ni complex **4a** was also analyzed by MALDI MS using a pyrene matrix (Figure 2.2). The mass spectrum showed no evidence of a signal for the molecular cation, but a major signal was found that had a m/z value and isotope pattern consistent with a fragment of the molecular ion $[\mathbf{4a}-(\text{Br})-(\text{H})]^{*+}$ (Figure 2.2 inset). This confirmed that the NHC is indeed coordinated to the metal center even though the bromide coordination was not observed. Literature data of related complexes also show ESI-MS peaks without the halide, this is likely due to the loss of the bromide during ionization.¹ A m/z value at 695 and isotope pattern denote the possibility of a monodentate Ni(II) bis-ligated complex as shown in Scheme 2.5. This was ruled out by carrying out a reaction with two equivalents of ligand **3a** and NiCp_2 under standard reaction conditions. The ^1H NMR spectrum of that reaction indicated a mixture of products being formed including the excess unreacted ligand **3a** and signals corresponding to complex **4a** (Figure 2.3). Therefore, the reaction requires only one

equivalent of **3a** to form **4a**, indicating a monoligated complex. **4a** was further treated with NEt_3 to confirm if X-type coordination has formed between the phenol group and Ni(II). No reactivity was observed when monitored through ^1H NMR spectroscopy further providing evidence that **4a** is a tridentate monoligated complex.

MALDI-MS (Pyrene matrix)

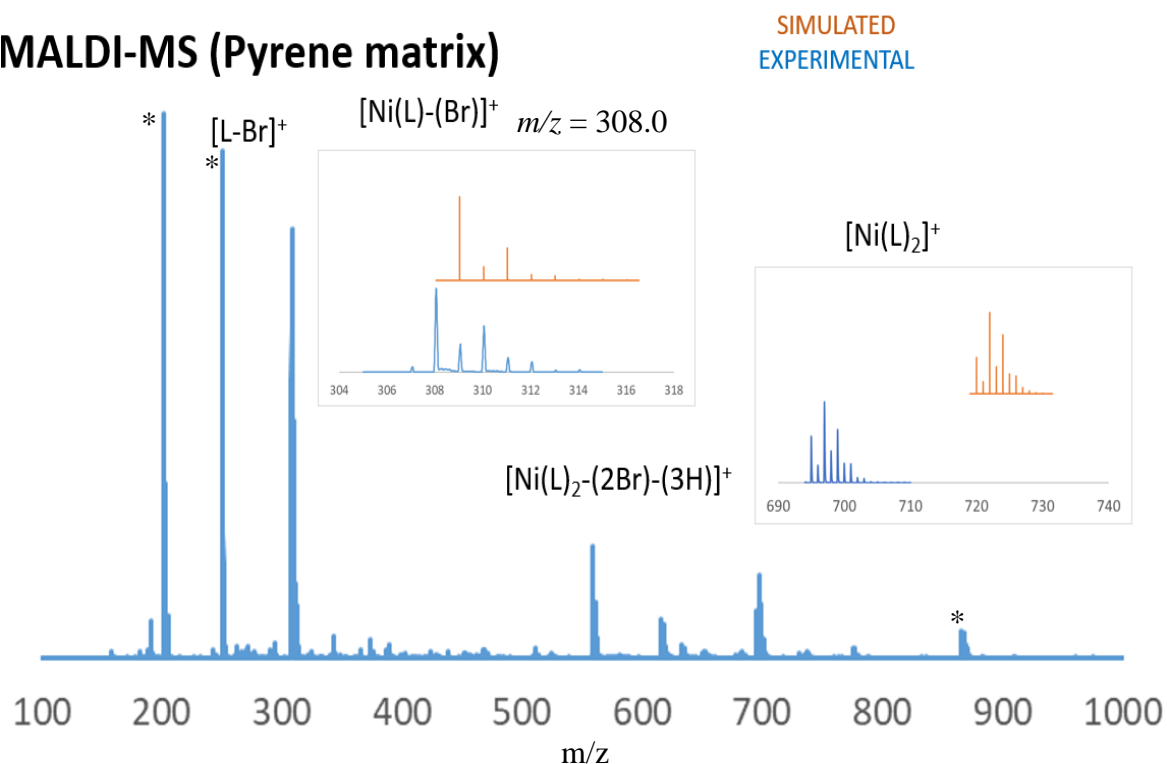
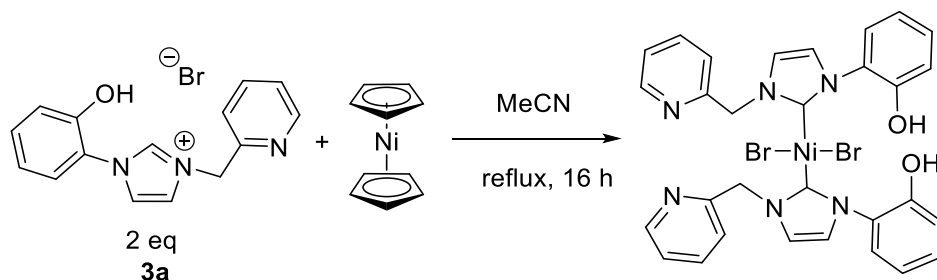


Figure 2.2. MALDI MS of **4a** with pyrene as the matrix. The inset depicts the simulated and observed isotope pattern for the abundant signals. Signals that do not contain Ni (as judged by the isotope pattern) are labeled with an asterisk (*). (L= ligand **3a**)



Scheme 2.5. Possible formation of monodentate bis-ligated Ni(II) complex.

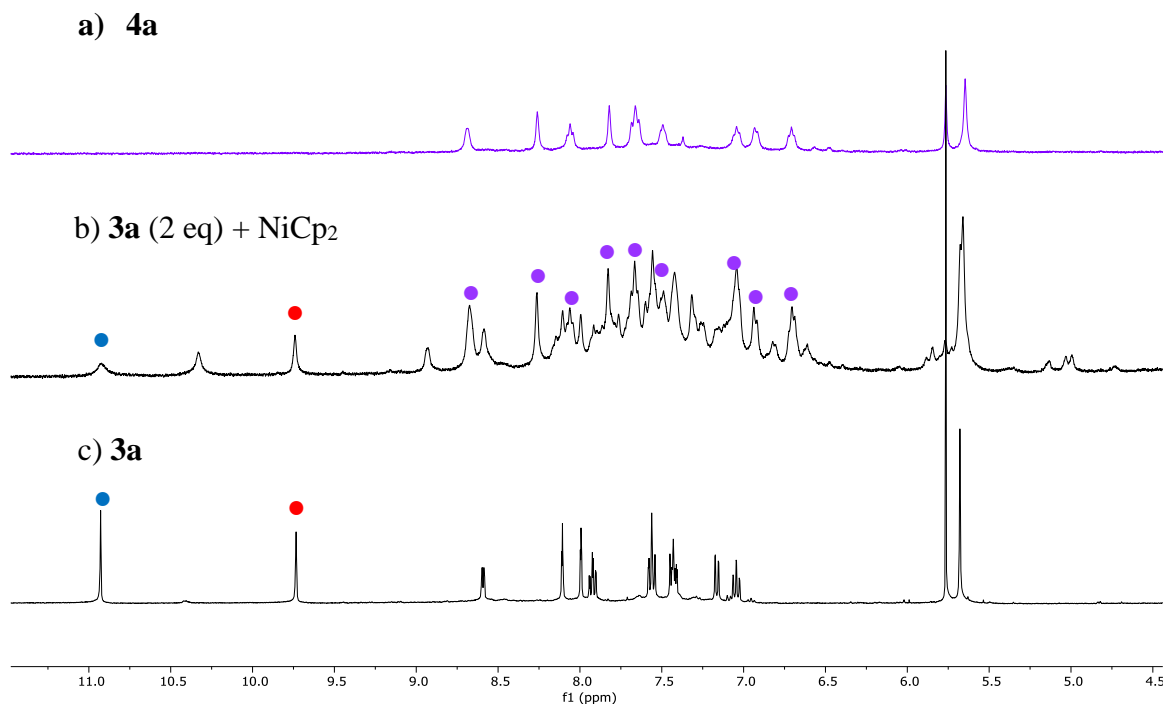


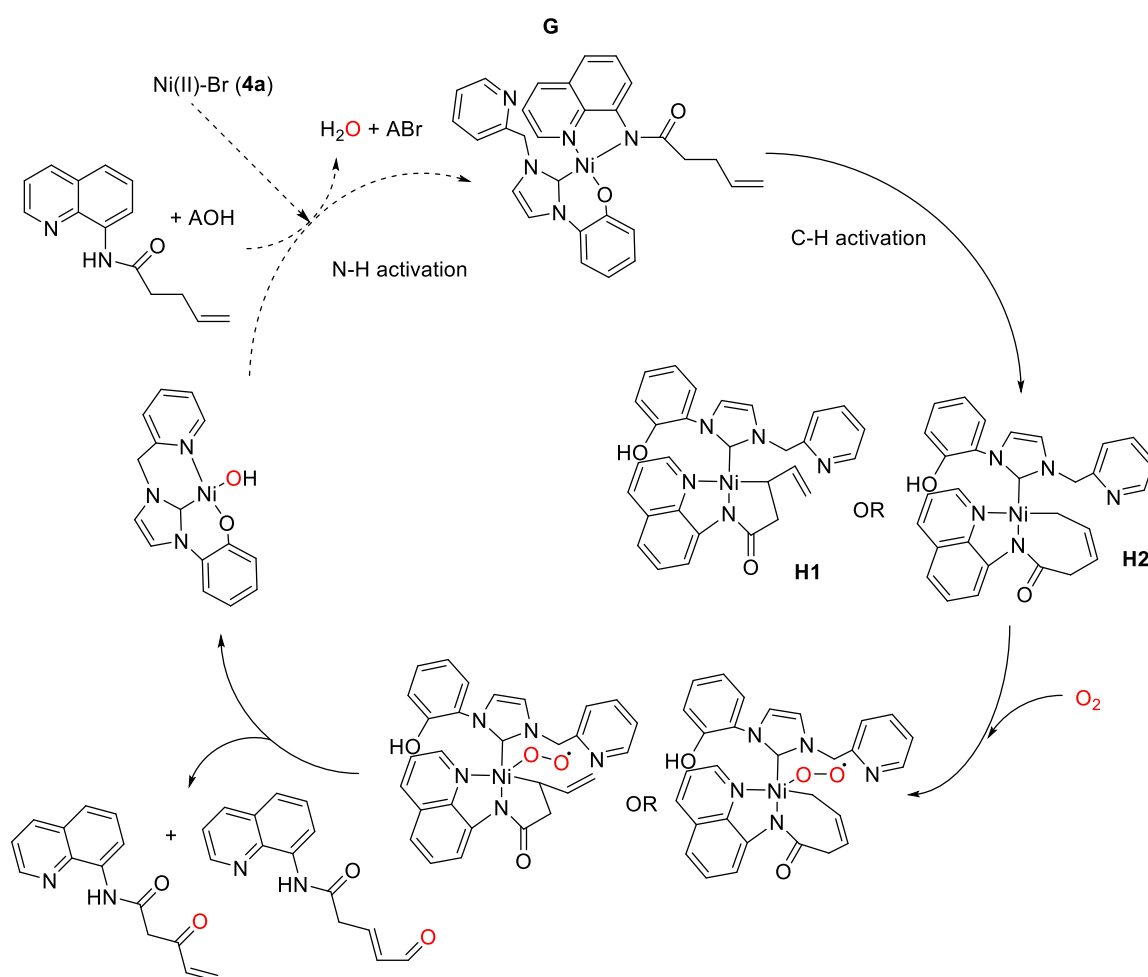
Figure 2.3. ^1H NMR stack plot of a) **4a** b) **3a** (2 equiv) + NiCp_2 under reaction conditions and c) **3a** in $\text{DMSO-}d_6$. Red dot (●) indicates the imidazolium peak and blue dot (●) indicated the hydroxy peak of the ligand. Signals corresponding to **4a** are denoted by purple dots (●).

EA (elemental analysis) was not done due to the inability to get the product free of residual solvents even after extensive drying under vacuum. Several crystallization attempts were carried out involving vapor diffusion and solvent diffusion techniques with no success.

2.3 Attempted Catalytic Aerobic Oxidations with **4a** and *N*-8-quinolinyl-4-pentenamide

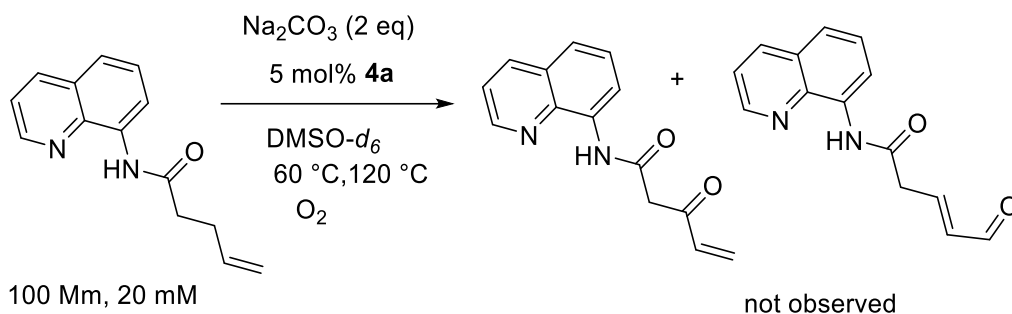
The potential of **4a** to act as a catalyst to facilitate aerobic oxidation of an allylic substrate having a directing group was tested. Theoretically, in the presence of *N*-8-quinolinyl-4-pentenamide (QPAH) and a base, the Ni(II) complex **4a** should coordinate with the substrate through the N,N bidentate 8-aminoquinoline directing group and form complex

G (Scheme 2.6). Complex **G** is hypothesized to activate the allylic C(sp³)-H bond to form a monodentate NHC Ni(II) intermediate **H1** or **H2**. The complex **H1** with a 5-membered metallocycle would be favoured over the 7-membered product **H2** due to the lower ring strain. The oxidation step would occur through a five-coordinate Ni(II) species, which ultimately forms the Ni(II)-OH complex that enters the cycle again and forms the oxidized organic products. The catalytic conditions were assessed under different solvents, temperatures, and the addition of two equivalents of base. Product formation was analyzed by ¹H NMR spectroscopy.



Scheme 2.6. Postulated mechanism for catalytic oxidation of *N*-8-quinolinyl-4-pentenamide utilizing **4a** as catalysts (A = alkali metal)

The initial reactions in DMSO-*d*₆ with Na₂CO₃ at various temperatures and concentrations mentioned in Scheme 2.7 showed no reaction when monitored by ¹H NMR spectroscopy. Deprotonation of the substrate did not occur possibly due to low basicity or poor solubility of Na₂CO₃ in DMSO. This is a possible reason for the absence of catalytic activity, hence catalytic reactions were attempted using different bases with higher basicity/solubility.

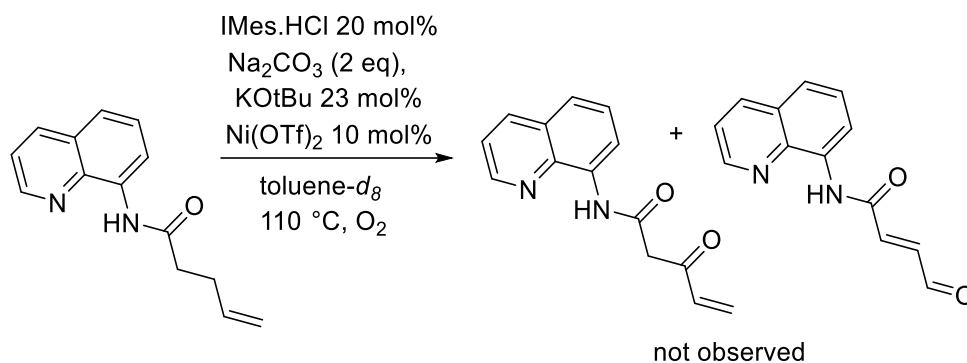


Scheme 2.7. Attempted catalytic aerobic oxidation of *N*-8-quinolinyl-4-pentenamide with **4a**, with conditions tested

Catalysis was attempted in DMSO-*d*₆ at 80 °C using 5 mol% of **4a** using the following bases: KH, NaOH, KOTBu and Cs₂CO₃. Deprotonation of the substrate was observed in the ¹H NMR spectra. However, no new peaks or consumption of the substrate was observed at the time points 1, 4, 24, and 48 hours for the bases KH, NaOH, and Cs₂CO₃. The reaction with KOTBu indicated full consumption of substrate and formation of a new compound in the ¹H NMR spectrum. Control reactions in the absence of the catalyst **4a** yielded similar results indicating that the base KOTBu was reacting with the substrate forming a new compound. Hence no catalytic activity was observed under above tested conditions.

One potential reason for the absence of catalytic activity in the above reaction could be the tridentate coordination mode of the NHC ligand. The presence of multiple coordinating sites at the Ni(II) center might have made the C-H activation step shown in Scheme 2.6 difficult due to steric overcrowding. Hence, a catalytic reaction was attempted by utilizing a monodentate NHC salt under conditions inspired by the catalytic reactions carried out by Chatani and the group (Scheme 2.8).⁹ Ni(OTf)₂ was used as the Ni(II) precursor, and the IMes•HCl salt was deprotonated *in situ* by the KOTBu base to form the monodentate NHC

Ni(II) catalyst. After 24 h when the reaction mixture after filtering through Celite was monitored by the ^1H NMR spectroscopy no catalytic turnover was observed. This indicated that the absence of catalytic activity with **4a** was likely not due to the limited availability of coordinating sites.

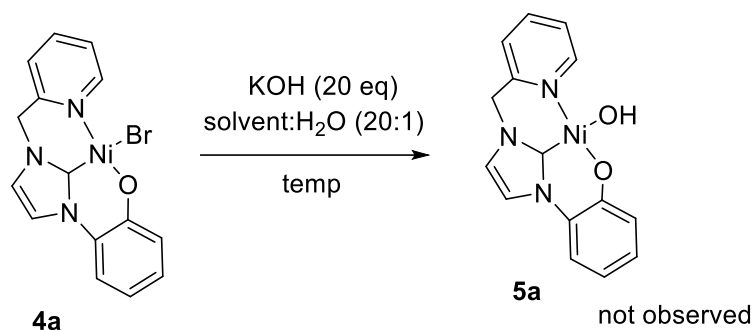


Scheme 2.8. Attempted catalytic aerobic oxidation of *N*-8-quinolinyl-4-pentenamide with monodentate NHC Ni(II) catalyst and the expected products.

2.4 Conversion of **4a** to Ni(II)-OH monomer **5a**

2.4.1 Attempted Synthesis with KOH

The first attempt to form a Ni(II)-OH complex **5a** from **4a** was carried out using an excess of strong base KOH based on previously established procedures^{10,11} with changes made to the solvent system used. A mixed solvent system of DCM, THF, or DMSO and H₂O at a ratio of 20:1 was used to enhance the solubility of both the complex and the base. Sonication of **4a** with KOH at temperatures varying from 25 to 70 °C was conducted (Scheme 2.9). The obtained ^1H NMR spectra had many unknown peaks with no aryl or methylene peaks indicating the possibility of decomposition. Hence, this attempt was considered unsuccessful.

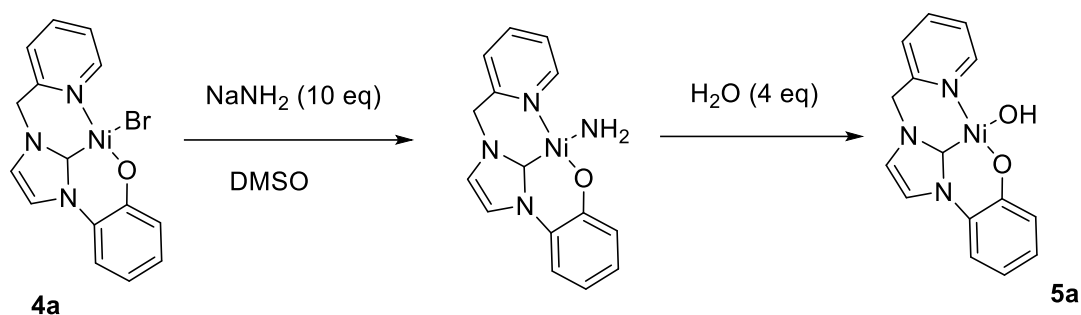


Scheme 2.9. Reaction of **4a** with KOH, at variable solvent systems (DCM, THF, and DMSO) and temperatures (from room temperature gradually increased to 70 °C).

2.4.2 Attempted Synthesis via a Ni-Amido Complex

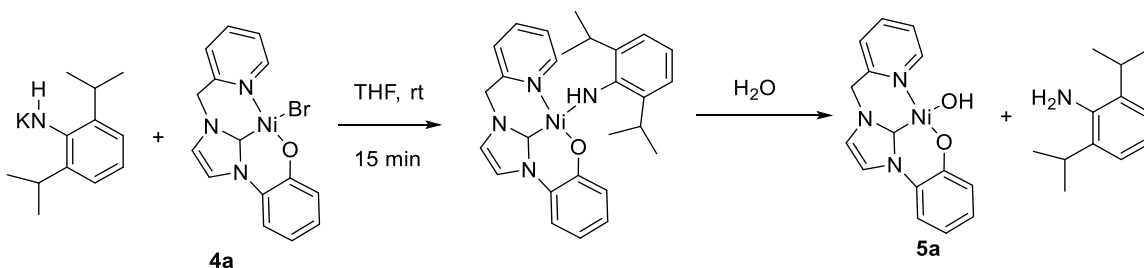
Since the above-mentioned experiments did not result in the successful formation of a Ni(II)-OH complex **5a**, a new route to achieve this product was considered. Based on published procedures,^{11,12} by forming a Ni(II) amido complex followed by conversion to the hydroxide Ni(II) complex by reaction with H₂O.

First, an attempt to synthesize the **5a** complex through a Ni(II)-NH₂ was carried out. The reaction was done on a small scale, using DMSO-*d*₆ as the solvent to monitor the progress of the reaction through ¹H NMR spectroscopy. **4a** was exposed to an excess of NaNH₂, followed by the addition of H₂O at room temperature (Scheme 2.10). The methylene peak observed at 5.64 ppm for the **4a** complex shifted giving rise to two peaks at 5.47 ppm and 5.34 ppm after NaNH₂ addition. With the water addition, a single peak at 5.34 ppm was observed when kept overnight. The aryl peaks were also shifted when compared to the **4a** ¹H NMR spectrum. Though these observations indicated the occurrence of a reaction, characterization of the new product was unsuccessful due to the inability to isolate the pure product. The solubility of the **4a** complex is limited to very polar, high boiling point solvents such as DMSO and DMF, hence the reactions were conducted in these solvents resulting in difficulty of removal.



Scheme 2.10. Reaction of **4a** with NaNH_2 followed by H_2O addition.

To improve the solubility of the hypothetical Ni(II) amido and make the isolation of the complex easier, an organoamide with *iPr* groups was used to make the new Ni(II) amido complex. Two equivalents of KNHAr ($\text{Ar} = 2,6\text{-}^i\text{Pr}_2\text{C}_6\text{H}_3$) were added to **4a** in dried THF and a reaction was observed in 15 mins (Scheme 2.11). The ^1H NMR spectrum in $\text{DMSO-}d_6$ indicated complete disappearance of the signals corresponding to the KNHAr compound, and the new set of signals had similar shifts to 2,6-diisopropyl aniline (Figure 2.4b). The methylene peak of **4a** at 5.67 ppm disappeared and two new broad peaks at 4.93 and 4.50 ppm appeared after the benzene wash, indicating a change in the Ni(II) complex (Figure 2.4c).



Scheme 2.11. Proposed reaction of **4a** with KNHAr ($\text{Ar} = 2,6\text{-}^i\text{Pr}_2\text{C}_6\text{H}_3$) in THF

The formation of 2,6-diisopropyl aniline was not expected at this point of the reaction and indicated the possibility of two scenarios. First, **4a** might be protonated resulting in the deprotonation by KNHAr and formation of 2,6-diisopropyl aniline. The second possibility being Ni(II)- NHAr formed and deprotonated the H_2O present in the solvent resulting in aniline formation. In this case, the anticipated Ni(II)-OH complex would be observed. The later scenario was more likely hence it was assumed that the Ni(II)-OH complex was

formed. Attempts on the purification of the product were conducted, but due to the inability to remove any remaining KNHAr and other unknown impurities another synthetic route was explored.

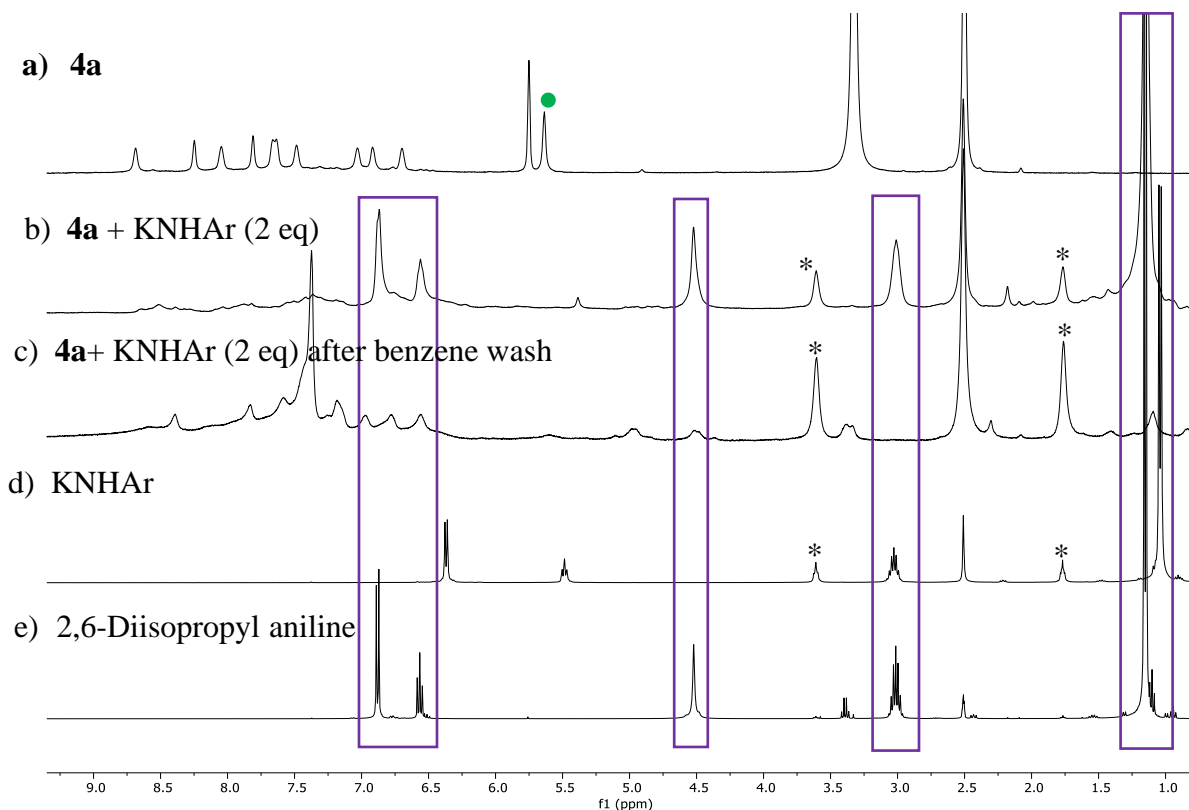


Figure 2.4. ¹H NMR stack plot of a) **4a** b) **4a** + KNHAr (2 eq) c) **4a** + KNHAr (2 eq) after washing with benzene to remove aniline d) KNHAr and e) 2, 6-diisopropyl aniline all taken in DMSO-*d*₆. Green dot (●) indicates the methylene peak of **4a**, which has disappeared after the addition of KNHAr. The purple boxes highlight the similarity of amide signals formed in **4a** + KNHAr reaction to diisopropyl aniline. (THF is denoted by ‘*’)

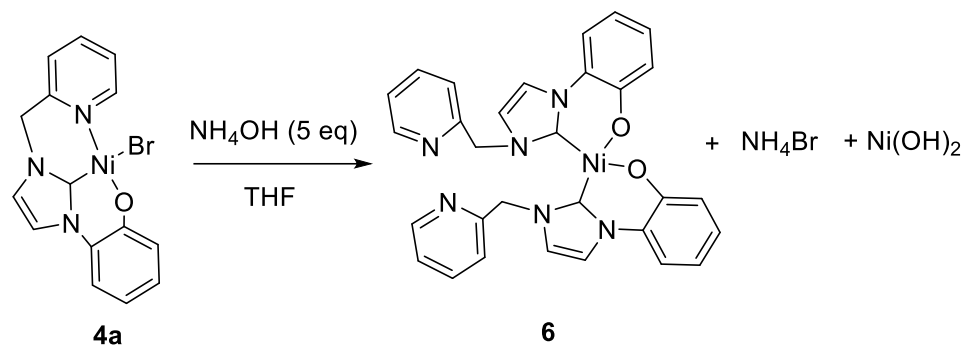
2.4.3 Attempted Synthesis with NH₄OH

An alternative route to form the Ni(II)-OH monomer without side reactions was considered. Et₄NOH has been utilized in the formation of Ni(II)-OH in literature.¹³ Preliminary studies were done to see if this route was promising using NH₄OH. Excess NH₄OH (28-30% volume in H₂O, 10 equiv.) was added to **4a** in THF and DCM separately at room temperature and left to stir for 24 hours. Immediately after the addition of NH₄OH,

the formation of a sticky red-brown precipitate was observed in both reaction flasks. The ^1H NMR spectra of both reactions after filtering out the precipitate and taken in $\text{DMSO-}d_6$ indicated the formation of aryl signals different from **4a** and the formation of two new signals at 4.93 and 4.51 ppm similar to what was observed in the above reaction with **4a** + KNHAr (Section 2.4.2). The reaction done in DCM had a better yield (71%), but had many unknown signals, whereas the reaction in THF had a yield of 50% with very few unknown peaks. The observation of similar signals in the ^1H NMR spectra from both reactions with KNHAr and NH_4OH with **4a** was promising as it indicated the formation of similar products. Hence, characterization of the formed product **6** was carried out.

2.5 Synthesis and Characterization of Complex **6**

Complex **6** was synthesized using a single step, where NH_4OH (28-30% volume in water, 5 equiv.) was added to a Schlenk flask containing **4a** with dry THF and was left to stir overnight at room temperature (Scheme 2.12). The obtained brown solid had a yield of 50% after filtering out the sticky brown solids assumed to be NH_4Br and $\text{Ni}(\text{OH})_2$, which were formed right after NH_4OH addition. The complex was insoluble in toluene, hexane, and diethyl ether, but dissolved in DCM, chloroform, MeCN, DMF, and DMSO.



Scheme 2.12. Formation of **6** by reacting **4a** with NH_4OH in THF.

Although the NMR spectroscopy data provided the evidence of the formation of a new Ni(II) complex, they do not indicate the exact coordination of atoms. Hence, there is a need to prove this structure by X-ray crystallography.

An X-ray quality crystal of **6** was obtained by layering hexanes into a solution of **6** in DCM which was analyzed by X-ray diffraction (Figure 2.5). The obtained data confirmed the structure of complex **6** in the solid state, showing a monometallic Ni complex with a nickel atom coordinated to two aryloxy-NHC ligands to form a distorted square-planar geometry with a τ_4 value of 0.2286. A *cis* arrangement is observed around the Ni atom, with the two NHC ligands in the adjacent position. The crystal data and structure refinement parameters for complex **6** are summarized in Table A1 displayed in the appendices and the selected bond length and bond angles are depicted in Table 2.1. A comparison of the bond parameters for the nickel-ligand bonds to related literature complex **7** which have *t*-butyl groups in their *ortho* and *para* positions of the aryl ring shows close correlation (Figure 2.6 and Table 2.1).^{1,14} The Ni–C_(NHC) bonds (1.8491(12) and 1.8613(12) Å) for **6** are similar to the bis ligated Ni–C bond in Ni(II) aryloxy NHC complex **7** synthesized by Wang (1.833(3) and 1.866(3) Å).

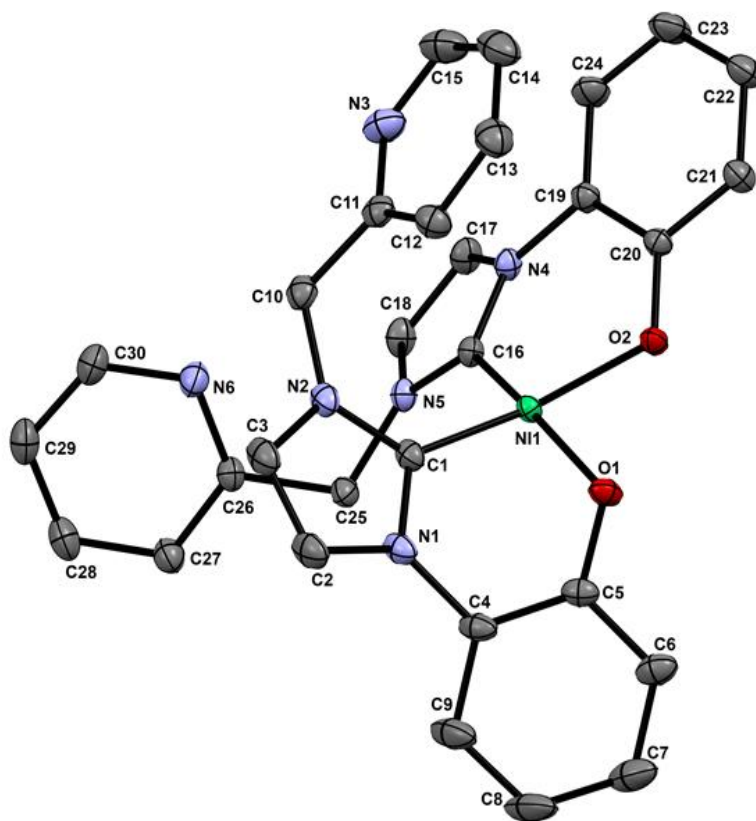


Figure 2.5. Thermal ellipsoid plot drawing of **6** showing naming and numbering scheme for selected atoms of interest. Ellipsoids are at the 50% probability level and hydrogen atoms were omitted for clarity.

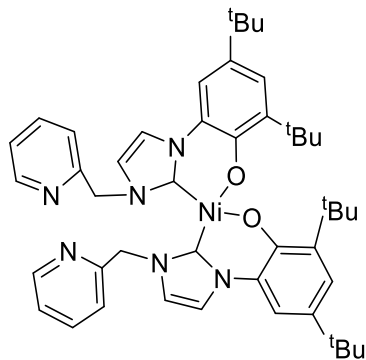


Figure 2.6. Complex **7** synthesized by Wang et al. analogous to **6**¹

Table 2.1. Selected bond lengths (Å) and bond angles (°) for solid-state structures of **6** and **7**.¹

Bond	6	7 ¹
Ni(1)-C(1)	1.8491(12)	1.833(3)
Ni(1)-C(16)	1.8613(12)	1.866(3)
Ni(1)-O(1)	1.8901(10)	1.885(2)
Ni(1)-O(2)	1.8771(10)	1.886(2)
C(16)-Ni(1)-C(1)	97.88(6)	97.19(14)
O(1)-Ni(1)-O(2)	85.30(5)	86.88(10)
C(1)-Ni(1)-O(1)	89.39(6)	89.53(12)
C(16)-Ni(1)-O(2)	91.22(5)	90.07(12)

The numbers listed for **7** are for the analogous bonds, but the labels do not correspond to the reported structure for that compound.

The Ni complex **6** was further characterized by ESI-MS using DCM as the solvent. The resulting spectrum, showed evidence of a signal for **[6-H]**⁺ (Figure 2.7). Thus, providing

further evidence of the coordination of two NHC ligands to the metal. Another signal was identified with a m/z value and isotope pattern that is consistent with a fragment of the molecular ion, $[\mathbf{6}\text{-NHC ligand}]^+$.

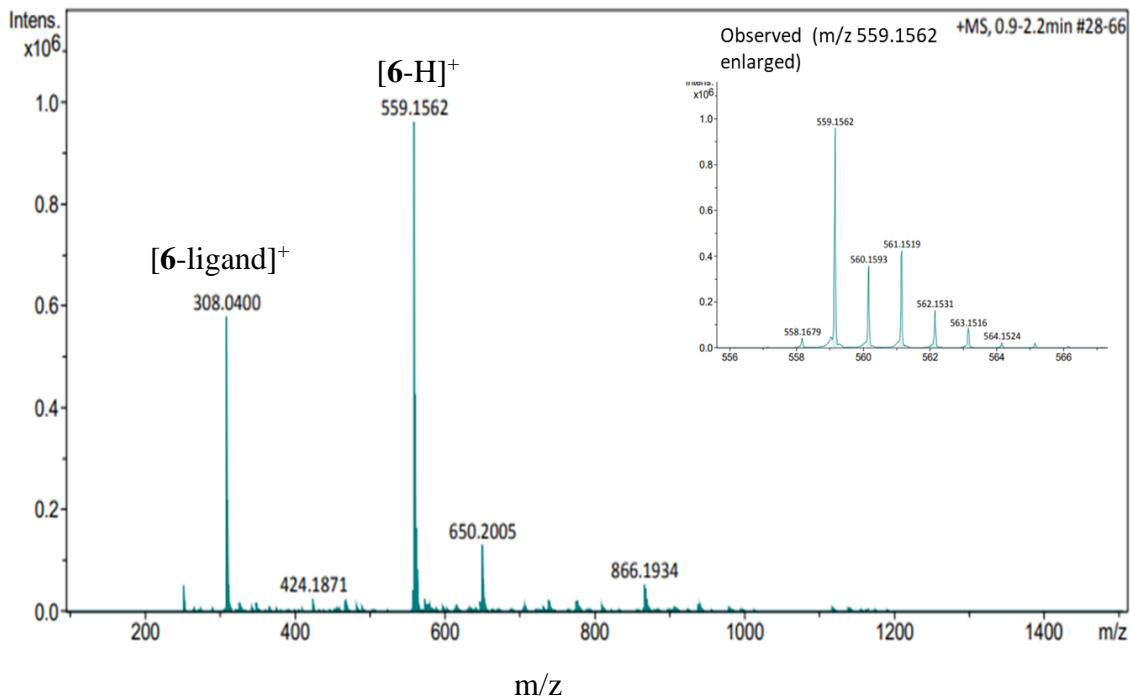
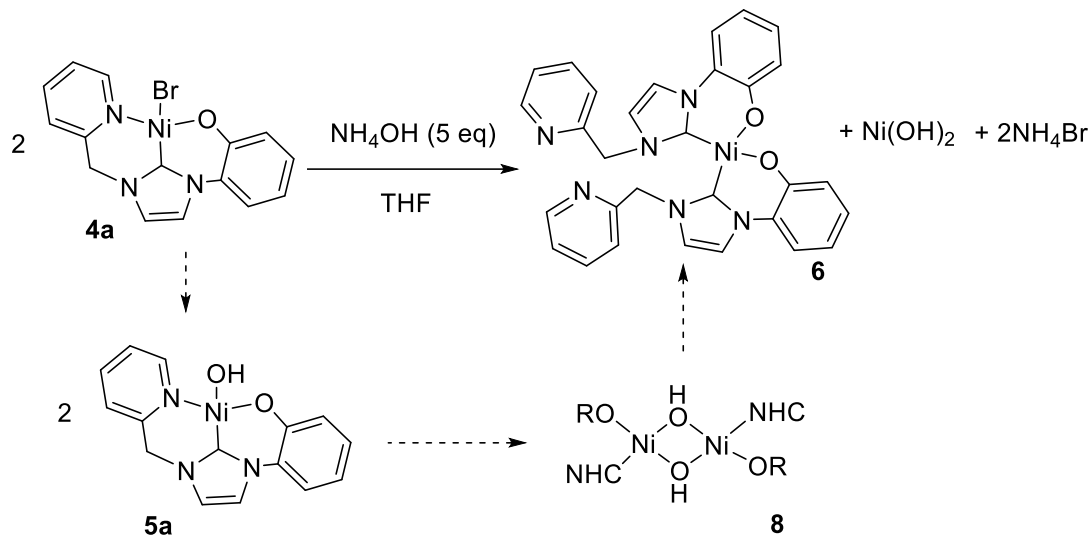


Figure 2.7. ESI-MS of **6** with DCM as the solvent. The inset depicts the observed isotope pattern for the most abundant signal.

The ^1H NMR spectrum of the bis-ligation reaction indicated the presence of a mixture of products even after the removal of the NH_4Br and $\text{Ni}(\text{OH})_2$ by-products. Through HSQC and HMBC NMR spectroscopy the presence of two compounds was determined: complex **6** (53 mass%) and the mono cationic **3a** ligand. The formation of the mono cationic ligand **3a** was due to the water present in the 28-30% NH_4OH reagent which might have protonated the hydroxy group of **3a**. Several washing and crystallization attempts were carried out to remove the mono cationic ligand **3a** to yield pure **6**, but no success was achieved due to similar solubility profiles of both the compounds.

Based on the above results, it can be hypothesized that the formation of complex **6** is due to the instability of the $\text{Ni}(\text{II})\text{-OH}$ monomer **5a** which immediately upon formation undergoes dimerization leading to the formation of **6**. The proposed pathway for the

formation of the bidentate bis-ligated complex **6** through the Ni(II)-OH monomer (**5a**) and dimer (**8**) is shown in Scheme 2.13.

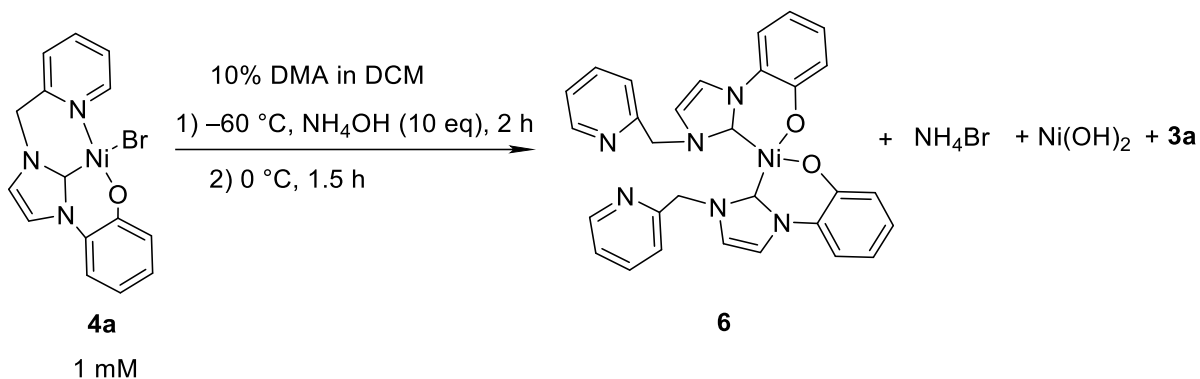


Scheme 2.13. Proposed pathway for the formation of bis ligated Ni(II) complex **6**.

2.6 Low Temperature UV-vis study to Determine **4a** + NH_4OH Reaction Intermediates

From the above section, it was found that at room temperature the attempts to convert the NHC complex **4a** to **5a** forms the bis-ligated complex **6**. A potential pathway was proposed for the formation of complex **6** which involves the Ni(II)-OH monomer and dimer intermediates (Scheme 2.13). To gain a better handle on the pathway, low temperature studies were conducted to attempt to trap out reaction intermediates. The expected intermediates are **5a** and **8** that are potentially unstable at room temperature and are anticipated to have better stability at lower temperature.

Low temperature UV-vis spectroscopy studies were performed in order to determine temperature ranges that would allow for trapping of the reaction intermediates. The experiments were conducted using a 1 mM solution of **4a** in 10% DMA in DCM to make **4a** fully soluble in the solvent. UV-vis spectra were obtained at various temperatures and times after NH_4OH (28-30%_{vol} in water, 10 equiv.) addition (Scheme 2.14).



Scheme 2.14. General reaction scheme for low temperature UV-Vis experiments.

Upon cooling **4a** to $-60 \text{ }^\circ\text{C}$ there was no change in the UV-vis spectrum compared to room temperature. After NH_4OH addition to **4a** at $-60 \text{ }^\circ\text{C}$, an immediate, but minor, change to the absorption spectra was observed with in 30 seconds and remained constant by 0.5 h. During the reaction, the UV-vis spectrum showed a decrease in the absorbance compared to the spectrum before NH_4OH addition (Figure A15). An isosbestic point was observed indicating potential formation of a single intermediate.

During subsequent studies to determine the basicity of the formed potential intermediate, it was observed that the phenolphthalein was not miscible with the reaction solution below $0 \text{ }^\circ\text{C}$. Rather it remained as a layer, presumably because the NH_4OH was not soluble at lower temperature due to the presence of water. Hence, the change observed above could not be due to reactivity between NH_4OH and **4a**. The changes observed in the UV-vis spectra could be due to temperature fluctuations.

Upon warming of the mixture of **4a** and NH_4OH to $-15 \text{ }^\circ\text{C}$ the UV-vis spectrum remained constant and when further warmed to $0 \text{ }^\circ\text{C}$ it showed a rapid change for nearly 1 h. There was no observed isosbestic point, which suggests that intermediate does not cleanly convert one species at $0 \text{ }^\circ\text{C}$. There were no further spectral changes observed above $0 \text{ }^\circ\text{C}$, even with continued warming up to room temperature ($20 \text{ }^\circ\text{C}$). As there was no further reactivity observed, it was presumed that the products formed at $0 \text{ }^\circ\text{C}$ are the bis-ligated complex **6** with its by-products (NH_4Br , Ni(OH)_2 and deprotonated **3a**) that were studied previously

by room temperature ^1H NMR spectroscopy and X-ray crystallography studies (Section 2.5). The reaction likely proceeded rapidly at $0\text{ }^\circ\text{C}$ due to melting of water in the base reagent and then reaction with Ni.

2.7 Preliminary Synthesis of Ni(II) Allyl Complex **9a**

The formation of unreactive **6** should be prevented and the anticipated Ni(II)-OH monomer **5a** must be formed in order to activate allylic C-H bonds. This can be achieved by forming **5a** *in situ* under catalytic conditions which would kinetically disfavor the dimerization due to the lower concentration of the ligand. Hence, the formation of a Ni(II) allyl complex **9a** (Figure 2.8) with the above tridentate ligand design was targeted in order to achieve catalysis.

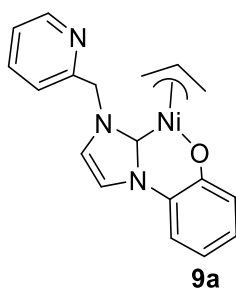
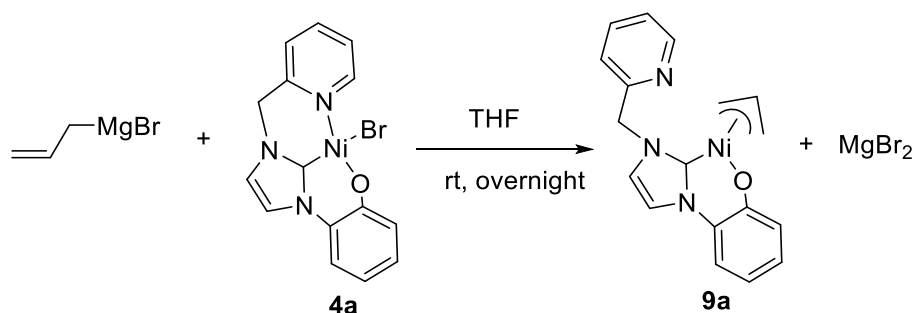


Figure 2.8. Target Ni(II) allyl complex to favour formation of Ni(II)-OH monomer *in situ* for C-H activation.

Previous work on the formation Ni(II) allyl complexes involved a two-step, one pot procedure utilizing free carbenes and Ni(II) allyl halide complexes.^{15,16} Due to the absence of precedence for isolation/use of the free carbene of **3a** ligand, an alternative route was followed to synthesize the target Ni(II) allyl complex.

A Grignard reaction was conducted by reacting allyl magnesium bromide with **4a** overnight at room temperature in THF to form the anticipated Ni(II) allyl complex **9a** (Scheme 2.15). Complex **4a**, which is insoluble in THF dissolved overtime with the addition of Grignard to form a dark brown solution, which gave qualitative evidence for the reaction of **4a** with the Grignard.



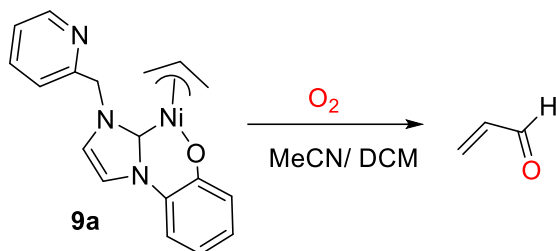
Scheme 2.15. Formation of **9a** by reacting 2-propenyl magnesium bromide with **4a** in THF

The ¹H NMR spectrum of **9a** in common solvents (DMSO-*d*₆, MeCN-*d*₃, DCM-*d*₂ and acetone-*d*₆) indicated broad signals which could be due to the dynamic nature of the molecule. Two high intense peaks corresponding to THF were observed even after keeping the sample under vacuum for 3 days. The coordination of THF molecules to the reaction by-product MgBr₂ is a common occurrence in Grignard reactions based on literature data.¹⁷ Hence, this could have been the reason for the observation of THF peaks in the ¹H NMR spectrum even after intense drying for several days. Removal of the THF coordinated salt was attempted by washing the sample in different solvents such hexane, pentane, toluene, and diethyl ether resulting in no success. A water wash was also attempted under inert conditions to avoid the reaction with molecular oxygen but resulted in **9a** reacting with water/O₂ from the water. Hence new methods to remove the THF coordinated MgBr₂ is still under way. Crystallization of **9a** was attempted through solvent diffusion method utilizing different solvents at room and low temperatures. Due to similar solubilities of both the MgBr₂-THF salt and **9a**, the precipitation of both complexes occurs yielding no success.

2.8 Reactivity of **9a** with Molecular Oxygen

Based on preliminary data, the reactivity of **9a** towards O₂ was tested, despite the fact it was not purified or fully characterized. It was hypothesized that the oxidized organic product formed from the aerobic oxidation of the Ni(II) allyl complex would yield the same outcome as products of closely related complexes by Sigman with the monodentate NHC ligand¹⁵ and the Blacquiere group with the pendant H-bond donor on the NHC ligand.¹⁶

The expected oxidized product was 2-propenal (Scheme 2.16), however, a different result was also a possibility due to the difference in ligand structure.



Scheme 2.16. Reactivity of **9a** with molecular oxygen.

Preliminary aerobic oxidation tests were conducted by exposing a 4 mL vial containing a dark brown solution of **9a** in MeCN/ DCM to ambient air. These tests were done to see if the Ni(II) complexes with the new NHC ligand react with O_2 , as some NHCs used by Sigman were air stable.¹⁸ Upon exposure to the air, a color change of the solution was noted immediately in both solutions from a dark brown solution to greenish-brown solution. It also formed brown precipitates at the bottom of the vial (Figure 2.9). The change in colour indicated the possibility of aerobic oxidation as similar observations were reported in previous studies.¹⁶ To rule out the possibility of reactivity of **9a** with moisture present in the air, new samples of **9a** in DCM and MeCN solvents in NMR tubes were purged with dry molecular oxygen. Similar observations were seen, indicating that water was not involved in the reactivity.

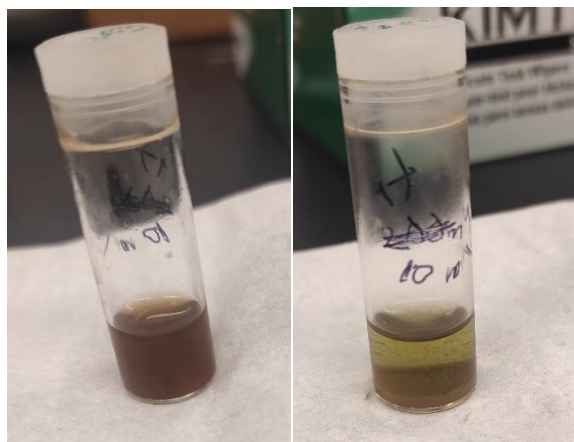
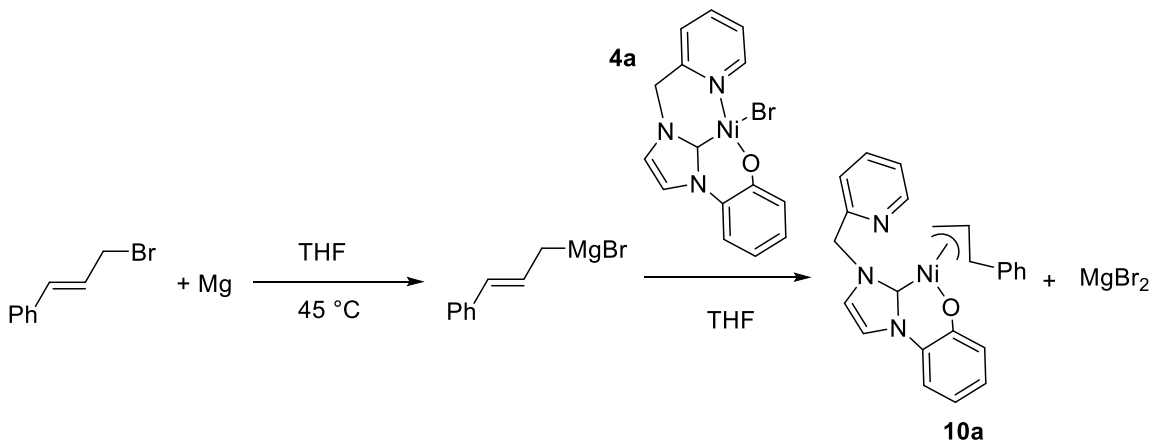


Figure 2.9. Solution of **9a** in MeCN in 4 mL vial. Left picture taken before oxygen exposure, right picture taken 3h after exposure to oxygen.

When the above solution was monitored using ^1H NMR spectroscopy, no new peaks were observed. The absence of peaks corresponding to 2-propenal was expected due to its small molecular size and instability. The obtained precipitates were filtered through Celite, redissolved in $\text{DMSO-}d_6$ and analyzed using ^1H NMR spectroscopy. The obtained ^1H NMR spectrum had peaks overlapping with the ^1H NMR spectrum of the Ni(II) bis ligated complex **6**. This indicated that upon exposure of **9a** to O_2 , it formed **6** as the by product and possibly an oxidized organic product which was not observed. The evidence for the formation of the oxidized organic product would further confirm the occurrence of aerobic oxidation. Hence, a Ni(II) allyl complex which yields stable oxidized organic products was targeted next to confirm the oxidation reaction.

Ni(II) cinnamyl complex would theoretically yield stable oxidized organic products such as cinnamaldehyde and phenyl vinyl ketone. Consequently, attempts for the synthesis of Ni(II) cinnamyl complex **10a** were conducted following the same procedure as above. First the formation of cinnamaldehyde magnesium bromide was attempted by reacting (3-bromo-1-propenyl)benzene with Mg turnings in dry THF overnight at room temperature (Scheme 2.17). Since no qualitative observation indicated any reaction, it was left to stir overnight at $45\text{ }^\circ\text{C}$ for another day. It was then directly added to **4a** and left to stir at room temperature. After stirring for two days at elevated temperatures ($50\text{ }^\circ\text{C}$), no reactivity was

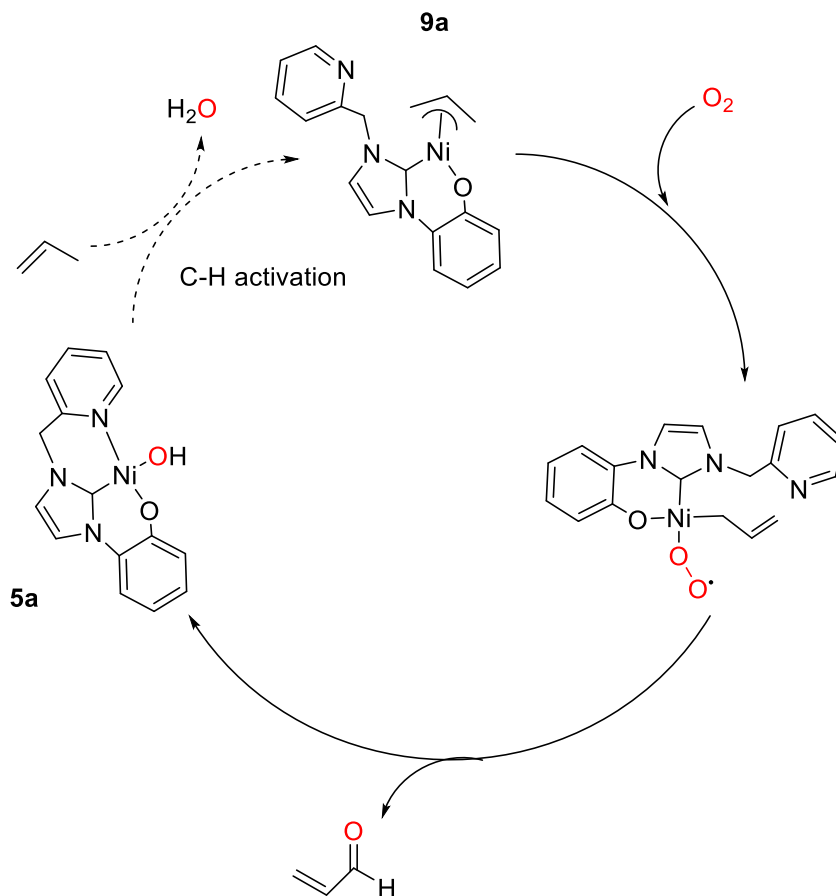
observed based on ^1H NMR spectroscopy data. There are two possible reasons for the absence of reactivity: firstly, the synthesis of cinnamaldehyde magnesium bromide did not occur due to the instability of the compound (no literature precedence for this compound); secondly, the reaction between **4a** and the cinnamaldehyde Grignard reagent simply did not occur under tested conditions.



Scheme 2.17. Cinnamaldehyde Grignard formation by reacting (3-Bromo-1-propenyl) benzene with Mg followed by **4a** addition to form **10a**.

2.9 Attempted Catalytic Aerobic Oxidations with **9a**

The possibility of achieving catalytic turn over using **9a** was explored. The reaction of Ni(II) allyl (**9a**) with molecular oxygen should ideally release the oxidized organic molecules and the Ni(II)-OH monomer **5a**. The Ni(II)-OH intermediate would subsequently need to perform a C(sp³)-H activation on another allylic substrate to regenerate another Ni(II) allyl complex (Scheme 2.18). It is hypothesized that under catalytic conditions, the formation of a Ni(II)-OH dimer **8**, which is assumed to form the unreactive bis ligated complex **6**, will be kinetically prevented due to the low Ni(II) allyl concentration, which is more likely to interact with the substrate than with each other.

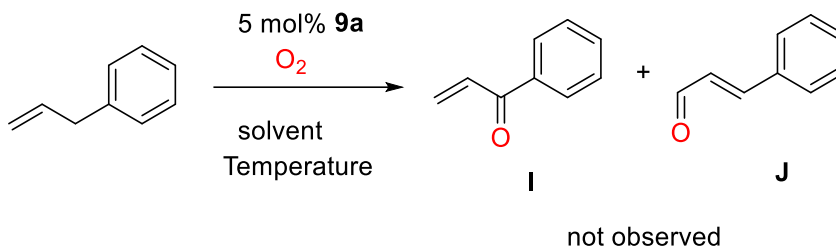


Scheme 2.18. Proposed mechanism for catalytic aerobic oxidation of **9a** through tridentate Ni(II)-OH monomer **5a** intermediate.

It was assumed that the THF coordinated $MgBr_2$ impurity present in the **9a** sample does not affect the catalytic reactivity. The percentage purity of **9a** was calculated to be 45 mass%. The catalytic reactions were carried out using different substrates under different conditions.

2.9.1 Allyl Benzene as a Substrate

Catalytic oxidation of allyl benzene was attempted with 5 mol% of **9a** (Scheme 2.19) and mesitylene as the internal standard. The catalytic conditions were assessed under various solvents, temperatures, and substrate concentrations aiming to increase the chances for catalytic turnover. The product formation was analyzed by 1H NMR spectroscopy.



Scheme 2.19. Attempted catalytic aerobic oxidation of allylbenzene with **9a**, with conditions tested.

The catalytic reaction was first attempted in an NMR tube using 100 mM of allyl benzene in DMSO-*d*₆ at 120 °C (Table 2.2, Entry 1). The brown solution was exposed to dry O₂, and a colour change to light green with brown precipitates was observed, similar to the qualitative observations made during the stoichiometric oxidation of **9a** (Section 2.8). The reaction mixture was then analyzed by ¹H NMR spectroscopy at the following time points: 30 minutes, 1, 4, and 18 hours. Data obtained from this experiment suggested no catalytic activity as no peaks for the expected oxidized products or consumption of substrate was observed. The formation of the bis ligated Ni(II) complex **6** when exposed to O₂ even under catalytic conditions could be a possible reason for the absence of catalytic activity. To overcome this issue several reaction conditions were altered.

The solvent was switched from DMSO-*d*₆ to MeCN-*d*₃ since observed yields in the oxidation stoichiometric reactions for similar Ni(II) allyl complexes utilized by the Blacquiere group were highest for MeCN¹⁶ and MeCN as a coordinating solvent could possibly stabilize a monomer. Secondly, the reaction temperature was attempted at both 80 °C and –40 °C. Other decomposition products may exist due to oxidation of the NHC ligand. Upon lowering the temperature, these competitive decomposition products may become kinetically unfavourable. Lastly, the concentration of allylbenzene was lowered to 20 mM which would theoretically reduce the favourability of dimerization.

Analysis of the reaction mixtures (Table 2.2, Entries 2-5) using ¹H NMR spectroscopy showed no catalytic activity. It can be concluded that the allylic C-H bond activation does

not occur for the conditions listed in Table 2.2 with **9a** as the catalyst and allyl benzene as the substrate.

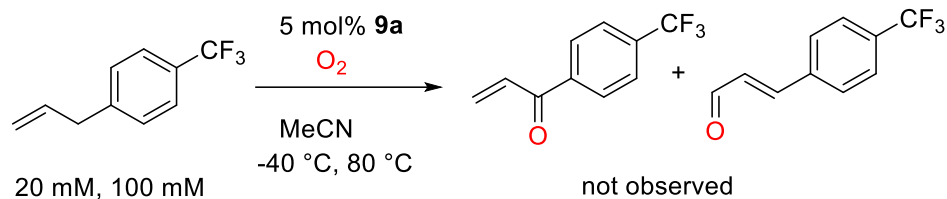
Table 2.2. Conditions screened for attempted catalytic oxidation of allylbenzene.^a

Entry	Concentration of substrate (Mm)	Solvent	Temp. (°C)	% I	% J
1	100	DMSO- <i>d</i> ₆	120	0	.0
2	100	MeCN- <i>d</i> ₃	80	0	0
3	100	MeCN- <i>d</i> ₃	-40	0	0
4	20	MeCN- <i>d</i> ₃	80	0	0
5	20	MeCN- <i>d</i> ₃	-40	0	0

^aConditions: 5 mol% **9a**, and reaction were analyzed by H NMR spectroscopy at 0.5, 1, 4, and 18 hours. The 18 h time point data is provided here. Mesitylene used as internal standard.

2.9.2 Allyl-4-(trifluoromethyl) Benzene as a Substrate

A possible explanation for no catalytic activity of **9a** could be that the C-H bond activation barriers of allyl benzene was too high under tested conditions. Hence, utilizing a different substrate with lower C-H bond activation energies can provide a solution to this issue. 1-Allyl-4-(trifluoromethyl) benzene was chosen as the substrate since it has strongly deactivating CF₃ group in the para position of the phenyl group. The CF₃ weakens the alpha hydrogens and subsequently weakens the C-H bond. The CF₃ group can also provide an NMR handle in which the reaction progress can be monitored via ¹⁹F NMR spectroscopy. The potential catalytic reaction starting from **9a** would generate an equivalent of non-fluorinated products, in addition to the CF₃ derivatives of these products (Scheme 2.20).

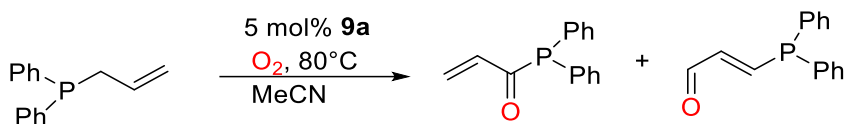


Scheme 2.20. Reaction conditions of aerobic oxidation catalysis of 1-allyl-4-(trifluoromethyl) benzene with **9a** with proposed products.

The conditions mentioned in Scheme 2.20 were tested for the 1-allyl-4-(trifluoromethyl) benzene substrate. The resulting ^{19}F NMR showed one singlet at -62.2 ppm, corresponding to unreacted 1-allyl-4-(trifluoromethyl)benzene. In conclusion, complex **9a** is inactive towards catalysis with 1-allyl-4-(trifluoromethyl) benzene with as the substrate under the tested conditions.

2.9.3 Allyldiphenyl Phosphine as the Substrate

The formation of a C-H agostic interaction (or σ -complex) before C-H activation is an important step.¹⁹ By having a directing group that can coordinate to the Ni(II) center through donor atoms, the formation of the C-H agostic complex can be promoted favouring the activation reaction. Hence, allyldiphenyl phosphine was chosen as the next substrate since it can coordinate to the metal center through the phosphorus atom and form the agostic complex in an intramolecular reaction.



Scheme 2.21. Attempted aerobic oxidation catalysis of allyl diphenyl phosphine with **9a**.

A catalysis attempt was carried out using 5 mol% of **9a** at 80 °C in MeCN with allyl diphenyl phosphine as the substrate and triphenyl phosphine oxide as the internal base (Scheme 2.21). Consumption of the substrate and formation of a new peak at 28 ppm was observed when monitored through $^{31}\text{P}\{^1\text{H}\}$ NMR spectroscopy. A control reaction in the

absence of the catalyst revealed that the substrate oxidized to form a new complex at 28 ppm when exposed to O₂. Hence the usage of allyl diphenyl phosphine as a substrate to test catalytic activity was discontinued.

2.10 Conclusions

A new tridentate bifunctional NHC ligand **3a**, designed to hypothetically stabilize the Ni(II)-OH monomer **5a** was successfully synthesized and characterized following three steps starting from a methoxy aniline precursor. The first two steps involved imidazole synthesis and picolyl installation using modified literature procedures. The final deprotection step, which was done using BBr₃, was optimized by changing the temperature, solvent, and duration of the reaction. Metalation of the synthesized ligand **3a** with Ni to form the Ni(II)-Br complex **4a** was achieved based on preliminary data. The ¹H, ¹³C{¹H} NMR spectroscopy, and IR spectroscopy of **4a** provided evidence of metalation by indicating the disappearance of imidazolium proton peak, the appearance of carbene peak, and the absence of an O-H peak. MALDI and ESI mass spectrometry data confirmed the metalation of Ni with the ligand, although it did not yield a molecular ion for the complete complex. Crystallization of **4a** was not achieved to confirm the exact structure, but ¹H NMR spectroscopic studies confirmed the formation of a tridentate complex. Catalysis attempts to aerobically oxidize an alkenamide substrate QPAH with a bidentate directing group using **4a** as a catalyst were conducted resulting in no success.

Attempts to convert **4a** to Ni(II)-OH monomer **5a** were performed. The first attempt using a strong base such as KOH was deemed unsuccessful based on ¹H NMR spectroscopic results, which had many unknown signals and indicated a possible decomposition of the Ni(II) complex. A different route of synthesizing a Ni(II)-NH₂ complex and reacting it with H₂O to form the Ni(II)-OH in DMF/DMSO was considered. This route although looked promising, was difficult to purify due to the difficulty of removing the DMSO/DMF solvents. Hence a Ni(II)-NHAr (Ar = 2,6-ⁱPr₂C₆H₃) with *i*Pr groups was targeted for better solubility in organic solvents, which are easier to work with. The occurrence of a reaction was indicated by the ¹H NMR spectroscopy when KNHAr (Ar = 2,6-ⁱPr₂C₆H₃) was added

to **4a** in THF giving out 2,6-diisopropyl aniline as a byproduct. Similar product (**6**) formation was observed when **4a** was reacted with NH₄OH (28-30% in water). The obtained product **6** was characterized through X-ray crystallography, ESI-MS, NMR and IR spectroscopy which indicated a bis-ligated Ni(II) complex. The formation of the bis ligated Ni(II) complex **6** was hypothesized due to potential instability of Ni(II)-OH dimer **8** and was proposed to go through a pathway consisting of the Ni-OH intermediates. Low temperature UV-vis studies were conducted to trap any potential intermediates. The studies were unsuccessful due to the immiscibility of the NH₄OH reagent at the temperature range of -60 °C to 0 °C. Hence, the synthesis of an allylnickel NHC complex **9a** with the same ligand design was attempted instead to achieve aerobic oxidation catalysis. Preliminary catalytic studies on **9a** were tested indicating no catalytic activity. The formation of **6** as a precipitate was observed when **9a** was exposed to molecular oxygen, which potentially hindered the catalytic turnover.

2.11 References

- (1) Yang, D.; Dong, J.; Wang, B. *Dalton Trans.* **2018**, 47 (1), 180–189.
- (2) Pratt, D. A.; Pesavento, R. P.; Van Der Donk, W. A. *Org. Lett.* **2005**, 7 (13), 2735–2738.
- (3) Nareddy, P.; Mantilli, L.; Guénée, L.; Mazet, C. *Angew. Chem. Int. Ed.* **2012**, 51 (16), 3826–3831.
- (4) Kirsch, P.; Jakob, V.; Oberhausen, K.; Stein, S. C.; Cucarro, I.; Schulz, T. F.; Empting, M. *J. Med. Chem.* **2019**, 62 (8), 3924–3939.
- (5) Kosak, T. M.; Conrad, H. A.; Korich, A. L.; Lord, R. L. *Eur. J. Org. Chem.* **2015**, 2015 (34), 7460–7467.
- (6) Lu, Q.; Hou, J.; Wang, J.; Xu, B.; Zhang, J.; Yu, X. *Chin. J. Chem.* **2013**, 31 (5), 641–650.
- (7) Collman, J. P.; Yang, Y.; Decréau, R. A. *Org. Lett.* **2007**, 9 (15), 2855–2858.
- (8) Yang, D.; Tang, Y.; Song, H.; Wang, B. *Organometallics* **2016**, 35 (10), 1392–1398.
- (9) Aihara, Y.; Wuelbern, J.; Chatani, N. *Bull. Chem. Soc. Jpn.* **2015**, 88 (3), 438–446.

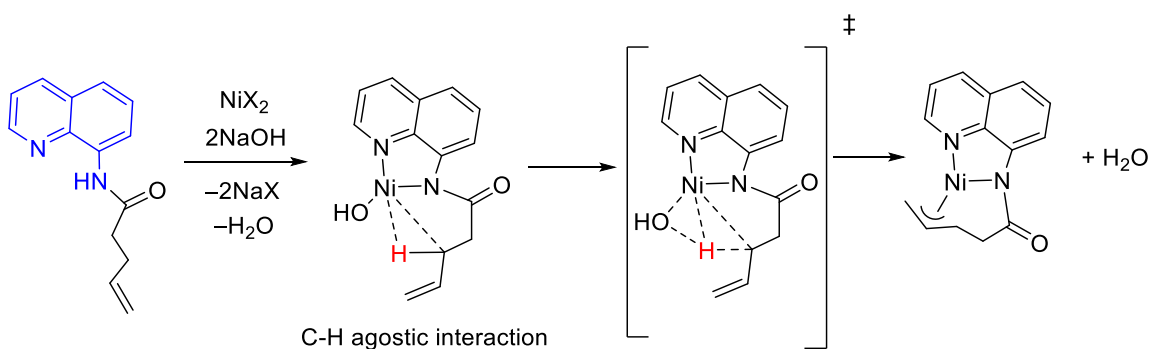
- (10) Cámpora, J.; Palma, P.; Del Río, D.; Álvarez, E. *Organometallics* **2004**, *23* (8), 1652–1655.
- (11) Mousa, A. H.; Bendix, J.; Wendt, O. F. *Organometallics* **2018**, *37* (15), 2581–2593.
- (12) LendeVander, D. D.; Abboud, K. A.; Boncella, J. M. *Inorg. Chem.* **1995**, *34* (21), 5319–5326.
- (13) Huang, D.; Holm, R. H. *J. Am. Chem. Soc.* **2010**, *132* (13), 4693–4701.
- (14) Nirmala, M.; Prakash, G.; Ramachandran, R.; Viswanathamurthi, P.; Malecki, J. G.; Linert, W. *J. Mol. Catal. A Chem.* **2015**, *397*, 56–67.
- (15) Dible, B. R.; Sigman, M. S. *J. Am. Chem. Soc.* **2003**, *125* (4), 872–873.
- (16) Hazlehurst, R. J.; Hendriks, S. W. E.; Boyle, P. D.; Blacquiere, J. M. *ChemistrySelect.* **2017**, *2* (23), 6732–6737.
- (17) Sarnia, R.; Ramirez, F.; Brian McKeever, Ib; Fen Chaw, Y.; James Marecek, Ib F.; Nierman, D.; McCaffrey, T. M. *J. Am. Chem. Soc.* **1977**, *99*, 5285.
- (18) Dible, B. R.; Sigman, M. S. *Inorg. Chem.* **2006**, *45* (20), 8430–8441.
- (19) Altus, K. M.; Love, J. A. *Commun. Chem.* **2021**. 4.1-11.

Chapter 3

Synthesis of 8-Aminoquinoline Derived Allyl Ni(II) Complex for C(sp³)-H Bond Activation Study

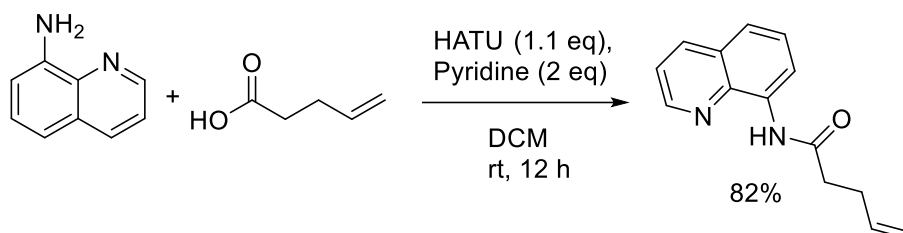
3.1 Reactivity of Ni(II) with *N*-8-Quinolinylnyl-4-pentenamide

The NHC Ni(II)-OH monomer **5a** was proposed to have the ability to activate allylic C(sp³)-H bonds through a CMD pathway promoted by the internal hydroxo base. The experimental results from Chapter 2 indicated the instability of the target tridentate NHC Ni(II)-OH monomer, which resulted in the absence of catalytic activity for aerobic oxidation reactions with various alkene substrates tested under different conditions. Hence, to promote the Ni(II) mediated activation of allylic C(sp³)-H bonds by hydroxo base the new allyl substrate *N*-8-quinolinylnyl-4-pentenamide (QPAH) that include a directing group was chosen instead. The bidentate 8-aminoquinoline directing group of the substrate should theoretically bind to the Ni(II) metal through the N donor atoms and favor the formation of C-H agostic interactions (Scheme 3.1). The agostic interaction is then anticipated to promote the intramolecular CMD pathway through the hydroxo base to cleave the allylic C(sp³)-H bond. Prior reports have shown effective C-H activation leading to functionalization utilizing the 8-aminoquinoline directing group with nickel and carboxylate/carbonate bases.¹⁻⁴



Scheme 3.1. Proposed CMD pathway through deprotonation by a hydroxo base for allylic C(sp³)-H activation using 8-aminoquinoline (denoted in blue) derived allyl substrate.

The QPAH ligand was synthesized following an established synthetic route⁵ with no changes made to any of the steps and the product was purified by column chromatography (Scheme 3.2). The obtained yellow-brown oil was confirmed to be QPAH through ¹H NMR spectroscopy matching reported literature values.

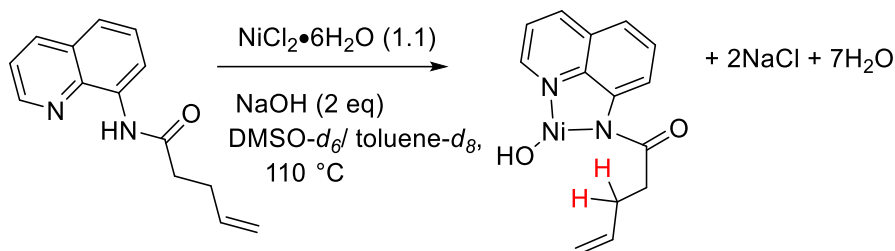


Scheme 3.2. Synthesis of the 8-aminoquinoline derived allyl QPAH. (HATU = hexafluorophosphate azabenzotriazole tetramethyl uronium)

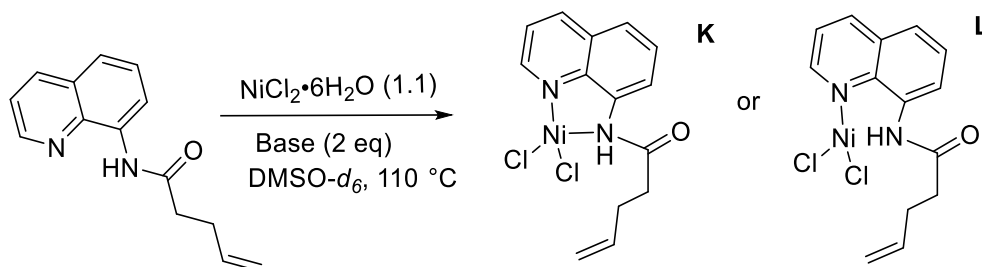
3.1.1 Reactivity of NiCl₂•6H₂O with QPAH

Initial attempts to metalate the *N*-8-quinolinyl-4-pentenamide ligand were conducted using NiCl₂•6H₂O in the presence of NaOH (2 equiv). The reactions were done in DMSO-*d*₆ and toluene-*d*₈ solvents at 110 °C (Scheme 3.3). No reactivity was observed in the ¹H NMR spectrum of the reaction in the toluene-*d*₈ solvent, likely due to the insolubility of the Ni precursor and the base. A colour change from green to dark brown was noted in the reaction in the DMSO-*d*₆ solvent. The ¹H NMR spectrum of the reaction in DMSO-*d*₆ showed slight shifts in the QPAH ligand peaks with the presence of the amide NH peak at 10.25 ppm which was expected to disappear due to the deprotonation by the base and coordination to Ni(II). Extremely broad, low-intense peaks were observed in the region 30-10 ppm outside the diamagnetic region of the ¹H NMR spectrum. The presence of broadened NMR signals outside the diamagnetic region indicated the formation of a new paramagnetic complex or complexes. Further assessment of the ¹H NMR data was not conducted due to the poor quality of the spectrum obtained due to shimming issues caused by the chemistry of the reaction mixture. This indicated the occurrence of three possibilities; 1) Adduct formation between the amide NH and Ni(II) to give **K**; 2) Coordination of Ni(II) to the pyridine N

site of QPAH resulting in a monodentate complex, **L**; or 3) The existence of a potential equilibrium between paramagnetic complex(s) and the QPAH ligand (Scheme 3.4).

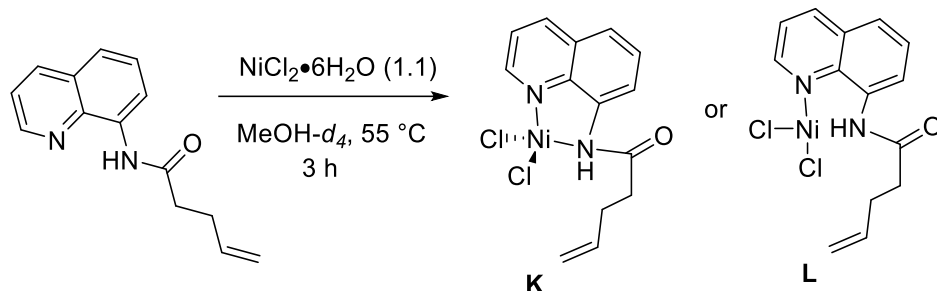


Scheme 3.3. Metalation attempts of Ni(II) with QPAH in DMSO-*d*₆ and toluene-*d*₈ with NaOH and the proposed product.



Scheme 3.4. Proposed potential products from the metalation reaction in DMSO-*d*₆ based on the ¹H NMR spectrum.

To isolate and study further the formed complex, metalation reactions were conducted in methanol solvent, which can be more easily removed due to its lower boiling point compared to DMSO. The addition of NiCl₂·6H₂O to a solution of QPAH in MeOH-*d*₄ in the absence of any base (Scheme 3.5) resulted in large upfield shifts of all the ligand peaks when monitored through ¹H NMR spectroscopy. This indicated successful coordination with Ni(II) (formation of **K** or **L**) or effects of paramagnetism (Figure A9 appendix). Attempts to isolate the formed product were unsuccessful, leading to only the isolation of the ligand QPAH. This could be due to weak Ni(II)-N adduct bond strength, which could have broken during the isolation process. The above reaction in the presence of different bases (NaOH and NEt₃) did not result in any reactivity based on ¹H NMR spectroscopy.

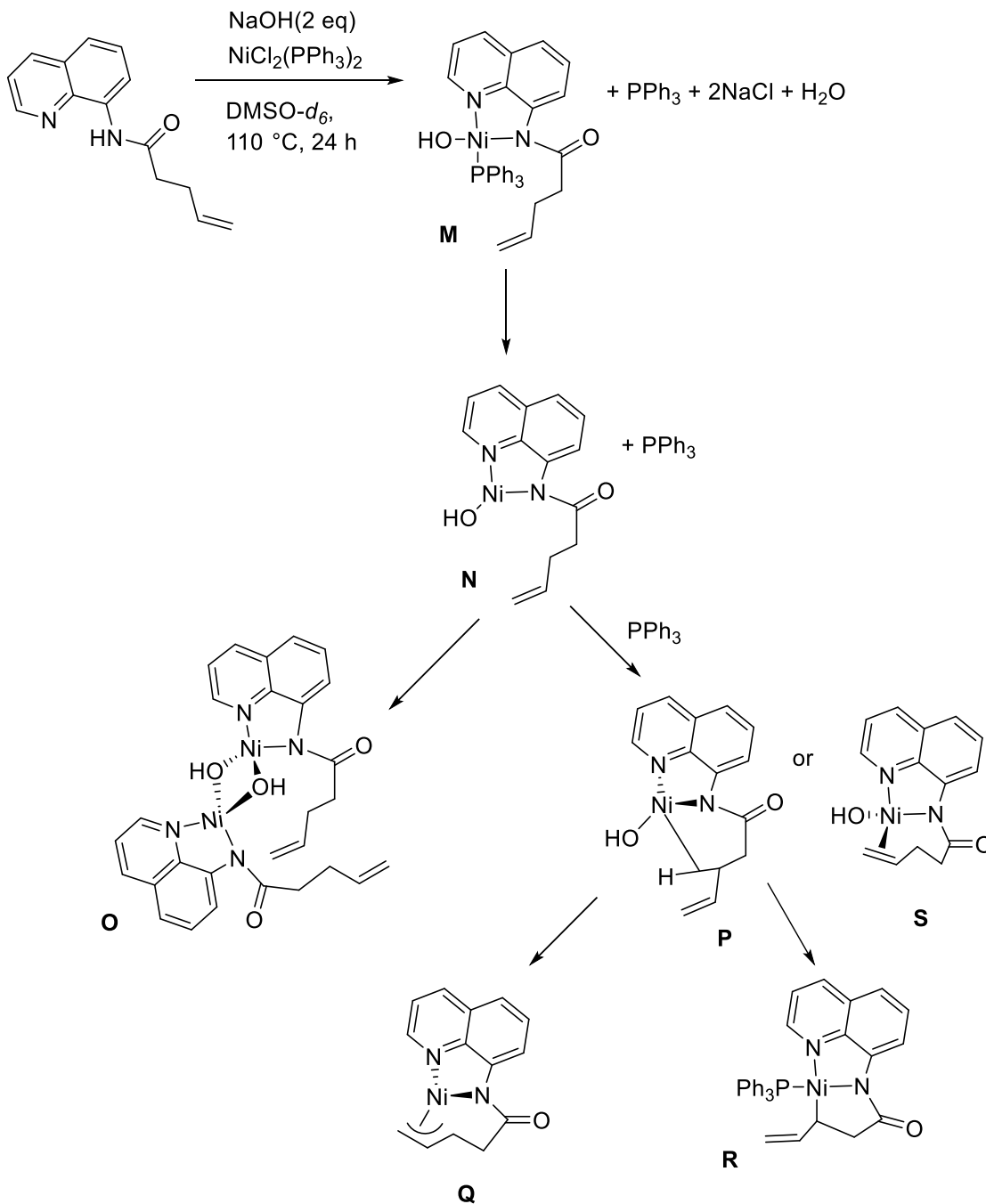


Scheme 3.5. Metalation attempt of *N*-8-quinolinyl-4-pentenamide using $\text{NiCl}_2 \cdot 6\text{H}_2\text{O}$ in MeOH in the absence of a base and proposed *in situ* formed products.

3.1.2 Reactivity of $\text{NiCl}_2(\text{PPh}_3)_2$ with QPAH

$\text{NiCl}_2(\text{PPh}_3)_2$ was chosen as the new Ni(II) precursor for the metalation of the *N*-8-quinolinyl-4-pentenamide ligand. This is because there is literature precedence on using $\text{NiCl}_2(\text{PPh}_3)_2$ as the precursor for metalation reactions,⁶ $\text{NiCl}_2(\text{PPh}_3)_2$ has better solubility in common solvents, is free from water, and has phosphine groups that can act as a handle to monitor reaction progress using $^{31}\text{P}\{^1\text{H}\}$ NMR spectroscopy.

Following the procedure of related reported reactions,² the metalation reaction was carried out in $\text{DMSO-}d_6$ using one equivalent of $\text{NiCl}_2(\text{PPh}_3)_2$ at 110 °C (Scheme 3.6). Two equivalents of NaOH were used for the deprotonation of the amide ligand, and to provide the hydroxide ion to form the Ni(II)-OH complex. The reaction mixture immediately turned dark green and subsequently dark brown after 2 h. The reaction did not show any peaks at any stages of the reaction when monitored by $^{31}\text{P}\{^1\text{H}\}$ NMR spectroscopy, either due to paramagnetism or the high fluxionality of molecules. After 24 h the ^1H NMR spectrum indicated the presence of neutral QPAH and new broad peaks in the range of 10 to 30 ppm indicating the presence of paramagnetic product(s). Three major peaks at 27.65, 26.30 and 15.74 ppm were observed in the presence of minor peaks at 22.96, 17.70, and 12.48 ppm (Figure 3.1a).



Scheme 3.6. Metalation reaction of QPAH with $\text{NiCl}_2(\text{PPh}_3)_2$ in the presence of NaOH base and the proposed potential products.

There are many possible products for the metalation reaction shown in Scheme 3.6. The formed paramagnetic complex or complexes could be the anticipated Ni(II) hydroxide **M**

or the complex **N** after phosphine dissociation. The Ni(II) hydroxides **M** and **N** can further undergo dimerization to form complex **O**, as dimerization is common for Ni-OH complexes. It is also possible to form the C-H agostic complex **P** leading to the C-H activated products **Q** and **R**. Literature findings of C-H activated intermediates having structures closely related to **R** with 8-aminoquinoline derived ligands and phosphine groups resulted in diamagnetic complexes.^{2,6} This gives a strong indication that the complex **R** would be a diamagnetic complex. Hence, the probability of the formed paramagnetic complex having the structure of **R** is quite low.

Isolation of the formed paramagnetic complex/complexes and further characterization must be conducted to determine the structure of the complex to assign the observed ¹H NMR peaks. In order to isolate the paramagnetic complex, the above reaction was conducted in DMF under the same conditions mentioned in Scheme 3.6. The boiling point of DMF is relatively lower than DMSO; hence, it is easier to remove during isolation of the complex. The crude ¹H NMR spectrum of the reaction conducted in DMF showed the formation of similar broad peaks in the range of 10-30 ppm and signals corresponding to ligand QPAH as previously seen for the reaction in DMSO. Attempts made to purify the complex from the QPAH ligand were unsuccessful. The recovery of the sample with the paramagnetic complex and QPAH ligand with the same relative intensity after each purification attempt indicated this could be due to a potential equilibrium between ligand QPAH and complex. Crystallization attempts were conducted following the layering technique using various co-solvents such as diethyl ether, toluene, hexane, and pentane, but none were successful.

Control reactions were carried out to deduce the identity of the formed paramagnetic compounds in the above standard metalation reaction shown in Scheme 3.6 (Figure 3.1a). The ¹H NMR spectra of NiCl₂(PPh₃)₂ and NiCl₂(PPh₃)₂ treated with NaOH (2 equiv) (Figure 3.1 b and c) displayed no paramagnetic signals in the range of 10-30 ppm. These observations led to the conclusion that the observed paramagnetic peaks were not due to NiCl₂(PPh₃)₂ or the reaction of NaOH with the Ni precursor. The metalation reaction of QPAH in the absence of any base (Figure 3.1d) resulted in QPAH peaks and paramagnetic peaks that were observed in minor amounts in the standard reaction but did not correspond

to the obtained major product(s) signals. Hence, it was determined that the standard metalation reaction did not result in $\text{NiCl}_2(\text{QPAH})$ as a major product. Metalation reaction conducted in a different solvent THF and temperature $60\text{ }^\circ\text{C}$ (Figure 3.1e) compared to the standard conditions resulted in a set of paramagnetic peaks at 22.22, 17.75, and 12.00 ppm. The peaks observed in this reaction were slightly upfield compared to the peaks in the standard reaction (Figure 3.1a) by 0.81, 0.08, and 0.55 ppm respectively and indicated the formation of a single product. Subsequent studies (below) suggest that this product is $\text{Ni}(\text{QPA})_2$. The above ^1H NMR spectra observations indicated the potential formation of three paramagnetic products by the metalation reaction conducted in $\text{DMSO-}d_6$ consisting of the $\text{Ni}(\text{QPA})_2$, minor quantities of $\text{NiCl}_2(\text{QPAH})$ and an unknown product **12**.

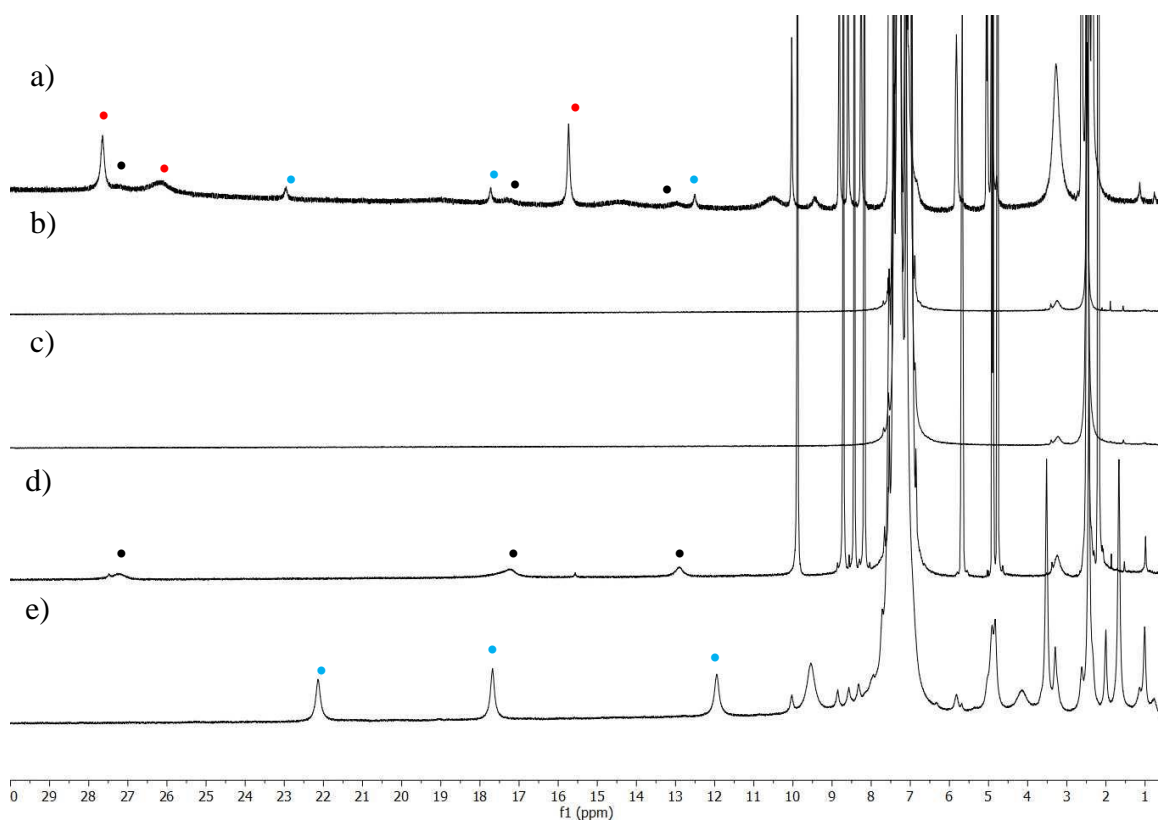


Figure 3.1. ^1H NMR stack plot of a) $\text{QPAH} + \text{NiCl}_2(\text{PPh}_3)_2 + \text{NaOH}$ (2 eq) (standard metalation reaction) b) $\text{NiCl}_2(\text{PPh}_3)_2$ c) $\text{NiCl}_2(\text{PPh}_3)_2 + \text{NaOH}$ (2 eq) d) $\text{QPAH} + \text{NiCl}_2(\text{PPh}_3)_2$ all reactions heated at $110\text{ }^\circ\text{C}$ in $\text{DMSO-}d_6$ for 24 h, and e) $\text{QPAH} + \text{NiCl}_2(\text{PPh}_3)_2 + \text{NaOH}$ (2 eq) heated at $60\text{ }^\circ\text{C}$ in THF for 24 h. All spectra taken in $\text{DMSO-}d_6$. The ‘•’ indicate the major paramagnetic peaks observed in the standard reaction, ‘•’

indicate the peaks that have nearby peak shifts to spectrum e), and ‘•’ indicate the peaks that have nearby peak shifts to spectrum d). Peaks in the range of 0-10 ppm correspond to the QPAH ligand.

Variable temperature (VT) ^1H NMR studies were explored to further characterize the reaction mixture. Since DMSO has a relatively high freezing point (19 °C), it has limited use in low temperature VT NMR studies. Hence, high-temperature VT ^1H NMR spectra were obtained to study any potential dynamic behavior of the complex (Figure 3.2). Heating the NMR sample from 25 to 125 °C and cooling it back to 25 °C caused shifts in the signals indicating the dynamic nature of the formed paramagnetic species. A reduction in the QPAH ligand signals relative to the paramagnetic peaks with the increase in temperature was also observed, indicating a potential equilibrium between the paramagnetic complex and the ligand.

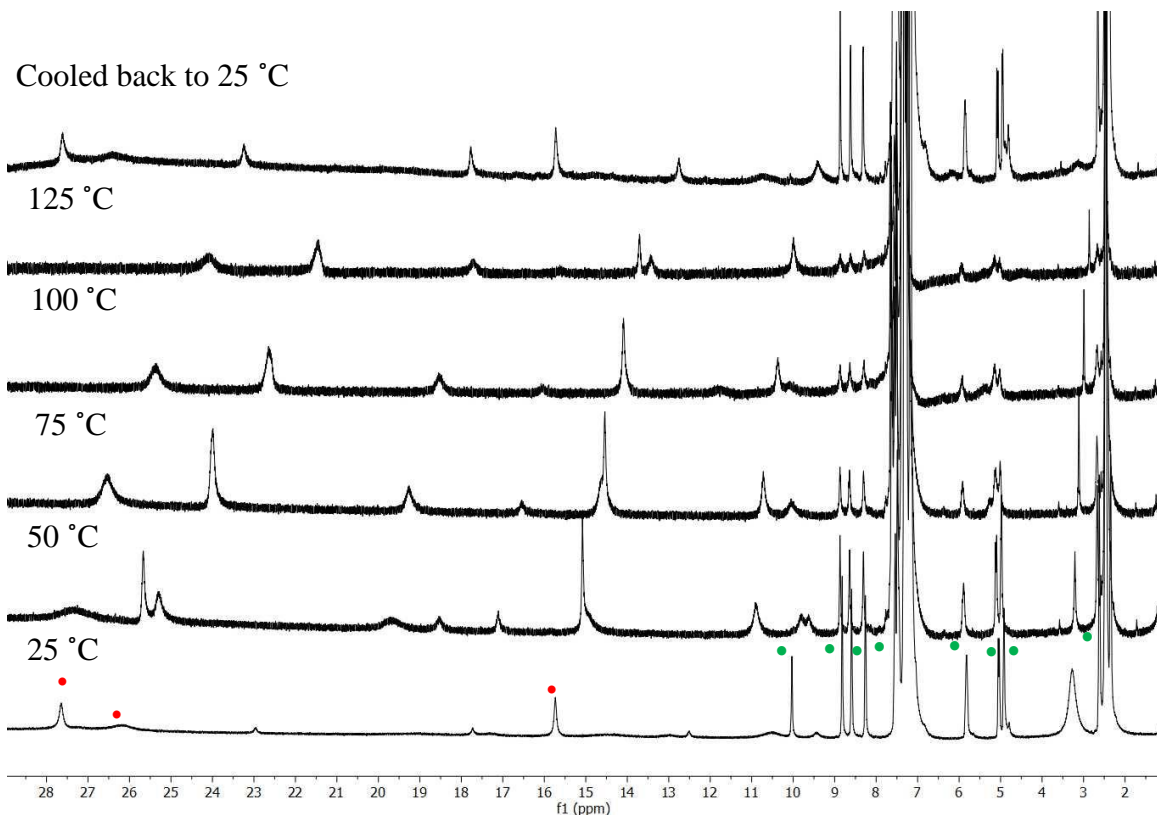
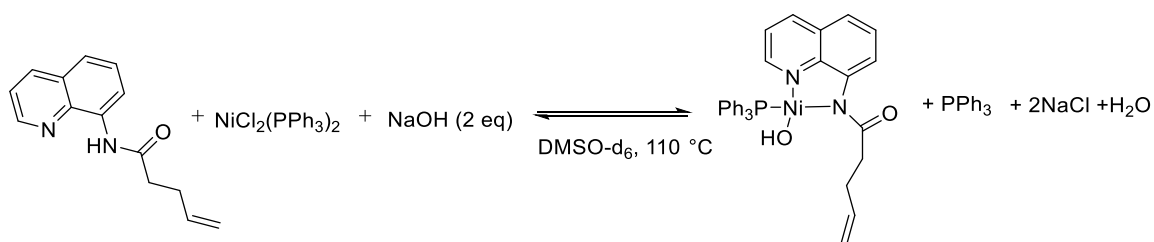


Figure 3.2. Variable-temperature ^1H NMR experiment of the reaction mixture QPAH + $\text{NiCl}_2(\text{PPh}_3)_2$ + NaOH (2 eq) kept at 110 °C for 24 h in $\text{DMSO-}d_6$. All spectra taken in

DMSO-*d*₆, I600 MHz, except the spectrum at 25 °C which is taken by B600 MHz instrument. Signals corresponding to the neutral ligand QPAH are denoted in red (•). Signals corresponding to the major peaks of unknown product are denoted in red (◦).

The water formed as a by-product in the above metalation reaction could have reacted with the coordinated QPA ligand in the Ni(II)-OH complex forming the neutral QPAH ligand, since the basicity of the coordinated ligand is unknown. This could have resulted in a potential equilibrium shown in Scheme 3.7. To push the reaction forward and promote the formation of the product in the equilibrium, the reaction was conducted in the presence of 4 Å sieves as a strategy to remove the water which is being formed. By removing the water, the reaction will be favored towards product formation according to Le Chatelier's principle. The ¹H NMR spectrum of the metalation reaction in the presence of sieves resulted in the formation of paramagnetic signals and the QPAH ligand as in the previous reaction (Figure 3.3), but the peaks corresponding to the QPAH ligand had lower intensity relative to the paramagnetic peaks. This observation implied the removal of water could have potentially favored the equilibrium toward product formation. Notably, the relative ratio of the two paramagnetic products changed and both the products had equal intensities.



Scheme 3.7. Proposed equilibrium for the metalation reaction forming free QPAH.

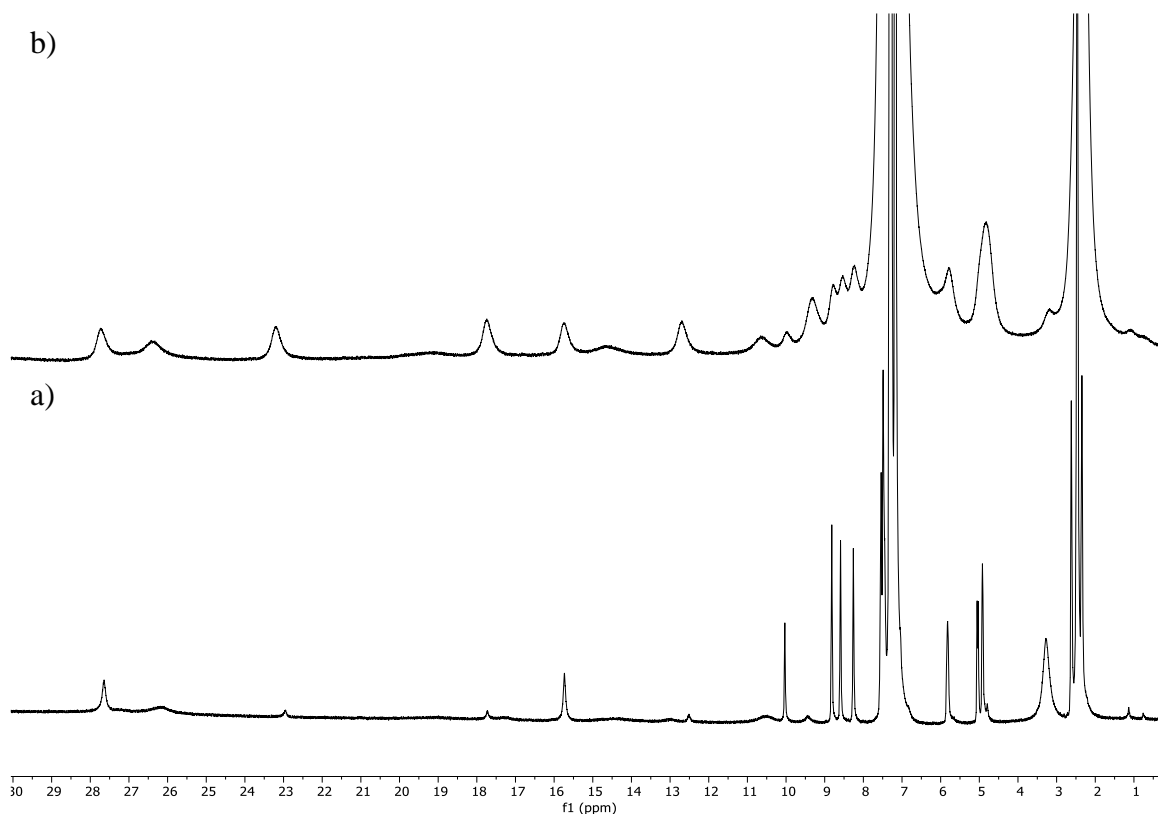
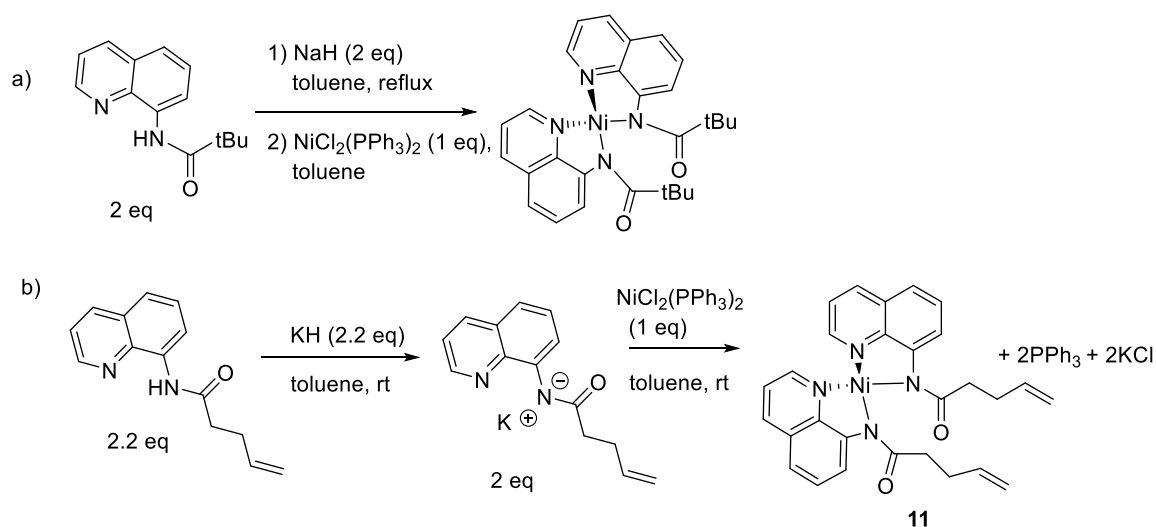


Figure 3.3. ^1H NMR stack plot of a) QPAH + $\text{NiCl}_2(\text{PPh}_3)_2$ + NaOH (2 eq) in the absence of sieves b) QPAH + $\text{NiCl}_2(\text{PPh}_3)_2$ + NaOH (2 eq) in the presence of 4 Å sieves. Both reactions heated at 110 °C in $\text{DMSO-}d_6$ for 24 h and taken in $\text{DMSO-}d_6$.

A report by Johnson et al.⁶ demonstrated the potential for the formation of a bis-ligated Ni(II) complex, analogous to **11** (Scheme 3.8 b). The bis-ligated Ni(II) complex formed by Johnson, from a reaction of $\text{NiCl}_2(\text{PPh}_3)_2$ with an 8-aminoquinoline derived amide, is a dark brown paramagnetic complex (Scheme 3.8 a). Since similar observations were seen in the previously discussed reaction with a structurally related compound to QPAH, this outcome was considered a possibility. In order to confirm the occurrence of a bis-ligation, the intentional synthesis of a bis-ligated Ni(II) complex **11** was conducted using 2.2 equivalents of QPAH and base KH (Scheme 3.8 b). The reaction solution turned dark green and turned brown within 24 h. After removing the reaction solvent, the ^1H NMR spectrum of the crude sample in $\text{DMSO-}d_6$ indicated the presence of a set of paramagnetic peaks at 21.42, 17.60, and 11.48 ppm and peaks corresponding to the QPAH ligand (Figure 3.4 a).

The paramagnetic signals observed in this reaction had very similar peak shifts to the signals observed in the ^1H NMR spectrum of the metalation reaction done in THF (Figure 3.1 e) with small differences of 1.25, 0.17, and 0.89 ppm respectively, which might have been due to effects of paramagnetism. This indicates the possibility of bis-ligation as the major product in the metalation reactions conducted in THF, likely due to the poor solubility of $\text{NiCl}_2(\text{PPh}_3)_2$ in this solvent. The above observations suggest the bis-ligated complex **11** did not correspond to the major paramagnetic product(s) signals observed for the metalation reactions shown in Scheme 3.6, but presumably correspond to the minor signals.



Scheme 3.8. a) Bis-ligated Ni(II) complex formed in the metalation reactions by Johnson *et al* using $\text{NiCl}_2(\text{PPh}_3)_2$ with 8-aminoquinoline derived amide.⁶ b) Synthesis of bis ligated Ni(II) complex **11**.

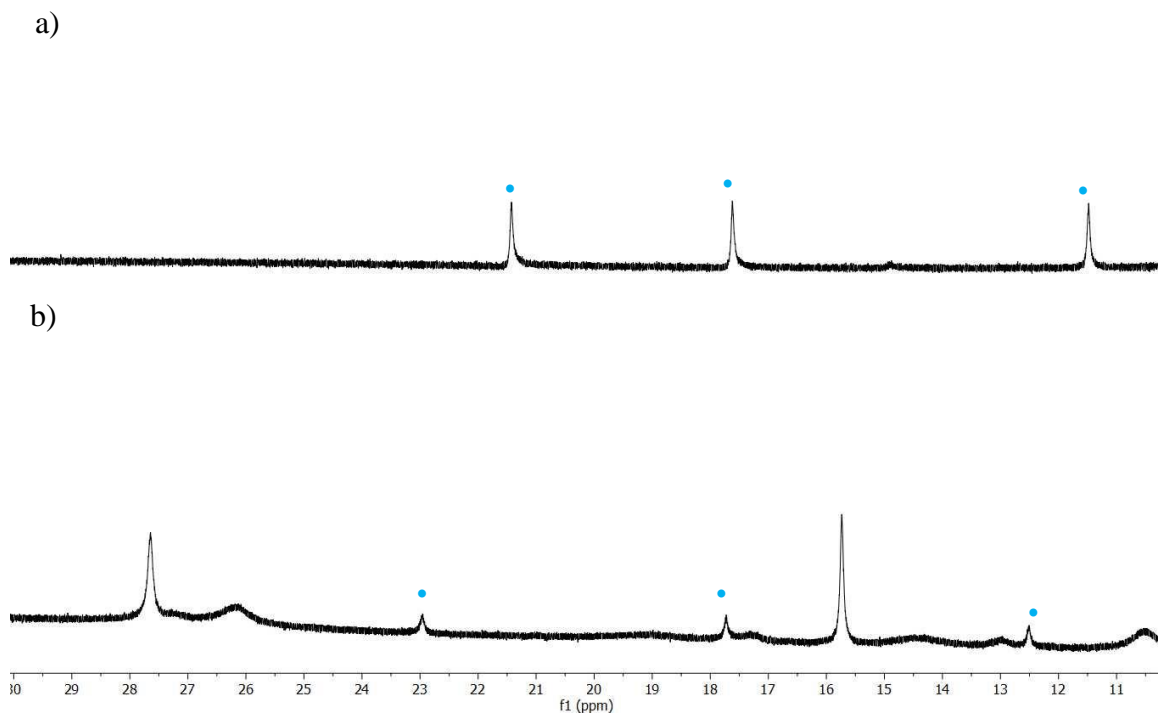


Figure 3.4. Wide range ^1H NMR stack plot of a) QPAH (1 eq) + $\text{NiCl}_2(\text{PPh}_3)_2$ (1 eq) + NaOH (2 eq) heated to $110\text{ }^\circ\text{C}$ for 24 h in $\text{DMSO-}d_6$, b) QPAH (2.2 eq) deprotonated with KH (2.2 eq) followed by $\text{NiCl}_2(\text{PPh}_3)_2$ (1 eq) addition in toluene at RT. Both spectra taken in $\text{DMSO-}d_6$. The ‘•’ indicate the peaks that have nearby peak shifts to spectrum b).

To promote the formation of the major paramagnetic product **12** relative to the presumed by-product **11**, the standard metalation reaction in DMSO was carried out at different temperatures in the presence of 4 \AA sieves. A low temperature might not provide sufficient energy to overcome the activation energy barriers of both products. Hence, the reactions were conducted at temperatures lower than $110\text{ }^\circ\text{C}$. The reactions done at RT had both paramagnetic products at equal intensities and did not seem to favour a specific product (Figure 3.5). When the reaction was conducted at $60\text{ }^\circ\text{C}$ there was a slight reduction in the intensity of the presumed bis-ligated product **11** signals compared to the unknown product **12**. These observations implied that by increasing the temperature the unknown paramagnetic product might be potentially favoured. But the standard metalation reaction

carried out at 110 °C did not further reduce the intensity of the signals corresponding to **11** relative to **12**. Additionally, the metalation reaction carried out at 160 °C resulted in the formation of dark brown solids and absence of any paramagnetic peaks in the ^1H NMR spectrum and the presence of peaks corresponding to the neutral QPAH ligand. These observations implied the potential decomposition of the paramagnetic product(s) at 160 °C. Hence, changing the temperature of the metalation reaction did not result in the promotion of the formation of the unknown paramagnetic product **12** over the by-product.

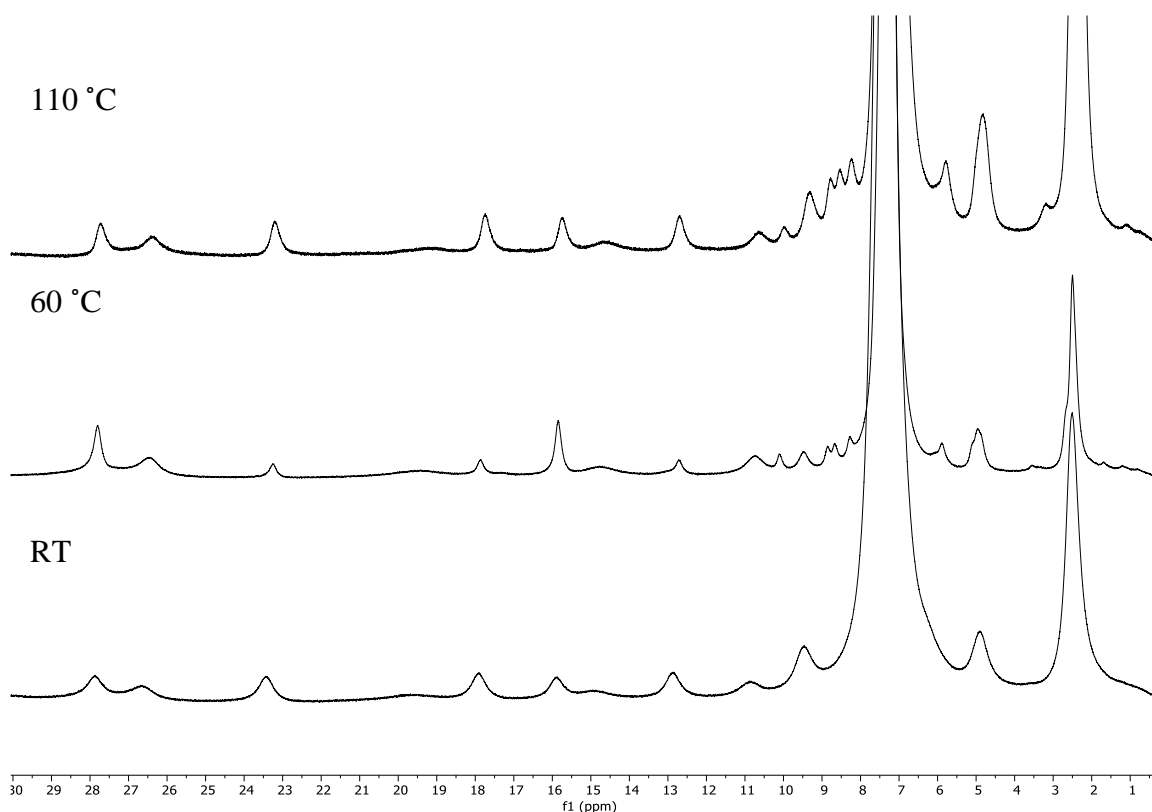
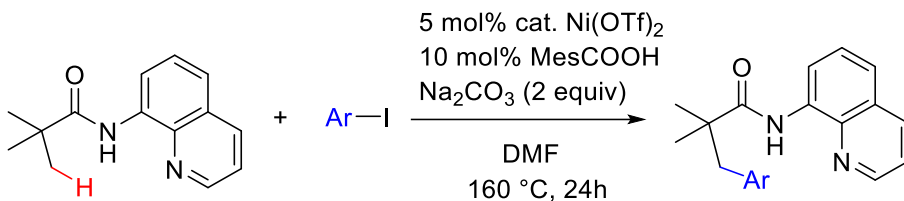


Figure 3.5. QPAH (1 eq) + $\text{NiCl}_2(\text{PPh}_3)_2$ (1 eq) + NaOH (2 eq) heated at different temperatures for 24 h in $\text{DMSO}-d_6$ in the presence of sieves.

3.2 Catalysis to Test C-H Bond Activation with NaOH as the Base

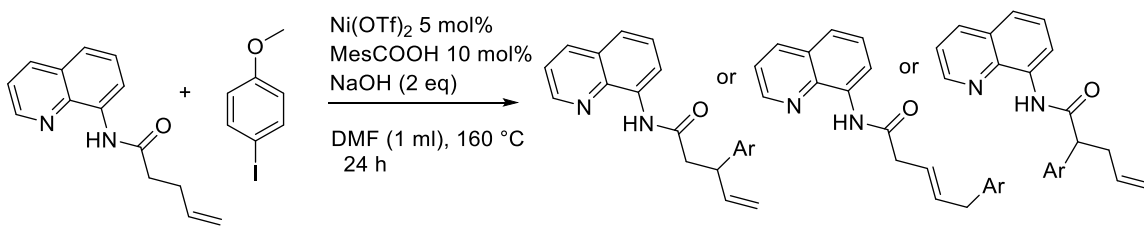
Isolation and characterization of the Ni(II) intermediate prior to the formation of the C-H activated product can be difficult due to its potential instability. Hence, as an attempt to gain information on whether a $\text{C}(\text{sp}^3)\text{-H}$ bond activation can be achieved using Ni(II)

catalysis was carried out. The catalytic reactions were inspired by the reactions reported by Chatani *et al.*,³ which involved direct arylation of an 8-aminoquinoline amide by activating primary C(sp³)-H bonds (Scheme 3.9). Ni(OTf)₂ catalysts were used with Na₂CO₃ as the base under the optimized conditions denoted in Scheme 3.9.



Scheme 3.9. Catalytic reaction by Chatani *et al.* involving C-H activation under optimized conditions.¹

A catalytic reaction was conducted with the above-mentioned conditions using *N*-8-quinolinyl-4-pentenamide as the substrate with the NaOH base instead of Na₂CO₃ (Scheme 3.10). The goal of the catalytic reaction was to understand if the allylic C(sp³)-H bond can be activated to give the arylated products with the hydroxide base.



Scheme 3.10. Proposed arylated products from Ni(II) mediated C-H activation catalysis.

The reaction mixture was analyzed by ¹H NMR spectroscopy in CDCl₃ after a water wash to quantify the consumption of starting material or the formation of any new products. The ¹H NMR spectrum indicated the presence of the starting material QPAH with the formation of a new product in the ratio 1:2 (Figure 3.6 b). Column chromatography was conducted to separate the formed yellow oily product from the starting material (Figure 3.6 c). Control reactions in the absence of Ni(OTf)₂ and iodoanisole indicated that the QPAH reacts with NaOH forming the same product as the product isolated in the above catalysis reaction. Hence, the catalytic reaction did not result in a Ni(II) mediated C-H activated aryl product

as anticipated, instead, the base NaOH reacted with the substrate to form a deleterious side reaction.

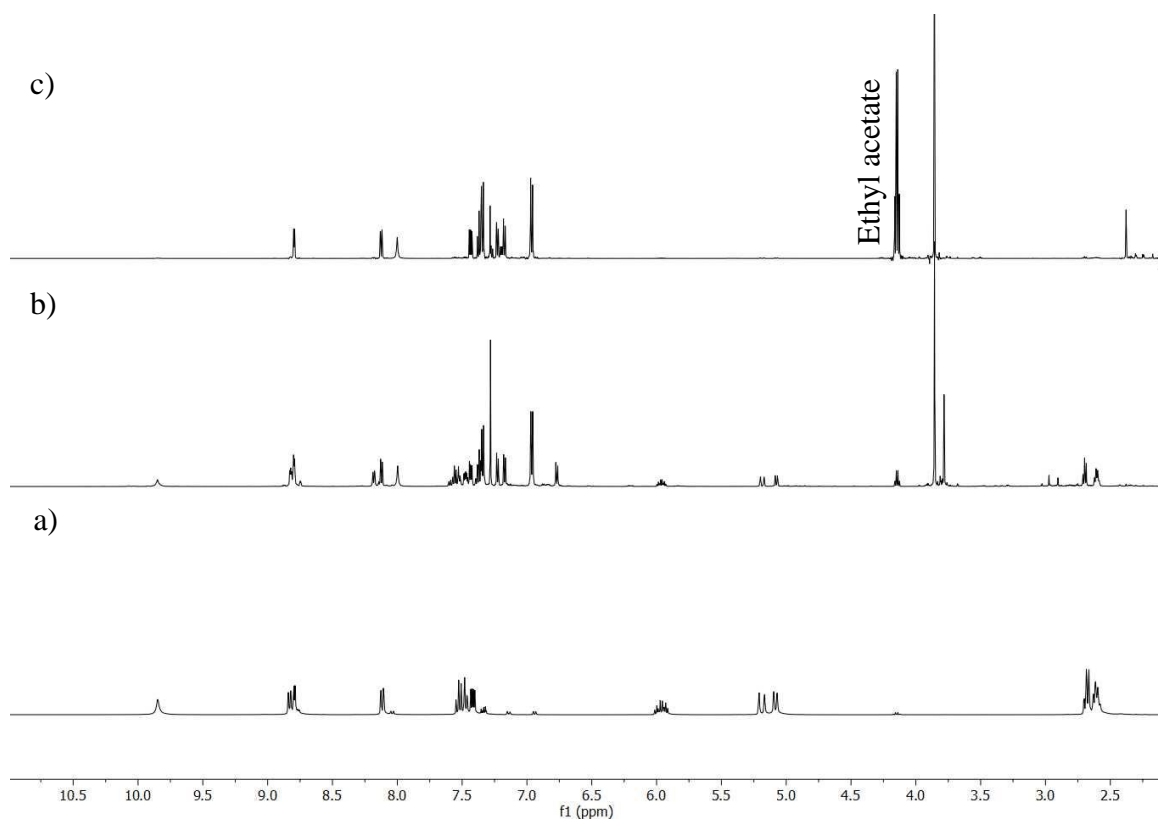


Figure 3.6. ^1H NMR stack plot of a) QPAH b) Crude reaction mixture obtained from catalysis c) Isolated product obtained after QPAH removal through column chromatography. All spectra taken in CDCl_3 .

3.3 Conclusions

The ability of Ni(II) to activate an allylic $\text{C}(\text{sp}^3)\text{-H}$ bond of an 8-aminoquinoline derived allyl substrate was studied. The goal of the study was to promote the CMD mediated C-H activation reaction with the help of a bidentate directing group through an internal hydroxyl base. Attempts to metalate *N*-8-quinolinyl-4-pentenamide with $\text{NiCl}_2\cdot 6\text{H}_2\text{O}$ in the presence of NaOH in $\text{DMSO-}d_6$ yielded the QPAH signals and low intense paramagnetic peaks when monitored through ^1H NMR spectroscopy. Further studies were not conducted due to the low-quality ^1H NMR spectra obtained due to shimming issues. Hence, a new

Ni(II) precursor $\text{NiCl}_2(\text{PPh}_3)_2$ was utilized for the metalation reactions based on previous studies.

Metalation reactions in $\text{DMSO-}d_6/\text{DMF}$ with NaOH (2 equiv) at $110\text{ }^\circ\text{C}$ resulted in a brown solution with a mixture of paramagnetic products and neutral QPAH ligand based on the ^1H NMR spectrum. Control reactions indicated the observed paramagnetic products were not $\text{NiCl}_2(\text{PPh}_3)_2$ or $\text{Ni}(\text{OH})_2(\text{PPh}_3)_2$, but had minor quantities of $\text{NiCl}_2(\text{QPAH})$. Characterization of the major paramagnetic complex was not performed due to the inability to isolate the complex from the ligand QPAH. High temperature ^1H NMR VT studies conducted by heating the sample to $125\text{ }^\circ\text{C}$ indicated the dynamic nature of the formed paramagnetic products and the existence of a potential equilibrium between the paramagnetic products(s) and the QPAH ligand. To favour the reaction forward 4 \AA sieves were added to the reaction as a strategy to remove the by-product water. Since, water might be likely reacting with the coordinated QPA ligand due to its unknown basicity causing an equilibrium. An increase in the intensity of the paramagnetic signals relative to the QPAH signals was observed in the ^1H NMR spectrum indicating a potential increase in product formation. The ^1H NMR spectrum of the bis-ligated complex **11** indicated the formation of paramagnetic signals having similar peak shifts to the metalation reactions in THF and one of the minor paramagnetic products observed in metalation reactions in DMSO. Hence, it was hypothesized the metalation reactions in DMSO in the presence of NaOH resulted in the formation of a presumed bis-ligated complex **11**, minor amounts of $\text{NiCl}_2(\text{QPAH})$ and another unknown paramagnetic complex **12**. To promote the formation of **12** the reactions were conducted at different temperatures. The ^1H NMR spectroscopy results implied that at higher temperatures the target complex **12** was favoured but increasing the temperature to $160\text{ }^\circ\text{C}$ caused the decomposition of the paramagnetic products. Instead of isolating the unknown Ni(II) intermediate prior to C-H activation, catalytic arylation of QPAH was attempted to test the ability of Ni(II) to activate $\text{C}(\text{sp}^3)\text{-H}$ bonds through a hydroxo-mediated CMD pathway. No catalytic activity was observed when analyzed through ^1H NMR spectroscopy due to the competitive reaction of the base with the QPAH substrate.

3.4 References

- (1) Aihara, Y.; Chatani, N. *J. Am. Chem. Soc.* **2013**, *135* (14), 5308–5311.
- (2) Beattie, D. D.; Grunwald, A. C.; Perse, T.; Schafer, L. L.; Love, J. A. *J. Am. Chem. Soc.* **2018**, *140* (39), 12602–12610.
- (3) Aihara, Y.; Chatani, N. *J. Am. Chem. Soc.* **2014**, *136*, 898–901.
- (4) Tang, H.; Zhou, B.; Huang, X. R.; Wang, C.; Yao, J.; Chen, H. *ACS Catal.* **2014**, *4* (2), 649–656.
- (5) Derosa, J.; van der Puyl, V. A.; Tran, V. T.; Liu, M.; Engle, K. M. *Chem. Sci.* **2018**, *9* (23), 5278–5283.
- (6) Liu, J.; Johnson, S. A. *Organometallics* **2021**, *40* (17), 2970–2982.

Chapter 4

General Conclusions and Future Work

4.1 General Conclusions

This report's main focus was to promote an allylic C-H activation with a Ni-OH moiety, leading to aerobic oxidation catalysis. This was approached through two strategies. The first method involved the synthesis and characterization of an NHC Ni(II)-Br complex **4a** and the attempts to convert it to a monomeric Ni(II)-OH complex **5a**. The novel NHC ligand **3a** was successfully synthesized in three steps: imidazole synthesis, picolyl group installation, and deprotection. By metalating **3a** with nickelocene, the new tridentate NHC Ni complex **4a** was synthesized in moderate yields following a modified one-step literature procedure. The new complex was characterized using MALDI-MS, ^1H and $^{13}\text{C}\{^1\text{H}\}$ NMR spectroscopy, and IR spectroscopy. Although crystallization of **4a** was not achieved to confirm the exact structure, ^1H NMR spectroscopic studies confirmed the formation of a mono-ligated tridentate complex. Catalysis attempts to aerobically oxidize an allyl substrate QPAH with **4a** as a catalyst resulted in no reactivity. By reacting **4a** with NH_4OH a bis-ligated Ni(II) complex **6** was formed based on X-ray crystallography, NMR spectroscopy, and ESI-MS analysis. The formation of the bis-ligated complex **6** was proposed to go through a pathway consisting of the Ni-OH monomer **5a** and Ni(II)-OH dimer **8**. Low-temperature UV-vis studies conducted to determine any intermediates that might be stable at low temperatures were not successful due to the presence of water in the NH_4OH reagent that prevented the solubility of the reagent at temperatures below $0\text{ }^\circ\text{C}$. Hence, a new route of synthesizing a Ni allyl complex **9a** with the same ligand design was conducted to achieve catalysis. Preliminary studies on the aerobic oxidation of **9a** indicated the formation of **6**. Aerobic oxidation catalysis reactions were attempted with different allyl substrates under different conditions to disfavor dimerization at low concentrations. All the attempts indicated the absence of catalytic activity and the formation of **6**, which might be hindering the catalytic cycle. Hence, this route was paused for the moment as experimental results did not indicate the formation of a stable Ni(II)-OH **5a** as anticipated.

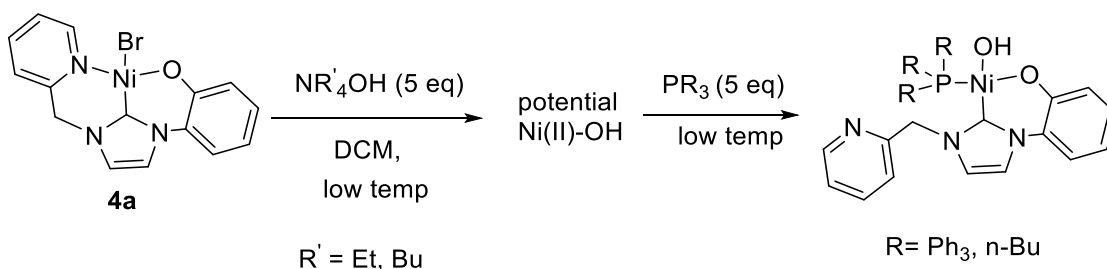
The second method involved the utilization of an allyl ligand QPAH with a bidentate directing group 8-aminoquinoline. The directing group was anticipated to promote the CMD mediated C-H activation in the presence of an internal hydroxide base. The ^1H NMR spectrum of the metalation reaction of QPAH with $\text{NiCl}_2(\text{PPh}_3)_2$ in the presence of NaOH (2 equiv) indicated the presence of QPAH ligand and a mixture of paramagnetic products. Control reactions indicated the observed paramagnetic products were not due to $\text{NiCl}_2(\text{PPh}_3)_2$ or $\text{Ni}(\text{OH})_2(\text{PPh}_3)_2$, but the reaction had minor peaks corresponding to $\text{NiCl}_2(\text{QPAH})$. A high-temperature VT NMR study implied the dynamic nature of the paramagnetic products and a potential equilibrium with the QPAH ligand. The proposed equilibrium was likely due to the by-product water reacting with the coordinated QPAH ligand. The addition of sieves as a strategy to remove water had a positive effect and increased the paramagnetic signal intensity relative to the QPAH signals. The bis-ligated complex **11** had very similar ^1H NMR peak shifts with slight differences from minor peaks observed in the paramagnetic region of the metalation reaction. Hence, the metalation reaction was proposed to form three potential paramagnetic products: an unknown complex **12**, the presumed bis-ligated complex **11**, and minor quantities of $\text{NiCl}_2(\text{QPAH})$. Isolation attempts on the formed Ni products were unsuccessful hence, catalytic arylation of QPAH was attempted to test the ability of Ni(II) to activate $\text{C}(\text{sp}^3)\text{-H}$ bonds through a hydroxo-mediated CMD pathway. No catalytic activity was observed when analyzed through ^1H NMR spectroscopy due to the competing side reaction of the base with the QPAH substrate.

Overall it can be understood that the tridentate NHC ligand **3a** was not able to stabilize the Ni(II)-OH monomer **5a** as anticipated. Hence, the proposed aerobic oxidation catalytic cycle consisting of the CMD-mediated activation of allylic $\text{C}(\text{sp}^3)\text{-H}$ bonds by **5a** was not tested. The studies on synthesizing a new allyl Ni-OH substrate with directing groups to achieve C-H activation indicated the formation of an unknown paramagnetic complex **12**. This complex could contain the Ni(II)-OH moiety that might lead to a CMD-mediated C-H activation. This could lead to an effective catalytic aerobic oxidation reaction utilizing the earth-abundant nickel metal to produce useful organic compounds in a sustainable way.

4.2 Future Work

Future work on this project will focus on first completely characterizing complexes **4a** as efforts so far have not proved satisfactory. The presence of a crystal structure and/or elemental analysis would confirm the exact structure of Ni(II)-Br complex **4a** and provide better leverage to the project.

The next focus should be to trap any potential Ni(II)-OH intermediates. Attempts at the formation of the Ni-OH monomer **5a** from **4a** have resulted in the bis-ligated Ni(II) complex **6**. Preliminary studies on the aerobic oxidation of **9a** have also resulted in the formation of **6**. Based on these observations a pathway for the formation **6** can be proposed for the **4a** + NH₄OH reaction, through potential Ni(II)-OH intermediates **5a** and **8** that might be unstable at room temperature. Low-temperature UV-visible experiment conducted at -60 C to trap potential intermediates was not successful due to the interference of water in the NH₄OH reagent. A possible solution for this issue would be to use [NR₄]OH (R = Et, Bu) reagent that is dissolved in an organic solvent such as MeOH instead of NH₄OH which is an aqueous solution. If the presence of an intermediate or intermediates is determined from the above experiment, attempts on trapping the intermediate using different phosphine donors (such as PPh₃ or P(n-Bu)₃) could be conducted (Scheme 4.1) and further studies on the chemistry of the Ni-OH can be probed.



Scheme 4.1. Ni(II)-OH intermediate trapping experiment at low temperature through phosphine groups.

From the experimental results of Chapter 2, it can be understood that the tridentate ligand **3a** was not able to stabilize the Ni(II)-OH monomer **5a** as proposed. Hence the viability of the hypothesized catalytic cycle for aerobic oxidation was not tested. To address this challenge, modification to the **3a** ligand should be considered. One potential reason for the lack of stability of Ni-OH monomer **5a** could be due to the small ligand size. By making the ligand bulkier the dimerization process might be prevented. Studies conducted by the previous Blacquiere group members at synthesizing the bulky NHC ligand which has *t*-butyl groups in the 2- and 4- positions of the phenol aryl ring were not successful (Figure 4.1). Hence, a new ligand consisting of different bulky groups substituted at the 2 and 4 positions of the phenol can be considered.

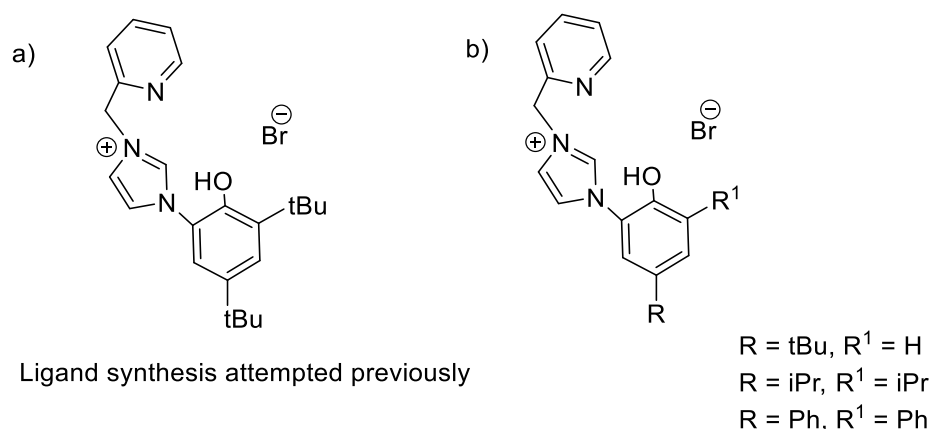


Figure 4.1. a) Synthesis of target NHC ligand attempted by previous group members. b) Proposed NHC ligand to prevent dimerization by having bulky groups in 2 and 4 positions of phenol.

The most essential part of the ligand design is the NHC donor group which is required to increase the electron density of Ni required for O₂ activation. Hence, modification of the other ligand segments can be considered. Replacing the picolyl group with the 8-aminoquinoline-derived allyl group might favor the C-H activation reaction by making the reaction intramolecular due to the presence of directing groups. The removal of the X-type aryloxide group might potentially prevent the occurrence of bis-ligation due to low coordination sites. Hence the synthesis of the following target ligand shown in Figure 4.2 can be proposed.

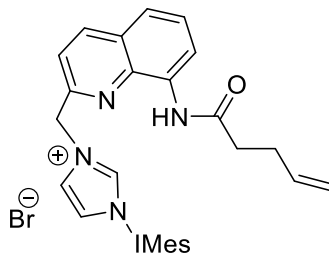


Figure 4.2. Proposed ligand design to stabilize the Ni(II)-OH complex

The final focus should be to identify and characterize the unknown paramagnetic product **12** formed in the metalation reaction of QPAH + NiCl₂(PPh₃)₂ + NaOH (2 equiv) conducted in DMSO-*d*₆. Based on the experimental results in Chapter 3, an equilibrium likely exists between the QPAH ligand and a mixture of paramagnetic products consisting of the unknown complex **12**. The presence of an equilibrium forming a mixture of paramagnetic products makes the isolation and characterization of the products challenging. Hence, different reaction conditions should be tested to favour the formation of the unknown paramagnetic product **12** which will help to make the isolation easier. Crystallization attempts should be pursued for both the bis-ligated complex **11** and the unknown complex **12** as efforts so far have not yielded success.

Chapter 5

Experimental

5.1 General Experimental Procedure

Unless otherwise stated, all reactions were conducted under an inert argon or nitrogen atmosphere following standard Schlenk or glovebox techniques, respectively. All NMR tubes and glassware were dried in an oven at 150–160 °C for at least 3 h and cooled under inert atmosphere or vacuum before use. All solvents were dried and degassed from an Innovative Technology 400-5 Solvent Purification system and stored over activated 4 Å molecular sieves for at least 24 h, with the exception of acetonitrile, which was stored over activated 3 Å molecular sieves before use unless otherwise stated. Molecular sieves were purchased from Fluka and activated under vacuum at 150 °C for 12 h prior to use. Chloroform was degassed and stored over activated 4 Å sieves. Dichloromethane-*d*₂, toluene-*d*₈, and DMSO-*d*₆ were purchased from Sigma Aldrich as ampules and stored over activated 4 Å molecular sieves for at least 24 h before use. Water was deoxygenated by sparging with nitrogen for 30 min before use. Dioxygen (99%) was purchased from Praxair and passed through a drying tube containing calcium sulphate to remove water prior to use. *N*-8-Quinoliny1-4-pentenamide was synthesized following a literature procedure and the obtained ¹H NMR spectrum matched reported characterization data.¹ All other reagents were purchased from Alfa Aesar, Sigma Aldrich or Oakwood and used without any further purification.

All NMR spectra were recorded on Bruker 400, Bruker 600 MHz, or INOVA 600 MHz instrument at 25 °C, unless stated otherwise. Variable temperature NMR experiments were performed by cooling an external heat exchanger on the spectrometer with liquid N₂ and managing the probe temperature through the spectrometer software (VnmrJ 3.2A). ¹H spectra acquired in CDCl₃ and DMSO-*d*₆ were referenced internally against the residual solvent signal (CHCl₃ at 7.26 ppm, DMSO at 2.50 ppm) to tetramethylsilane at 0 ppm. ¹³C{¹H} spectra acquired in CDCl₃ and DMSO-*d*₆ were referenced internally against the

residual solvent signal (CHCl_3 at 77.2 ppm, DMSO at 39.4 ppm) to tetramethylsilane at 0 ppm. $^{31}\text{P}\{^1\text{H}\}$ NMR spectra collected in protio solvents were referenced externally to 85% phosphoric acid (0 ppm) and referenced internally in deuterated solvents. Assigned multiplicities are abbreviated as: singlet (s), doublet (d), triplet (t), and multiplet (m). Infrared spectra were collected on solid samples using a Bruker ALPHA II FTIR spectrometer. Charge-transfer Matrix Assisted Laser Desorption/Ionization (MALDI) mass spectra were collected on an AB Sciex 5800 TOF/TOF mass spectrometer using a pyrene matrix in a 10:1 matrix: substrate molar ratio in DCM. ESI mass spectra were collected on Bruker MicroTOF II instrument using MeCN as the solvent. X-ray diffraction measurements were made on a Bruker Kappa Axis Apex2 diffractometer at a temperature of 110 K. UV-Visible spectra were collected using an Agilent Technologies Cary 8454 UV-Visible spectrometer, fitted with a Unisoko CoolspeK UV USP-203-A cryostat for low-temperature analyses.

5.2 General Procedure for Imidazole Synthesis

Substituted aniline (16 mmol; 2-methoxyaniline, 2-methoxy-6-methylaniline) was dissolved in MeOH (30 mL) in a 100 mL round-bottom flask. Glyoxal (1.0 equiv, 1.8 mL, 40% by weight in water) was added and the flask was sealed with a septum. The mixture was stirred at room temperature for 24 h. The rubber septum was removed, and NH_4Cl (1.10 equiv, 0.940 g, 17.6 mmol) was added followed by formaldehyde (1.0 equiv, 1.2 mL, 37% by weight in water) via pipette. The round-bottom flask was fitted with a reflux condenser, and the mixture was refluxed for 1 hour. H_3PO_4 (2.8 mL, 85% by weight in water) was added via pipette, and the mixture was refluxed for 24 h. The MeOH solvent was removed under reduced pressure. To the remaining solution was added KOH (7M in water, ca. 10 mL) until the pH of the solution measured 8-9. The solution was extracted with DCM (5×20 mL), and the combined organic layers were dried with anhydrous MgSO_4 . The mixture was then filtered, and the solvent of the filtrate was removed under reduced pressure to afford products **1a** or **1b**.²

1-(2-Methoxyphenyl)-imidazole (1a): Yield: 80% (2.28 g), dark brown oil. ^1H NMR (400 MHz, CDCl_3) δ : 7.80 (s, NCHN, 1H), 7.36 (ddd, $J = 8.3, 7.5, 1.7$ Hz, 1H), 7.31 (dd, $J =$

7.5, 1.7 Hz, 1H), 7.21 (d, imidazole backbone protons, 1H), 7.17 (d, imidazole backbone proton, 1H), 7.09-7.05 (m, 2H), 3.88 (s, OCH₃, 3H). The ¹H NMR spectrum values matched literature values.²

1-(2-Methoxy-3-methylphenyl)-imidazole (1b): Yield: 84%, dark brown oil. ¹H-NMR (400 MHz, CDCl₃) δ: 7.85 (s, NCHN, 1H), 7.25 (1H), 7.23 (d, 1H), 7.14 (d, 1H), 7.12-7.08 (m, 2H), 3.42 (s, OCH₃, 3H), 2.38 (s, Ar-CH₃, 3H).

5.3 General Procedure for Picolyl Group Installation

2-(Bromomethyl)pyridine hydrobromide (1.60 equiv, 1.01 g, 4.00 mmol) was neutralized by stirring it with a saturated aqueous solution of NaHCO₃ (20 mL) for 30 min. The liberated 2-(bromomethyl)pyridine was then extracted using DCM (3 × 30 mL). The combined organic layers were dried with Na₂SO₄, the mixture was filtered, and the DCM of the filtrate was removed under reduced pressure to produce a pink solid. 2-(Bromomethyl)pyridine (1.6 equiv, 0.69 g, 4.0 mmol) and the substituted imidazole (1.0 equiv, 2.5 mmol) were placed in a 100 mL round bottom flask containing MeCN (40 mL). The flask was fitted with a reflux condenser and the mixture was refluxed at 110 °C for 48 h. The reaction was cooled to room temperature, and the solvent was removed under reduced pressure. The solid crude material was added to DCM, filtered and the solvent of the filtrate was removed under vacuum to give the desired product.³

1-(2-Pyridinylmethyl)-3-(2-methoxyphenyl)-imidazolium bromide (2a): Yield: 68%, brown orange sticky solid. ¹H NMR (400 MHz, CDCl₃): δ 10.75 (s, NCHN, 1H), 8.59 (d, *J* = 8.0 Hz, 1H), 8.14 (d, *J* = 8.0 Hz, 1H), 7.93 (t, 1H), 7.83-7.79 (m, 1H), 7.59-7.56 (m, 1H), 7.53-7.49 (m, 1H), 7.45 (t, 1H), 7.36-7.33 (m, 1H), 7.14 (s, 1H), 7.12 (s, 1H), 6.13 (s, NCH₂C, 2H), 3.96 (s, OCH₃, 3H). ¹³C{¹H} NMR (101 MHz, CDCl₃): δ 152.4 (C-OCH₃), 152.0 (NCC=C), 149.2 (Ar), 138.3(N=CHN), 137.6 (NCC=C), 131.9 (Ar), 125.5 (Ar), 125.2, 124.3, 123.2, 122.6, 122.5, 121.7 (Ar), 112.8 (Ar), 56.4 (NCH₂C), 53.5 (CO-CH₃). HRMS (ESI, m/z): calcd. for [2a - Br]⁺ 266.1287, found 266.1285.

1-(2-Pyridinylmethyl)-3-(2-methoxy-3-methylphenyl)-imidazolium bromide (2b):
Yield: 82%, dark brown oily liquid. ¹H NMR (400 MHz, CDCl₃): δ 10.84 (s, NCHN, 1H), 8.61 (d, 1H), 8.30 (d, 1H), 8.09 (t, 1H), 7.90 (td, 1H), 7.56 (t, 1H), 7.49 (dd, 1H), 7.42 (d, 1H), 7.39 (dd, 1H), 7.23 (t, 1H), 6.21 (s, NCH₂C, 2H), 3.63 (s, OCH₃, 3H), 2.41 (s, Ar-CH₃, 3H).

5.4 Synthesis of 1-(2-Pyridinylmethyl)-3-(2-hydroxyphenyl)-imidazolium Bromide (3a)

In the glove-box, 1-(2-pyridinylmethyl)-3-(2-methoxyphenyl)-imidazolium bromide (**2a**) (0.330 g, 1.00 mmol) was dissolved in anhydrous CHCl₃ (20 mL) in a dry Schlenk flask. The flask was sealed with a rubber septum, and BBr₃ (5.0 equiv, 0.46 mL, 5.0 mmol) was added dropwise via ground-glass syringe to the reaction flask over a period of 30 min at room temperature under argon. After 30 min the temperature was increased to 60 °C and the reaction mixture was refluxed for 48 h. The resulting brown-yellow solution was cooled to 0 °C and MeOH (10 mL) was added dropwise via ground-glass syringe to quench any remaining BBr₃. The solvent was then removed under reduced pressure and the resulting dark brown residue was washed with ether. NH₃ (7M in MeOH, 10 mL) was added in excess and allowed to stir for 5 min. The solvent was then removed under reduced pressure, and the resulting pinkish brown solids were dissolved in DCM, filtered through Celite and the solvent of the filtrate was evaporated under vacuum to yield **3a** as a pink-brown solid. Yield: 55%.

¹H NMR (400 MHz, DMSO): δ 9.73 (s, N=CHN, 1H), 8.59 (d, Ar-H, *J* = 4.0 Hz, 1H), 8.10 (d, NHC=C, *J* = 4.0 Hz, 1H), 7.99 (d, NHC=C, *J* = 4.0 Hz, 1H), 7.94-7.90 (m, 1H), 7.57-7.54 (m, Ar-H, 2H), 7.45 - 7.42 (m, Ar-H, 2H), 7.15 (dd, Ar-H, 1H), 7.06-7.02 (m, Ar-H, 1H), 5.67 (s, NCH₂C, 2H). ¹³C{¹H} NMR (101 MHz, DMSO): δ 153.9 (C-OH), 150.9 (NCC=C), 150.1 (Ar), 138.1 (N=CHN), 138.0 (NCC=C), 131.7 (Ar), 126.2 (Ar), 124.2, 123.9, 123.5, 123.1, 122.7, 120.2 (Ar), 117.6 (Ar), 53.7 (NCH₂C). HRMS (ESI, *m/z*): calcd for [**3a**- Br]⁺ 252.1137, found 252.1137. IR (ATR, cm⁻¹): ν(OH) 3377.

5.5 Synthesis of NHC Ni(II)-Br Complex (4a)

1-(2-Pyridinylmethyl)-3-(2-hydroxyphenyl)-imidazolium bromide (**3a**) (0.166 g, 0.500 mmol), Cp₂Ni (1.10 equiv, 0.106 g, 0.560 mmol), and CH₃CN (20 mL) were placed in a dry round-bottom flask inside the glove box. The round bottom was sealed with a septum and removed from the glovebox and the reaction mixture was refluxed with stirring for 16 h. The reaction was then cooled to room temperature in open air, and the solvent was removed under reduced pressure. The brown residue was then washed with diethyl ether (3 × 10 mL) to give **4a** as a brown solid. The brown solids were further suspended in a mixture of DCM/Et₂O (1:2, 30 mL) and filtered through a frit and dried under vacuum. Yield (0.171 g, 63-88%). Followed a modified literature procedure.³

¹H NMR (400 MHz, DMSO): δ 8.69 (d, 1H), 8.25 (s, NHC=C, 1H), 8.04 (t, *J* = 8.0 Hz, 1H), 7.82 (s, NHC=C, 1H), 7.68-7.63 (m, 2H), 7.49 (t, 1H), 7.02 (t, *J* = 4.0 Hz 1H), 6.94 (d, 1H), 6.72-6.69 (m, 1H) 5.64 (s, NCH₂C, 2H). ¹³C{¹H} NMR (101 MHz, DMSO): δ 153.9 (Ni-C), 153.2 (C-O-Ni), 152.8, 140.6, 128.8, 127.6, 126.3, 125.8, 125.1 (imidazole backbone C), 124.9, 120.9, 118.6, 118.3 (imidazole backbone C), 116.1, 52.4 (NCH₂C).

5.6 Synthesis of Bis-ligated NHC Ni Complex (6)

In the glove box, **4a** (39 mg, 0.10 mmol) was suspended in THF (20 mL) in a dry Schlenk flask. The Schlenk flask was removed from the glove box and connected to a Schlenk line. NH₄OH (5.0 equiv, 65 μL, 0.50 mmol, 28-30% by volume in water) was transferred by syringe to the reaction flask and left to stir for 24 h at room temperature. The solvent was then removed under vacuum under an inert atmosphere. The resulting brown residue was taken into the glove box, redissolved in THF, and filtered through Celite affording dark brown precipitates. The solvent of the brown filtrate was removed under reduced pressure giving **6** as a brown solid. % Mass purity = 47-73% (The NMR spectra contains the free mono cationic ligand **3a** which was not removed even after several washing and crystallization attempts due to similar solubility. The following peaks corresponding to the complex **6** are assigned based on 2D NMR analysis).

^1H NMR (400 MHz, DMSO): δ 8.38 (d, 2H), 7.81 (d, $\text{NHC}=\text{C}$, $J = 16$ Hz 2H), 7.61-7.59 (m, $\text{NHC}=\text{C}$, 2H), 7.45-7.43 (m, 4H), 7.21-7.16 (m, 4H), 6.96 (d, $J = 4$ Hz, 2H), 6.73 (d, $J = 8$ Hz, 2H), 6.54 (t, $J = 4$ Hz, 2H), 4.93 (d, NCH_2C , $J = 12$ Hz, 2H), 4.51 (d, NCH_2C , $J = 12$ Hz, 2H) ppm. $^{13}\text{C}\{^1\text{H}\}$ NMR (101 MHz, DMSO): δ 157.7 (Ni-C), 155.8 (C-O-Ni), 149.6, 137.3, 136.4, 128.6, 127.5, 126.1, 123.1, 121.2, 120.5, 119.3, 119.1, 113.1, 55.0 (NCH_2C) ppm.

HRMS (ESI, m/z): calcd for $[\mathbf{6} - \text{H}]^+$ 559.1392, found 559.1562.

Gold prism crystals suitable for X-ray crystallography were grown from the slow vapour diffusion of hexane into a solution of **6** dissolved in a minimal amount of dichloromethane at room temperature.

5.7.1 Representative Procedure for Attempted Catalytic Aerobic Oxidation of *N*-8-Quinoliny-4-pentenamide (QPAH) with **4a** as Catalyst

A stock solution of **4a** (8.0 mg, 0.020 mmol, 10 mM) was prepared in $\text{DMSO-}d_6$ (2.0 mL), and 250 μL of the resulting solution was added to two separate NMR tubes. A second stock solution containing QPAH (68 mg, 0.30 mmol, 0.20 M) and the internal standard mesitylene (9.0 mg, 0.075 mmol, 50 mM) was prepared in $\text{DMSO-}d_6$ (1.5 mL) and 250 μL of this solution was added to each of the NMR tubes. The final concentrations in each NMR tube were 100 mM of QPAH, 25 mM of mesitylene, and 5 mol% of **4a**. To each of these NMR tube solutions, Na_2CO_3 (2.0 equiv, 10 mg, 0.10 mmol) was directly added. The NMR tubes were sealed with a septum, secured with electrical tape, and shaken well before being removed from the glovebox. Time = 0 ^1H NMR spectra were obtained for all the samples. Dry O_2 was bubbled approximately for 30 seconds through a stainless-steel needle into each tube, equipped with a bleed needle. After O_2 addition one tube was placed in a 60 $^\circ\text{C}$ oil bath, and the other in a 120 $^\circ\text{C}$ oil bath. After 0.5, 1, 4, and 18 hours of heating, each NMR tube was removed from the oil bath, the outsides of the tubes were washed with hexane and acetone, and the samples were analyzed by ^1H NMR spectroscopy. After analysis, the tubes were returned to the oil bath until the next time point.

5.7.2 Attempted Catalytic Aerobic Oxidation of QPAH at Low Concentration

This procedure follows the representative procedure as Section 5.7.1, differing only in the QPAH, internal standard, and **4a** concentrations. A stock solution of **4a** (0.004 mmol, 1 mM, 1 mL) was prepared by using 200 μL of the above 10 mM **4a** stock solution and adding 800 μL of $\text{DMSO-}d_6$ to it. 250 μL of this solution was added to NMR tubes. A second stock solution containing QPAH (0.060 mmol, 40 mM, 1.0 mL) and the internal standard mesitylene (0.015 mmol, 10 mM) was prepared by using 200 μL of above 200 mM substrate stock solution and adding 800 μL of $\text{DMSO-}d_6$ to it. 250 μL of this solution was added to the NMR tubes. The final concentrations of the reaction solutions in each NMR tube were 20 mM of QPAH, 5 mM of mesitylene, and 5 mol% of **4a**.

5.7.3 Attempted Catalytic Aerobic Oxidation of QPAH with Different Bases

The procedure follows the representative procedure as described in Section 5.7.1, except that the reaction tubes were immersed in a preheated oil bath set to 80 $^{\circ}\text{C}$ after O_2 addition, and KH (4 mg, 0.1 mmol, 2 equiv), NaOH (4 mg, 0.1 mmol, 2 equiv), KOtBu (11 mg, 0.10 mmol, 2.0 equiv) and Cs_2CO_3 (32 mg, 0.10 mmol, 2.0 equiv) as the bases.

5.7.4 Attempted Catalytic Aerobic Oxidation of QPAH with IMes•HCl and Ni(OTf)₂ as Catalyst

In the glovebox, QPAH (68 mg, 0.30 mmol), IMes•HCl (20 mg, 0.060 mmol), Ni(OTf)₂ (11 mg, 0.030 mmol), KOtBu (8 mg, 0.070 mmol), and Na_2CO_3 (64 mg, 0.60 mmol) were dissolved in toluene- d_8 solvent (1 mL) and added to an NMR tube. The NMR tube was sealed with a septum, secured with electrical tape, and shaken well before being removed from the glovebox. The T0 ^1H NMR spectrum of the sample was taken. The tube was equipped with a bleed needle and dry O_2 was bubbled through a stainless-steel needle into the tube for approximately 30 seconds. After the addition, the tube was kept in a 110 $^{\circ}\text{C}$

preheated oil bath for 24 hours. The outside of the tube was washed with hexane and acetone and the sample was analyzed by ^1H NMR spectroscopy

5.8 Low-Temperature UV-vis Spectroscopy Study to Trap Intermediates of the **4a + NH_4OH Reaction**

In a vial, a 1 mM solution of **4a** (4 mg, 0.01 mmol) in DCM (9.0 mL) and DMA (1.0 mL) was prepared. A glass cuvette was charged with 4 mL of the prepared **4a** solution, a stir bar, and sealed with a screw cap fitted with a septum. A 4 mL of a 9:1 mixture of DCM and DMA blank was also prepared. The UV-vis spectrometer sample holder was cooled to $-60\text{ }^\circ\text{C}$ and the blank spectrum was obtained. The **4a** solution was allowed to equilibrate for 5 minutes in the spectrometer at $-60\text{ }^\circ\text{C}$ and the low temperature spectrum was obtained. The kinetics experiment was started, collecting a UV-Visible spectrum every 30 seconds for 2 hours. 28-30% $\text{NH}_4\text{OH}_{\text{vol}}$ in water (10 equiv, 6.0 μL , 0.040 mmol) was injected into the cuvette through the septum and the reaction solution was allowed to stir. Changes in the spectral features were observed after addition and for 30 min, The sample was then warmed to $-45\text{ }^\circ\text{C}$, and a spectrum was collected every 30 seconds for 0.5 h, no changes were observed. The instrument was gradually warmed to $-30\text{ }^\circ\text{C}$ and $-15\text{ }^\circ\text{C}$ after which no changes were observed in the UV-vis spectra. Lastly, the reaction was warmed to $0\text{ }^\circ\text{C}$ and left to react for 30 minutes, collecting a UV-visible spectrum once every 5 minutes.

5.9 Preliminary Synthesis of Ni(II) Allyl Complex (9a**)**

In the glovebox, **4a** (0.39 g, 1.0 mmol) was suspended in dry THF (10 mL) in a 20 mL vial. A 1.0 M solution of allyl magnesium bromide in ether (1.00 equiv, 100 μl , 1.00 mmol) was syringe transferred to the vial, and the reaction was stirred for 24 h at room temperature. The obtained dark brown reaction mixture was filtered through Celite, and the solvent of the brown filtrate was removed under reduced pressure, giving **9a** as brown and white solids. The presence of high intensity THF peaks in the ^1H NMR spectrum and broad product peaks made it difficult to assign peaks corresponding to **9a**. The % mass impurity of the product was 65% and was calculated as shown below assuming 100% conversion of reactant to product. (The impurity was hypothesized to be the $\text{MgBr}_2\cdot\text{THF}$ salts)

$$\% \text{ Mass impurity} = \left(\frac{\text{Actual mass} - \text{Theoretical mass}}{\text{Theoretical mass}} \right) \times 100\%$$

5.10 Preliminary Study on the Reactivity of **9a** with O₂

In two NMR tubes, a solution was prepared to contain **9a** (8.0 mg, 45% purity, 0.010 mmol) dissolved in MeCN-*d*₆ or DCM-*d*₂ (1 mL). The tubes were sealed with a septum and secured with electrical tape. These samples were then removed from the glovebox. Dry O₂ gas was bubbled for ~30 seconds through a stainless-steel needle into each vial through the septum, fitted with a bleed needle. For both samples, an immediate colour change from dark brown to a pale greenish-brown with brown precipitates was observed. After 15 min, the suspensions were then analyzed using ¹H NMR spectroscopy. The mixtures were filtered through Celite and washed with ether (5 mL) to remove all soluble material. The obtained brown solids were redissolved in DMSO-*d*₆ and analyzed by ¹H NMR spectroscopy.

5.11.1 Representative Procedure for Attempted Catalytic Oxidation of Allylbenzene with **9a**

A stock solution of crude **9a** (16 mg, 45% purity, 0.020 mmol, 10 mM) was prepared in DMSO-*d*₆ (2.0 mL), and 250 μL of the resulting solution was added to a NMR tube. A second stock solution containing allylbenzene (35 mg, 0.30 mmol, 0.20 M) and the internal standard mesitylene (9.0 mg, 0.075 mmol, 50 mM) in DMSO-*d*₆ (1.5 mL) was prepared and 250 μL of this solution was added to the NMR tube. The final concentrations were 100 mM of allylbenzene, 25 mM of mesitylene, and 5 mol% of **9a**. The NMR tube was sealed with a septum, secured with electrical tape, and shaken well before being removed from the glovebox. Dry O₂ was bubbled for approximately 30 seconds, through a stainless-steel needle into the tube which was equipped with a bleed needle. The tube was subsequently heated in a 120 °C oil bath. After at 0.5, 1, 4, and 18 hours, the NMR tube was removed from the oil bath, the outside walls were washed with hexanes and acetone, and the sample was analyzed by ¹H NMR spectroscopy.

5.11.2 Attempted Catalysis of Allylbenzene with **9a at High and Low Temperatures in MeCN-*d*₃**

The procedure follows the representative procedure as Section 5.11.1, except MeCN-*d*₃ was used as the solvent and the NMR tube was immersed in a preheated oil bath set to 80 °C after O₂ addition. For low temperatures, the reaction flask was immersed in a dry ice/acetone bath held at -40 °C after O₂ addition.

5.11.3 Attempted Catalysis of Allylbenzene with **9a at Low Concentration in MeCN-*d*₃**

The procedure follows the procedure above (Section 5.11.2), except that the substrate, internal standard, and **9a** had different concentrations. A stock solution of **9a** (0.004 mmol, 2 mM) was prepared by using 200 μL of the above 10 mM **9a** stock solution and adding 800 μL of MeCN-*d*₃ to make a 1.0 mL solution, and 250 μL of the resulting solution was added to a NMR tube. A second stock solution containing allylbenzene (0.060 mmol, 40 mM) and the internal standard mesitylene (0.015 mmol, 10 mM) was prepared by using 200 μL of above 200 mM substrate stock solution and topping it up to 1.0 mL of MeCN-*d*₃, and 250 μL of this solution was added to the NMR tube. The final concentrations are 20 mM of allylbenzene, 5 mM of mesitylene, and 5 mol% of **9a**.

5.11.4 Attempted Catalytic Oxidation of 1-Allyl-4-(trifluoromethyl) Benzene with **9a**

A stock solution of **9a** (16 mg, 0.020 mmol, 10 mM) was prepared in MeCN-*d*₃ (2.0 mL), and 250 μL of the resulting solution was added to two separate NMR tubes. A second stock solution containing 1-allyl-4-(trifluoromethyl) benzene (56 mg, 0.30 mmol, 0.20 M) and the internal standard mesitylene (9.0 mg, 0.075 mmol, 50 mM) in MeCN-*d*₃ (1.5 mL) was prepared and 250 μL of this solution was added to each of the NMR tubes. The final concentrations of solutions in each NMR tube were 100 mM of 1-allyl-4-(trifluoromethyl) benzene, 25 mM of mesitylene, and 5 mol% of **9a**. The NMR tubes were sealed with a septum, secured with electrical tape, and shaken well before being removed from the

glovebox. Dry O₂ was bubbled through a stainless-steel needle into the tubes which were equipped with a bleed needle for approximately 30 seconds. One NMR tube was heated in an 80 °C oil bath and the other was immersed in a dry ice/acetone bath held at -40 °C after O₂ addition. After 0.5, 1, 4, and 18 hours, the NMR tubes were removed from the oil bath and ice bath, the outside walls were washed with hexanes and acetone, and the sample was analyzed by ¹H NMR spectroscopy.

For low concentration study, the procedure follows the procedure above, except that the substrate, internal standard, and **9a** had different concentrations. A stock solution of **9a** (0.004 mmol, 2 mM) was prepared by using 200 μL of the above 10 mM **9a** stock solution and adding 800 μL of MeCN-*d*₃ to make a 1.0 mL solution, and 250 μL of the resulting solution was added to NMR tubes. A second stock solution containing 1-allyl-4-(trifluoromethyl) benzene (0.06 mmol, 40 mM) and the internal standard mesitylene (0.015 mmol, 10 mM) was prepared by using 200 μL of above 200 mM substrate stock solution and adding MeCN-*d*₃ (800 μL) to it. 250 μL of this solution was added to the NMR tubes. The final concentrations were 20 mM of allylbenzene, 5 mM of mesitylene, and 5 mol% of **9a**.

5.11.5 Attempted Catalytic Oxidation of Allyl Diphenylphosphine with **9a**

In the glovebox, allyl diphenylphosphine (45 mg, 0.20 mmol), triphenylphosphine oxide (56 mg, 0.20 mmol), and **9a** (8 mg, 0.01 mmol) were dissolved in MeCN (1 mL) and added to an NMR tube. The NMR tube was sealed with a septum, secured with electrical tape, and shaken well before being removed from the glovebox. Dry O₂ was bubbled for approximately 30 seconds, through a stainless-steel needle into the tube, which was equipped with a bleed needle. After the addition, it was heated in an 80 °C oil bath. After 24 hours, the NMR tube was removed from the oil bath, the outside walls were washed with hexanes and acetone, and the sample was analyzed by ³¹P{¹H} NMR spectroscopy.

5.12 References

- (1) Derosa, J.; van der Puyl, V. A.; Tran, V. T.; Liu, M.; Engle, K. M. *Chem. Sci.* **2018**, 9 (23), 5278–5283.
- (2) Pratt, D. A.; Pesavento, R. P.; Van Der Donk, W. A. *Org. Lett.* **2005**, 7 (13), 2735–2738.
- (3) Yang, D.; Dong, J.; Wang, B. *Dalton Trans.* **2018**, 47 (1), 180–189.

Appendix

I NMR Spectra

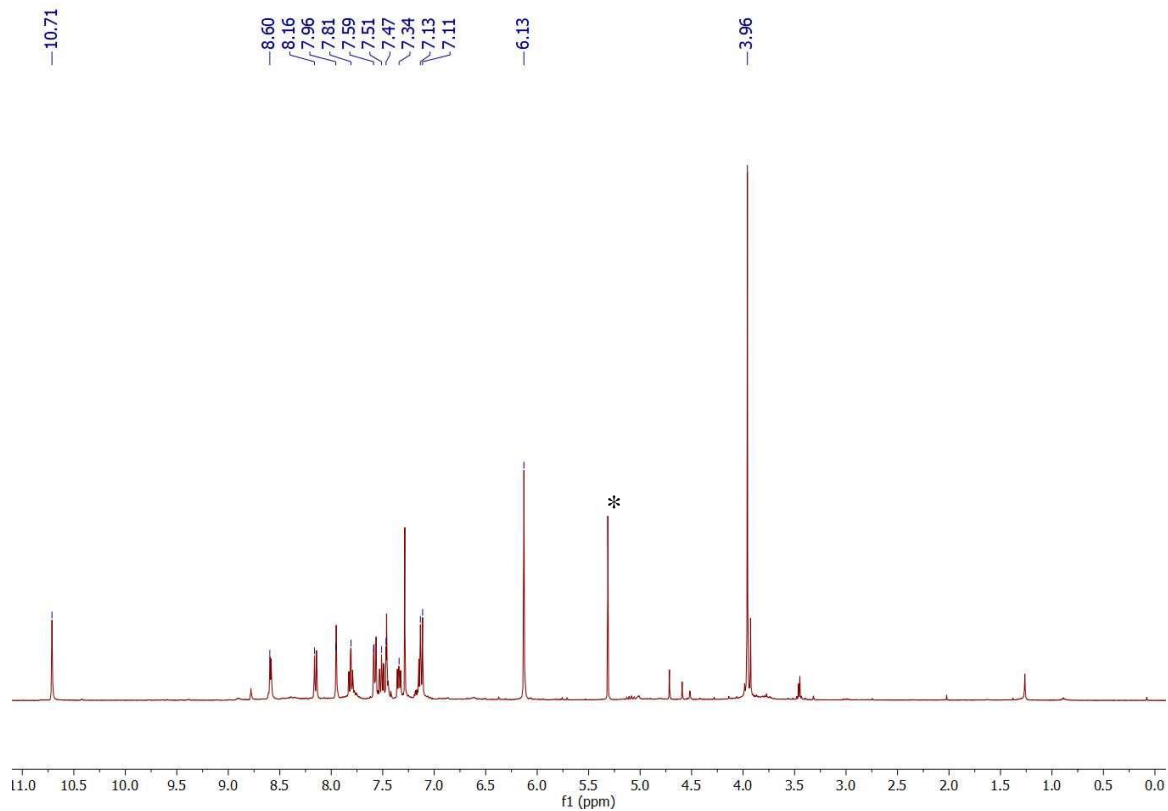


Figure A1. ^1H NMR spectrum (400 MHz, CDCl_3) of **2a**, DCM is denoted by ‘*’.

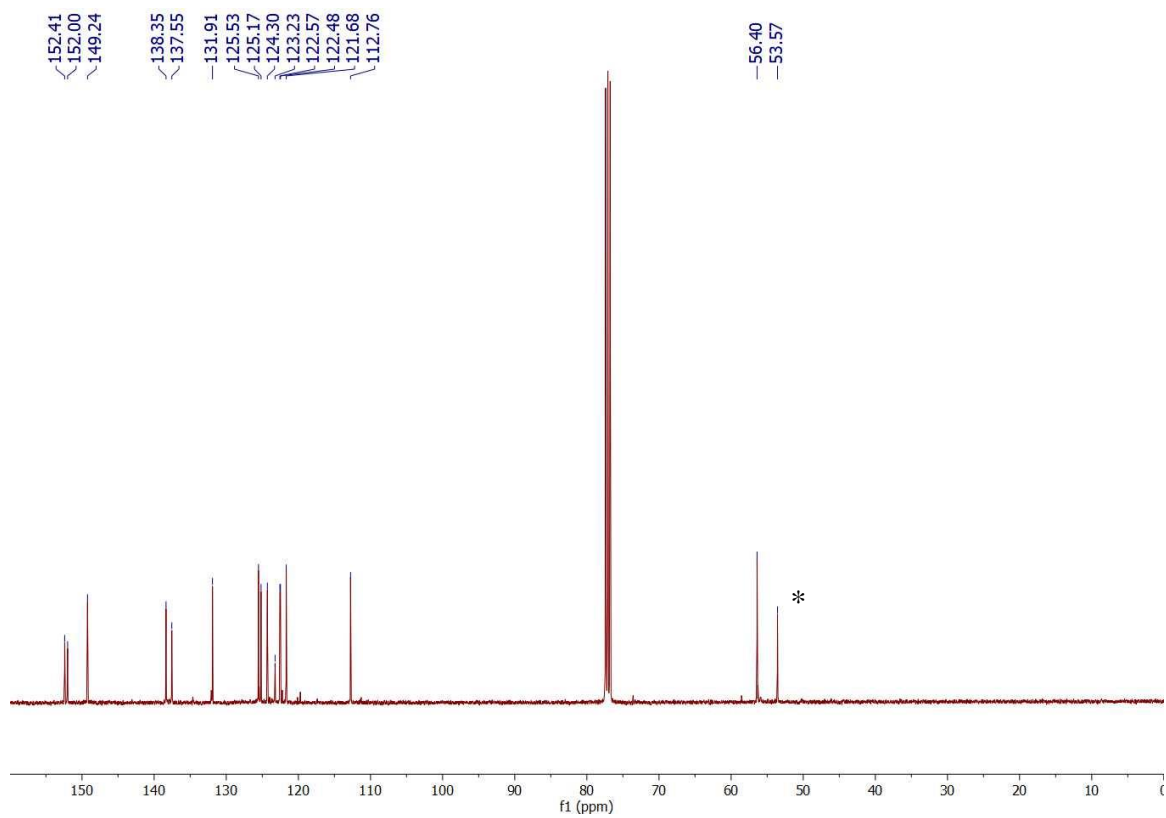


Figure A2. $^{13}\text{C}\{^1\text{H}\}$ NMR spectrum (101 MHz, CDCl_3) of **2a**, DCM denoted by ‘*’.

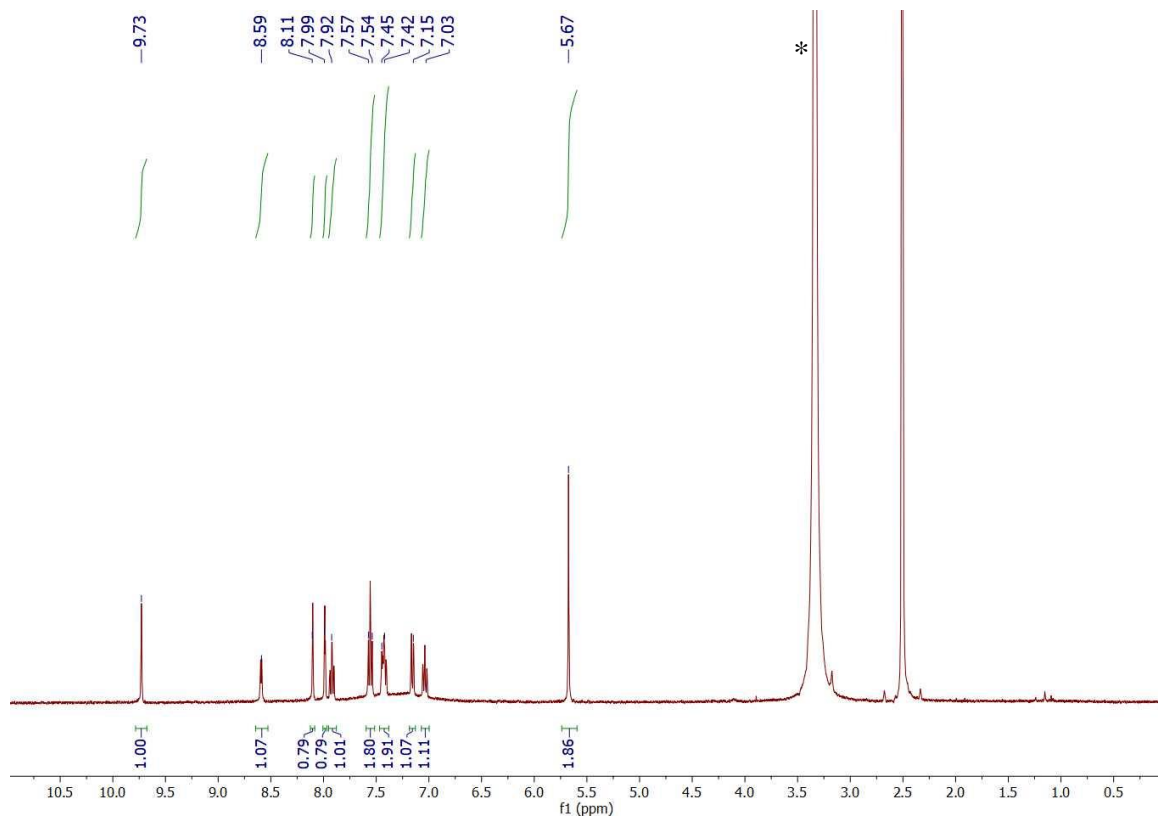


Figure A3. ^1H NMR spectrum (400 MHz, $\text{DMSO-}d_6$) of **3a**, water is denoted by ‘*’.

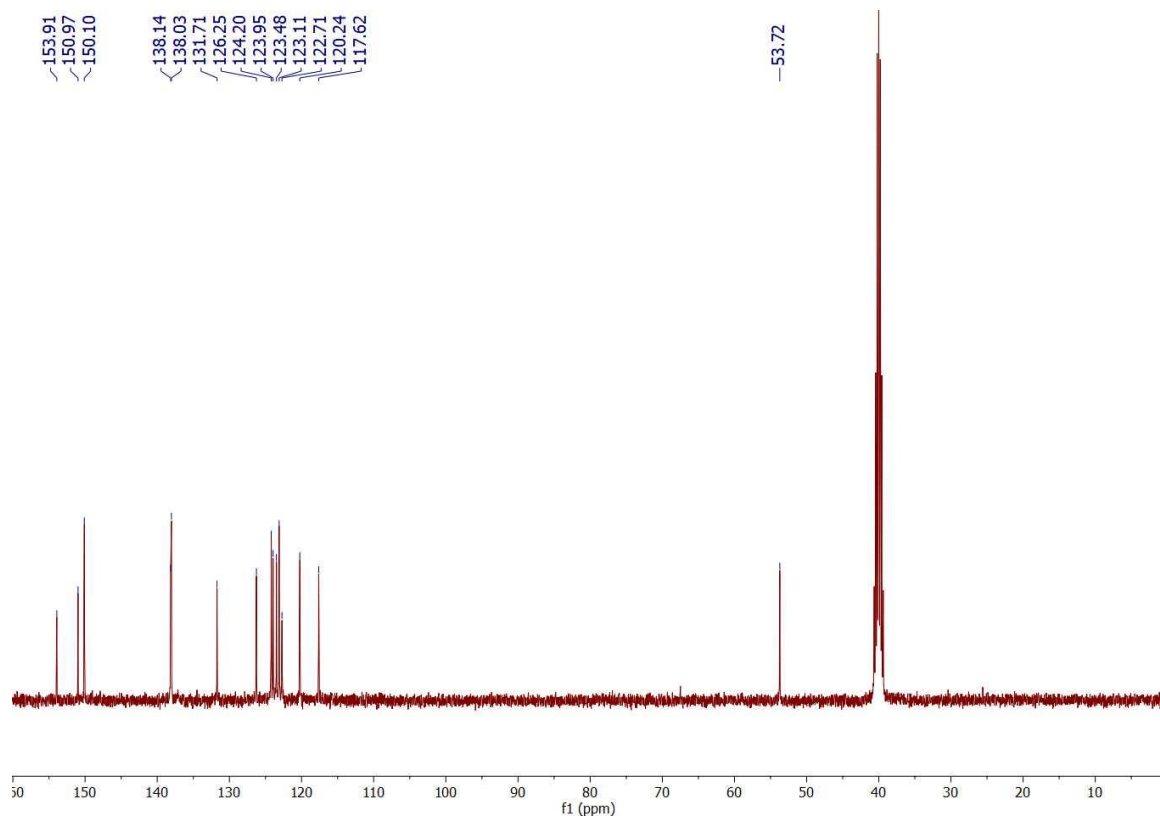


Figure A4. $^{13}\text{C}\{^1\text{H}\}$ NMR spectrum (101 MHz, $\text{DMSO-}d_6$) of **3a**.

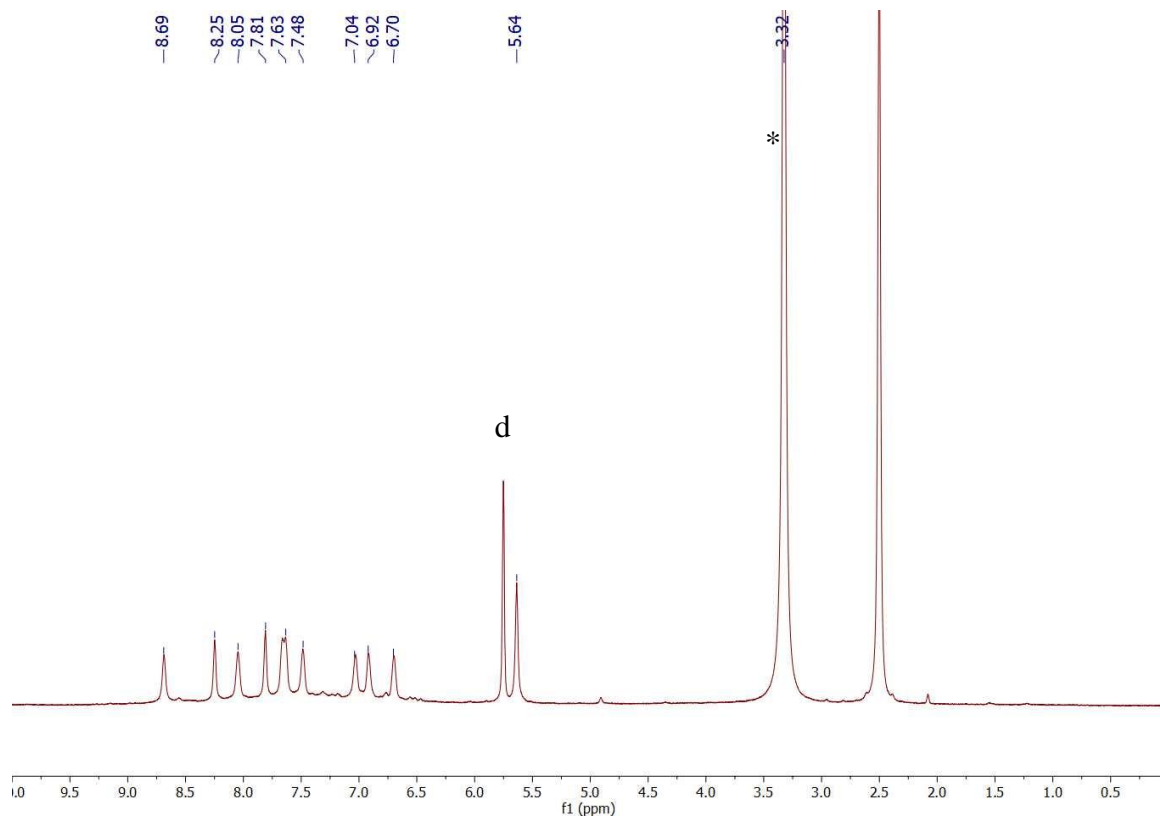


Figure A5. ^1H NMR spectrum (400 MHz, $\text{DMSO-}d_6$) of complex **4a**. DCM peak is denoted by 'd', water peak is denoted by '*'.

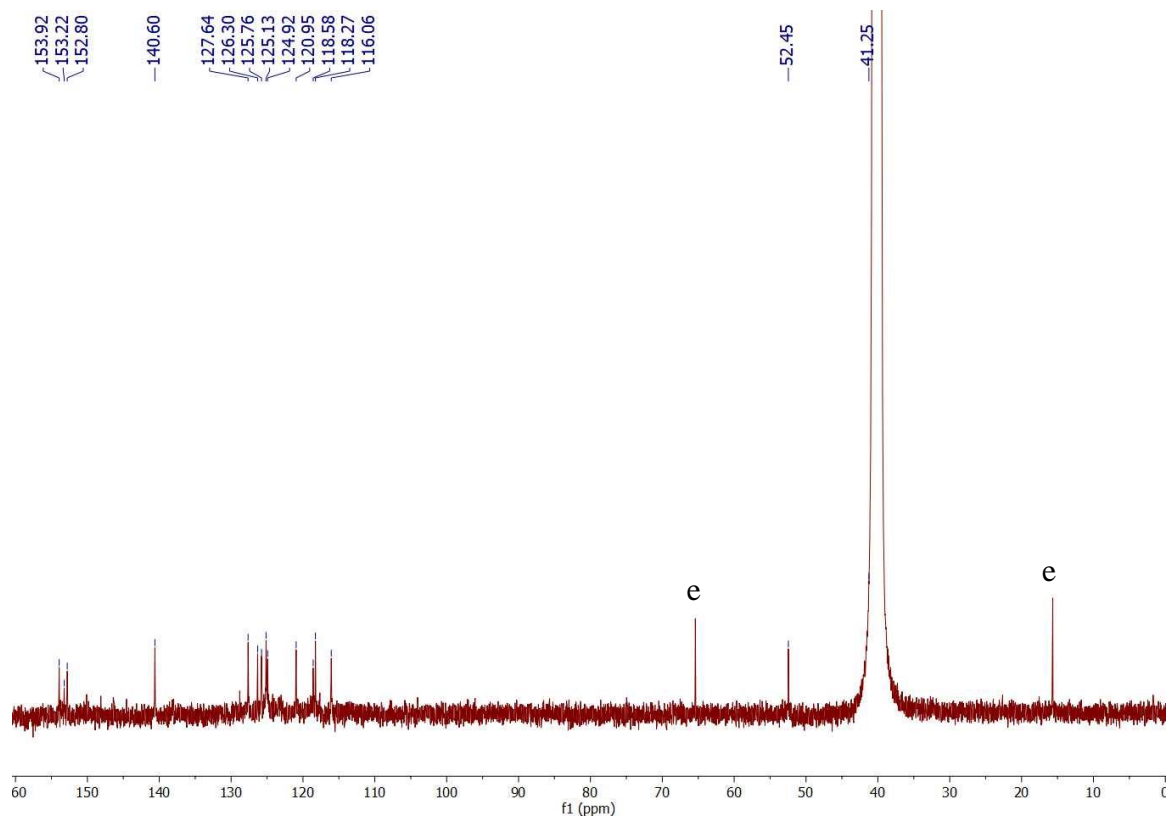


Figure A6. $^{13}\text{C}\{^1\text{H}\}$ NMR spectrum (101 MHz, $\text{DMSO-}d_6$) of complex **4a**. Diethyl ether is denoted by 'e'.

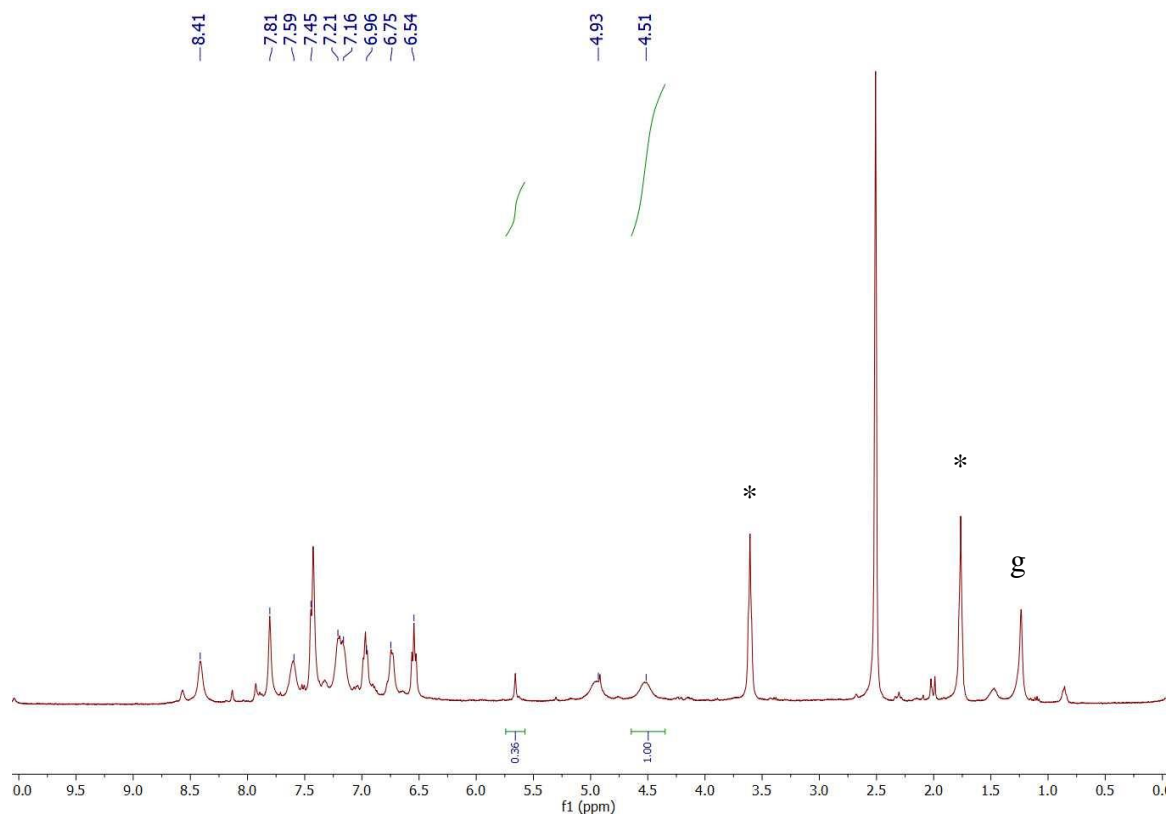


Figure A7. ^1H NMR spectrum (400 MHz, $\text{DMSO-}d_6$) of complex **6**. THF is denoted by ‘*’, grease denoted by ‘g’. Mass purity = 53% (Contains mono cationic ligand **3a**)

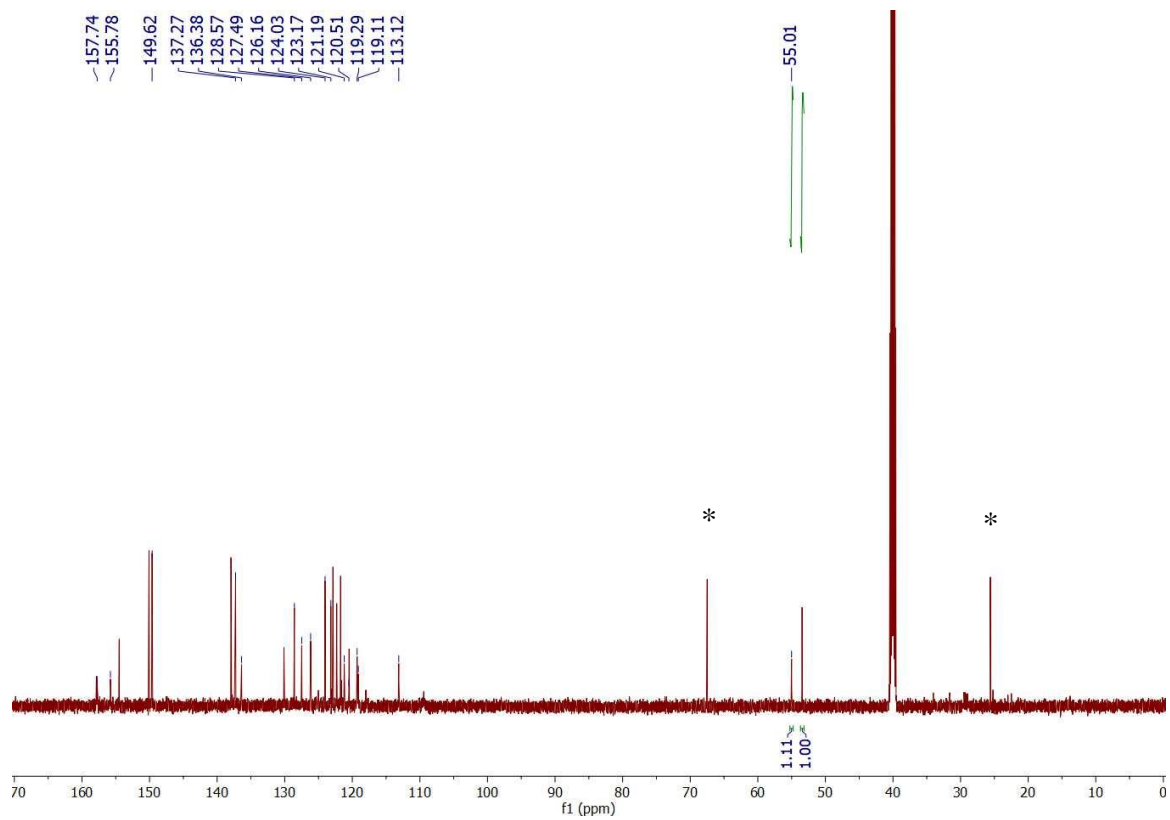


Figure A8. $^{13}\text{C}\{^1\text{H}\}$ NMR spectrum (101 MHz, $\text{DMSO-}d_6$) of **6**. THF is denoted by ‘*’. Mass purity = 53% (Contains mono cationic ligand **3a**)

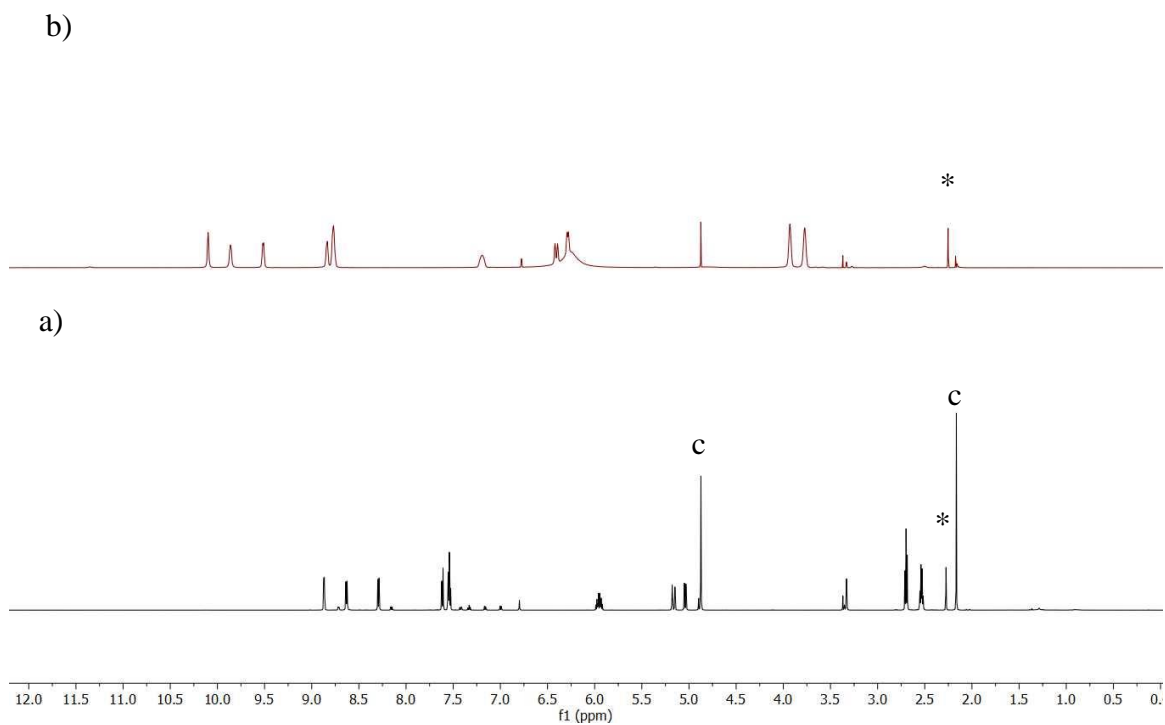


Figure A9. ^1H NMR stack plot (600 MHz, $\text{MeOH-}d_4$) of a) QPAH ligand b) QPAH treated with $\text{NiCl}_2 \cdot 6\text{H}_2\text{O}$ at 55 °C in $\text{MeOH-}d_4$. Internal standard denoted as ‘*’, traces of water and acetone denoted as ‘c’.

II IR Spectra

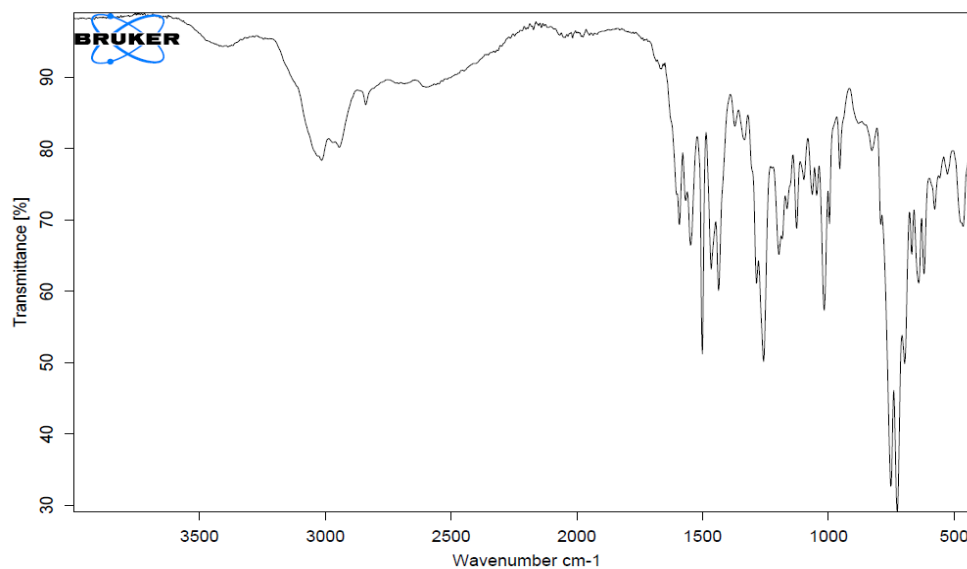


Figure A10. ATR-FTIR spectrum of solid **2a**.

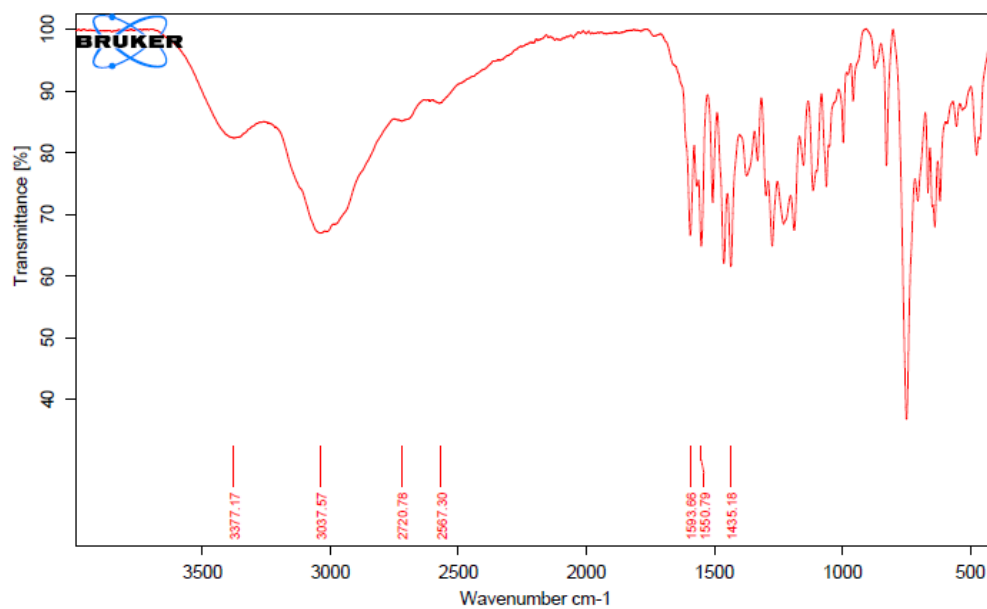


Figure A11. ATR-FTIR spectrum of solid **3a**.

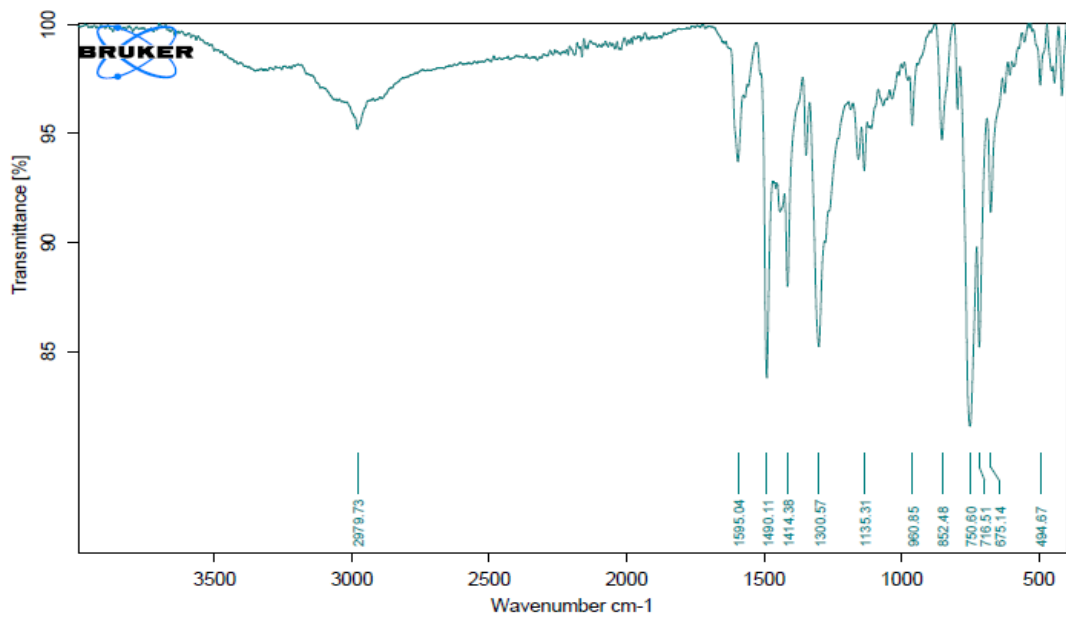


Figure A12. ATR-FTIR spectrum of solid **4a**.

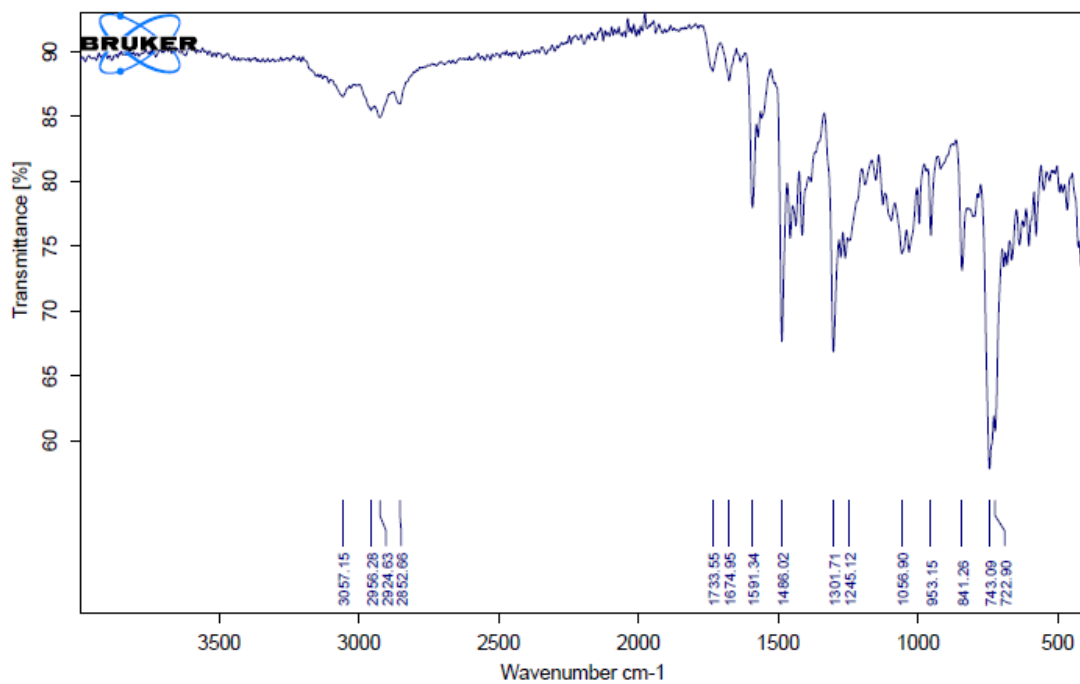


Figure A13. ATR-FTIR spectrum of solid **6**.

III Crystallographic Detail

Experimental for $C_{31}H_{26}Cl_2N_6NiO_2$ (6)

Data Collection and Processing. The sample was mounted on a Mitegen polyimide micromount with a small amount of Paratone N oil. All X-ray measurements were made on a Bruker Kappa Axis Apex2 diffractometer at a temperature of 110 K. The unit cell dimensions were determined from a symmetry constrained fit of 9914 reflections with $4.88^\circ < 2\theta < 58.5^\circ$. The data collection strategy was a number of ω and φ scans which collected data up to 70.022° (2θ). The frame integration was performed using SAINT.¹ The resulting raw data was scaled, and absorption corrected using a multi-scan averaging of symmetry equivalent data using SADABS.²

Structure Solution and Refinement. The structure was solved by using a dual space methodology using the SHELXT program.³ All non-hydrogen atoms were obtained from the initial solution. The hydrogen atoms were introduced at idealized positions and were allowed to ride on the parent atom. There were two regions of disordered CH_2Cl_2 molecules in the lattice. The first resided at a general position and was disordered over two sites. The occupancy for the predominant site refined to a value of 0.69(2). The second disordered solvent was in the vicinity of a crystallographic 2-fold axis. The array of peaks in the Fourier difference map could not be interpreted in a chemically sensible way. Therefore, the structure was subjected to a solvent masking procedure as implemented by the PLATON SQUEEZE routine.⁴ The structural model was fit to the data using full matrix least-squares based on F^2 . The calculated structure factors included corrections for anomalous dispersion from the usual tabulation. The structure was refined using the SHELXL program from the SHELX suite of crystallographic software.⁵ Graphic plots were produced using the Mercury program.⁶

References

- (1) Bruker-AXS, SAINT version 2013.8, **2013**, Bruker-AXS, Madison, WI 53711,

USA.

(2) Bruker-AXS, SADABS version 2012.1, **2012**, Bruker-AXS, Madison, WI 53711, USA.

(3) Sheldrick, G. M., *Acta Cryst.* **2015**, *A71*, 3-8.

(4) Sheldrick, G. M., *Acta Cryst.* **2015**, *C71*, 3-8.

(5) Macrae, C. F. B., I. J.; Chisholm, J. A.; Edington, P. R.; McCabe, P.; Pidcock, E.; Rodriguez-Monge, L.; Taylor, R.; van de Streek, J. and Wood, P. A. J., *Appl. Cryst.* **2008**, *41*, 466-470.

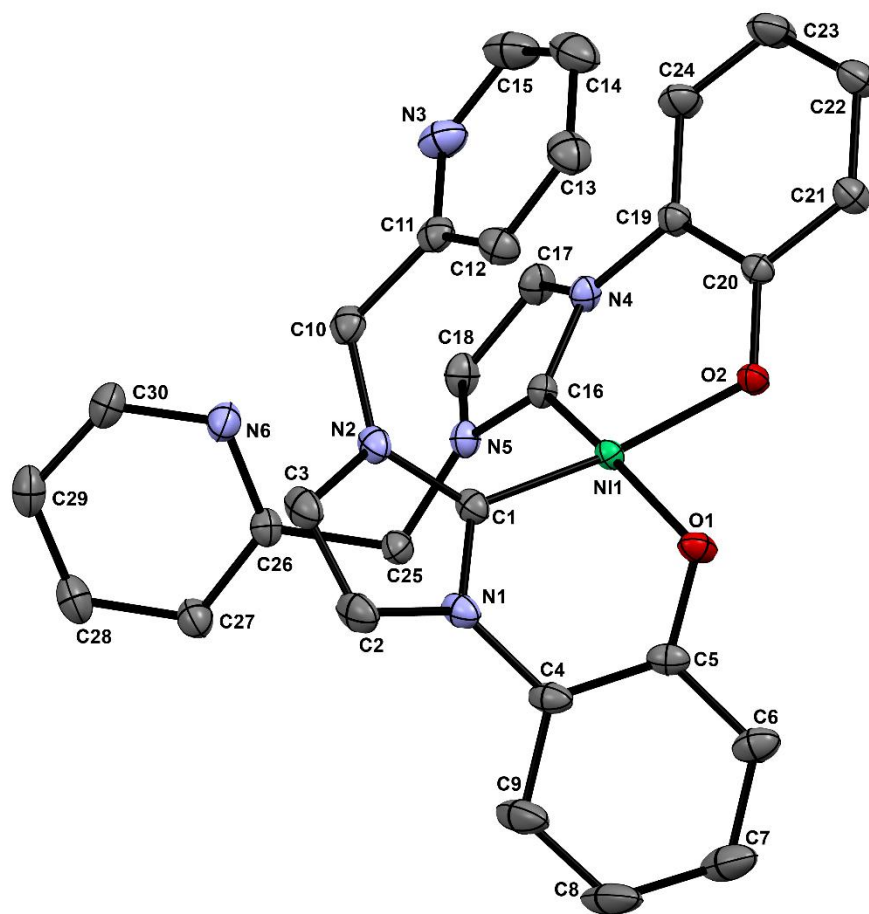


Figure A14. Drawing of **6** showing numbering scheme. Ellipsoids are at the 50% probability level and hydrogen atoms were omitted for clarity.

Table A1. Summary of Crystal Data for **6**

Formula	C ₃₁ H ₂₆ Cl ₂ N ₆ NiO ₂
Formula Weight (<i>g/mol</i>)	644.19
Crystal Dimensions (<i>mm</i>)	0.379 × 0.188 × 0.132
Crystal Color and Habit	gold prism
Crystal System	monoclinic
Space Group	C 2/c
Temperature, K	110
<i>a</i> , Å	28.060(9)
<i>b</i> , Å	11.481(4)
<i>c</i> , Å	21.363(8)
α , °	90
β , °	119.84(2)
γ , °	90
<i>V</i> , Å ³	5970(4)
Number of reflections to determine final unit cell	9914
Min and Max 2 θ for cell determination, °	4.88, 58.5
<i>Z</i>	8
F(000)	2656
ρ (<i>g/cm</i>)	1.433
λ , Å, (MoK α)	0.71073
μ , (<i>cm</i> ⁻¹)	0.869
Diffractometer Type	Bruker Kappa Axis Apex2
Scan Type(s)	π and Ω scans
Max 2 θ for data collection, °	70.022
Measured fraction of data	0.998
Number of reflections measured	222678
Unique reflections measured	13149

R _{merge}	0.0646
Number of reflections included in refinement	13149
Cut off Threshold Expression	I > 2Σ(I)
Structure refined using	full matrix least-squares using F ²
Weighting Scheme	w=1/[Σ ² (F _o ²)+(0.0508P) ² +4.9093P] where P=(F _o ² +2F _c ²)/3
Number of parameters in least-squares	398
R ₁	0.0358
wR ₂	0.0948
R ₁ (all data)	0.0507
wR ₂ (all data)	0.1031
GOF	1.044
Maximum shift/error	0.001
Min & Max peak heights on final ΔF Map (e ⁻ /Å)	-0.547, 0.575

Where:

$$R_1 = \frac{\sum | |F_o| - |F_c| |}{\sum F_o}$$

$$wR_2 = [\frac{\sum w(F_o^2 - F_c^2)^2}{\sum w F_o^4}]^{1/2}$$

$$GOF = [\frac{\sum w(F_o^2 - F_c^2)^2}{(\text{No. of reflns.} - \text{No. of params.})}]^{1/2}$$

IV UV Spectrum

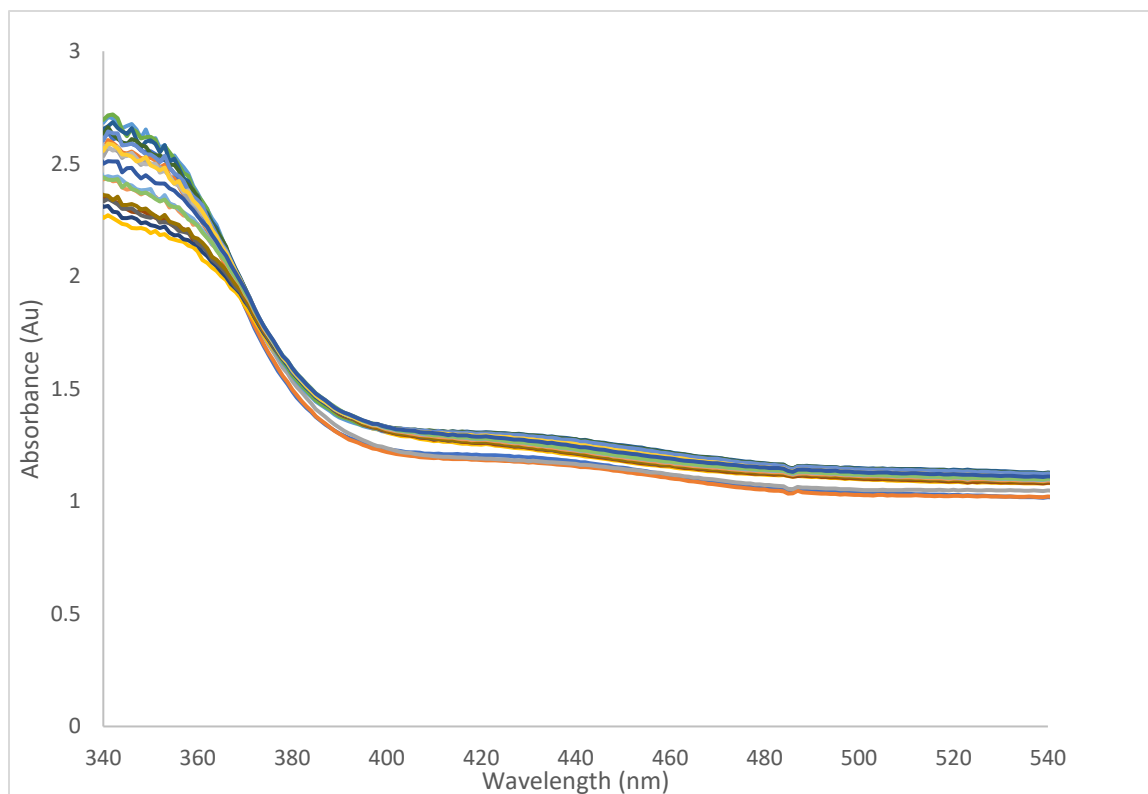


Figure A15. Kinetics trace of 1 mM **4a** at $-60\text{ }^{\circ}\text{C}$ depicted in blue and after addition of NH_4OH (28-30% in water) over 1 h. The reaction time between each trace is 5 min.

Curriculum Vitae

Shagana Kukendran

Education

M.Sc. Inorganic Chemistry January 2021- Present

The University of Western Ontario, London, ON

Thesis title: *Synthesis of Ni(II) Complexes for Allylic C(sp³)-H Bond Activation for Aerobic Oxidation Catalysis*

Supervisor: J.M. Blacquiere

B.Sc. Honours Specialization in Chemistry 2015- 2019

The University of Colombo, Sri Lanka

Fourth-year research project

Title: *Investigation of Copper Oxide Nanoparticles as Catalysts for “Click” Reaction*

Principal Supervisor: Dr. Sashiprabha Vithanarachchi

Graduate Courses Completed

9513S - Introduction to Physical Organic Chemistry (0.25 credits) Grade: 92%

9563S - Total Synthesis (0.25 credits) Grade: 90%

9555T - Organic Photochemistry (0.25 credits) Grade: 88%

9521S - Catalysis (0.25 credits) Grade: 87%

Honours and Awards

Gold Medal in Organic Chemistry - Undergraduate July 2019

The University of Colombo, Sri Lanka

Related Work Experience

Graduate Teaching Assistant

The University of Western Ontario, London, ON

Chemistry 2213A (Lab and Resource Room)

Summer 2021, Fall 2021, Fall 2022

Chemistry 2223B - Organic Chemistry of Biological Molecules

Winter 2022

Temporary Assistant Lecturer – Inorganic laboratory

March 2019-2020

The University of Colombo, Sri Lanka

Laboratory Techniques and Expertise

- Independently perform ligand and organometallic synthesis reactions
- Trained in the proper handling of air and moisture-sensitive materials (Schlenk and glovebox techniques)
- Characterized reaction products and monitored reactions in situ using NMR spectroscopy (1D, 2D, and VT) utilizing the MestReNova software
- Characterized reaction products using ATR-IR and MALDI-MS
- UV visible spectroscopy maintenance and handling including usage of Agilent ChemStation software to process data
- Prepared and analyzed catalytic reactions (NMR)
- Maintained standard operation of a MBraun glovebox
- Proficient in MS Office software- Word, PowerPoint, Excel, and Outlook as well as chemical drawing software ChemDraw

Conferences (OP = ORAL, PP = POSTER)

PP2. Shagana Kukendran, Johanna M. Blacquiere*, An Allylnickel NHC Complex to Promote Aerobic Oxidation Catalysis: Investigating the Role of a Tridentate Ligand, *Canadian Chemistry Conference and Exhibition (CCCE)*, Calgary, June 2022 (National).

PP1. Shagana Kukendran, Johanna M. Blacquiere*, A Monomeric Ni(II)-OH Complex for C-H Activation, *IUPAC World Chemistry Congress (WCC) and Canadian Chemistry Conference and Exhibition (CCCE)*, Virtual, August 2021 (International).

OP1: Shagana Kukendran, Sashiprabha Vithanarachchi, Investigation of Copper Oxide Nanoparticles as Catalysts for “Click” Reaction, *12th International Research Conference 2019, KDU, Sri Lanka*, September 2019 (National)

